Chromatin organisation in the spermatozoa of the dasyurid marsupial, *Sminthopsis crassicaudata*

by

Lilian LL Soon (BSc, Hons)

A thesis submitted for the degree of Doctor of Philosophy in the University of Adelaide

September, 1996

The Department of Anatomy and Histology, Faculty of Medicine, University of Adelaide
and The Department of Animal Genetics, Waite, University of Adelaide
SA, Australia

Fat-tailed dunnart

Sminthopsis crassicaudata

Order Dasyuromorphia
Family Dasyuridae
Head and Body: 6-9 cm
Tail: 4-7 cm

Oil by L Soon, adapted from photograph in "Encyclopedia of Australian Animals Series" A&R, Harper Collins

ABSTRACT

This research entailed investigations on the organisation of spermatozoa chromatin from the fat-tailed dunnart (*Sminthopsis crassicaudata*), an Australian insectivorous marsupial. The spermatozoa of this dasyurid species have two distinct nuclear regions; a homogeneous and amorphous interior (C1), and a fissured, peripheral region (C2). The objective of this research was to elucidate the molecular structural organisation of the spermatozoa nuclei. Some studies that were carried out include, (1) biochemical analyses of the nuclear proteins, (2) determination of the higher order chromatin structure using the atomic force microscope (AFM), and (3) molecular characterisation of DNA from the two nuclear regions.

Spermatozoa nuclear proteins were characterised using acetic acid-urea PAGE and fractionated by reverse-phase HPLC. The main protein component was partially sequenced and was determined to be protamine 1. A full histone complement consisting of H1, H2B, H2A, H3 and H4 was also detected and these histones constituted approximately 25-30% of total protein.

Immunofluorescence and immunoelectron microscopy revealed specific labelling of anti-histone antibodies to the C2 region. Treatment of nuclei with micrococcal nuclease showed that the C1 chromatin was resistant to digestion, a feature that is characteristic of nucleoprotamines. The enzyme, however, preferentially cleaved the C2 chromatin from the rest of the nucleus to produce 30-38 nm agglomerates.

AFM imaging demonstrated that the higher order chromatin structures in the C1 region were particles of 50-80 nm in diameter. The C2, nucleohistone region, however, contained clusters of 120-140 nm sized-particles.

DNA from the nucleohistone region was isolated using micrococcal nuclease, cloned into PCR-Script, and characterised by sequencing. A database search indicated shared sequence homology of the cloned fragments with a family of long interspersed repeat elements (LINEs).

Southern hybridisation using a probe made from a LINE insert named, L1Sc, did not label to DNA from the micrococcal nuclease-resistant, C1 region. By contrast, the probe hybridised to a large series of fragments from the untreated genomic DNA. These results indicate that L1Sc may occur exclusively in the nucleohistone region of the spermatozoa nuclei.

This was supported by fluorescence *in situ* hybridisation studies that demonstrated localisation of L1Sc probes to the peripheral chromatin of the spermatozoon nucleus, corresponding to the nucleohistone region. In *Sminthopsis* fibroblast chromosomes, L1Sc probes were localised within the dark R-bands that contain the AT-rich and gene-poor, isochores of the genome. Therefore, there may exist defined genomic clustering of LINE sequences in both the chromosomes and spermatozoa nuclei of this species.

In conclusion, spermatozoa of *Sminthopsis crassicaudata* appear to contain both histones and protamines in well-defined regions of the nucleus. Histones have been localised to the peripheral C2 region, whereas protamines are likely to occur in the nuclease-resistant C1 region. The histones organises DNA within the C2 region into 11 nm nucleosomal structures that form larger fibres of approximately 120-140 nm in diameter as measured from topographic AFM images. AFM also shows that the putative nucleoprotamine region (C1) may consist of tightly packed nodules of about 45-60 nm in diameter. Finally, the spermatozoa histones appear to have a preference for the packaging of the nongenic isochore, which consists mainly of LINE repeats, whereas protamines may bind to the gene-rich isochore of the genome.

DECLARATION

This work contains no material which has been accepted for the award of any other degree or diploma in any university or other tertiary institution and, to the best of my knowledge and belief, contains no material previously published or written by another person, except where due reference has been made in the text.

I give my consent to this copy of my thesis, when deposited in the University Library, being available for loan and photocopying.

Lilian Soon
September 1996

PUBLICATIONS

PAPERS

Breed WG, Leigh CM, Washington JM, Soon LLL (1994): Unusual nuclear structure of the spermatozoon in a marsupial, *Sminthopsis crassicaudata*. Mol Reprod Dev 37:78-86.

Soon LLL, Breed WG (1995): Ultrastructure of nuclear condensation and localisation of DNA and proteins in spermatozoa of a dasyurid marsupial, *Sminthopsis crassicaudata*. Mol Reprod Dev 43:217-227.

Soon LLL, Ausio J, Breed WG, Power JHT, Muller S (1996): Isolation of histones, and related chromatin structures from spermatozoa nuclei of a dasyurid marsupial, *Sminthopsis crassicaudata*. J Exp Zool (submitted).

Soon LLL, Bottema C, Breed WG (1996): Atomic force microscopy of three-dimensional nucleoprotamine and nucleohistone structures in the spermatozoa nuclei of marsupials. J Anat (in preparation).

Soon LLL, Bottema C, Breed WG (1996): Long interspersed repeats are packaged within the nucleohistone region of a marsupial spermatozoa nuclei (in preparation).

ABSTRACTS

Soon LLL, Power JHT, Breed WG (1993): Protamines and chromatin organisation in the spermatozoa of a dasyurid marsupial, *Sminthopsis crassicaudata*. Cell Biol Int 17:812.

Soon LLL, Breed WG , Webb G, Ford J (1994): Nuclear organisation in spermatozoa of a dasyurid marsupial. Proceedings of the 7th Int Conference on Spermatology. Section 4.3.

Soon LLL, Ausio J, Breed WG (1995): Histones and higher order chromatin structures in a dasyurid marsupial spermatozoa. Proceedings for the 27th Australian Society for Reproductive Biology conference p14.

Soon LLL, Breed WG (1995): Atomic force microscopy of sperm nuclear chromatin. Proceedings of the Australian and New Zealand Society for Cell Biology conference. Section 10 p55.

ACKNOWLEDGEMENTS

This study was conducted under the auspices of the Australian Research Council (grant [A09132094] to Dr. Breed) and the Faculty of Medicine, University of Adelaide (PhD scholarship [Alfred, Ferres and Scammell] to L Soon).

I would like to thank my supervisor, Associate Professor Bill Breed, and co-supervisor, Associate Professor Cynthia Bottema for their advice and support, and painstaking efforts at reading this thesis. Their comments and suggestions for the thesis and papers arising from this thesis have been invaluable. I am also grateful to Dr. Rod Balhorn from The Biology and Biotechnology Research Program Unit at Lawrence Livermore National Laboratory (LLNL), Livermore, California USA, for his early role in the discussion of ideas and studies for this project.

Antibodies (histones) used in this research have been obtained through the courtesy of Associate Professor Juan Ausio from The Department of Biochemistry and Microbiology, University of Victoria, Victoria, BC, Canada, and Professor Sylvianne Muller from The Institut de Biologie Moleculaire et Cellulaire du CNRS, Strasbourg, Cedex, France. I thank Juan, Sylvianne and Dr. John Power from The Department of Human Physiology, Flinders University of SA, for their collaboration in the protein chemistry aspect of this project.

I would like to thank Cindy and others at the Department of Animal Genetics, Waite, University of Adelaide, especially Dr. Graham Webb, Dr. Andrew Thompson and Miss Helena Cerin, who have been very helpful in the practical aspects and design of the molecular biological experiments.

Many thanks to Mr. John Terlet for his support of my use of the atomic force microscope housed at CEMMSA, University of Adelaide and the staff of CEMMSA for their friendly and competent service. I thank all members of The Department of Anatomy and Histology and The Department of Animal Genetics, University of Adelaide for their friendship and help.

I would like to especially thank my parents, Jeffrey and Alice Soon, and other members of my family, little Cheryl, Lynette, Penny, Rosaline, Seng and Stephen for their sacrifices, concern and patience over the years.

To Peter McPherson, warmest thanks and appreciation for being supportive and caring at all times.... :-)

ABBREVIATIONS

a = acrosome
AFM = atomic force microscope
C1 = homogenous, inner chromatin
C2 = indented, peripheral chromatin
cd = cytoplasmic droplet
Cyt = cytoplasm
DAPI = 4',6-diamidino-2-phenylindole
DMP 30 = tri-L-(dimethylaminomethyl)phenol
EDTA = ethylenediaminetetraacetic acid.
ENE = enlarged nuclear envelope
f = flocculent material
FITC = fluorescein isothiocyanate
HPLC = high performance liquid chromatography
mt = mitochondria
N = nucleus
ne = nuclear envelope
NM = nuclear mantle
np = nuclear pore
PMSF = phenylmethylsulfonyl fluoride
pr = periacrosomal ring
SNBP = sperm nuclear basic protein
s = subacrosomal space
t = sperm tail
tb = tubulobulbar complex
TEM = transmission electron microscope
TLCK = Nα-p-Tosyl-L-lysine chloromethyl ketone
w = membranous whorls

Chapter 1. LITERATURE REVIEW

1.1. INTRODUCTION

The spermatozoon is a highly specialised cell that fulfils roles in the transport of the haploid paternal genome within the female tract and in the fertilisation of the oocyte. Some key structures involved in these functions include a flagellum that is equipped with mitochondria and the machinery for motility, an acrosome which carries hydrolytic enzymes that aid in the penetration of oocyte coats, and a highly compacted nucleus that contains the male haploid genome. Although these features can be found in the spermatozoa of most species including invertebrates, there are, nevertheless, considerable differences in the morphology of the male gamete between species from different taxa. Sperm morphology is, however, conserved within taxonomic groups and has been used in comparative studies to determine or confirm phylogenetic relationships (Harding et al., 1982; Breed, 1983; Temple-Smith, 1984).

During vertebrate spermiogenesis, significant changes in the structure and biochemistry of chromatin occur, such as alterations in the methylation level of DNA (Mazo et al., 1994), and, with the exception of some fish and anurans, the replacement of histones with protamines (Balhorn, 1989). The DNA packaging protein, protamine, which is low molecular weight and highly basic, is largely responsible for the condensed and biochemically inert state of spermatozoa chromatin (Marushige and Dixon, 1969). There is large interspecies variation in the amino acid sequence of protamines and in the types expressed. This contrasts with the high degree of conservation in somatic cell histones. Histones have an important role in transcription by regulating the accessibility of DNA to transcription factors. This occurs through post-translational modifications of the proteins, such as acetylation of the amino terminus of histone H1 (Grunstein, 1991). In addition, the winding of the DNA helix around the histone octamer allows close range interactions between control elements that are separated within genes (van Holde, 1993).

Protamines, unlike histones, do not appear to have any specific roles in gene expression or replication. The high sequence divergence of protamines may reflect a lack of selective advantage in preserving characteristics that relate to

gene function. Protamines may have a primary role in the packaging of DNA to a minimal volume and may thus serve to protect the genetic material during transportation of the spermatozoa within a viscous medium. However, there exists some intriguing similarities between DNA packaging in somatic cells and spermatozoa, that is discussed in more detail in Section 1.4.

Somatic histones of germ cells are replaced by arginine-rich, sperm-specific protamines during spermiogenesis in mammals, however, a subset of histones are retained in the mature spermatozoa of some species such as mice, rams and humans (O'Brien and Bellvé, 1980; Biggiogera et al., 1992; Moss et al., 1989; Uschewa et al., 1982; Tanphaichitr et al., 1978; Gatewood et al., 1987; Gusse et al., 1986). In vertebrates, two major families of protamines, P1 and P2, are known to exist. The P2 protamines are, however, incorporated within the spermatozoa nuclei of only a small number of species that include mice, humans and stallions (McKay et al., 1986; Belaiche et al., 1987; Bellvé et al., 1988). Most vertebrate species express type I protamines, but, those of marsupials (Retief et al., 1995a; Fifis et al., 1990), birds (Chiva et al., 1987) and reptiles (Kasinsky et al., 1987) differ from eutherians in the general absence of inter- and intraprotamine disulphide bonds.

In this thesis, some basic questions regarding the organisation of the spermatozoa chromatin of a dasyurid marsupial, *Sminthopsis crassicaudata* have been addressed. The spermatozoon of this species displays a very peculiar nuclear morphology. Ultrastructurally, the nucleus consists of (1) a homogenous core structure and (2) fissured structures at the periphery. The morphology of spermatozoa nuclei in eutherians, is more akin to the first structure which has a condensed and homogenous appearance. In some species, however, irregularities such as the nuclear vacuoles of human spermatozoa, also exist (Tanphaichitr et al., 1982).

It is unknown how the variability in the morphology of mammalian chromatin relates to the diverse array of spermatozoa nuclear basic proteins (SNBPs) incorporated in the nuclei. For example, there is, hitherto, no comprehensive study on the localisation of different proteins such as sperm histones, and P 1 and P 2 protamines within the spermatozoon nucleus. It remains obscure whether or not this multiplicity of proteins translates into a heterogeneous chromatin organisation. With the pronounced features of the two chromatin regions in *Sminthopsis* spermatozoon, this animal lends itself as a good

model to study the disjunction or compartmentalisation of the chromatin and the cause and/or selective advantage for this occurrence.

In the following sections, several topics will be introduced including, (1) spermiogenesis during which nuclear condensation occurs, (2) the different types of sperm nuclear basic proteins (SNBPs), such as histones, histone-like proteins, intermediate proteins and protamines, that are incorporated in spermatozoa of various species, (3) protamine structure, function and evolution, (4) structures of nucleohistones and nucleoprotamines and, finally, (5) the organisation of DNA sequences such as the telomeres and satellite repeats in spermatozoa nuclei. These topics are designed to provide an overview of the morphogenesis of the sperm nucleus, the DNA packaging proteins involved including some aspects of their evolution, and the spatial distribution of certain DNA elements in the spermatozoa nuclei.

1.2. SPERMATOGENESIS IN MAMMALS

Spermatogenesis encompasses two meiotic divisions of a male germ cell to produce four haploid spermatids and their subsequent transformation into spermatozoa that is equipped with flagella, acrosomes, and compact nuclei. The morphological changes that take place during spermatogenesis are essentially the same in all mammals and can be divided into several stages. Each stage is represented by four or five layers of germ cells that exhibit various degrees of development (Fig. 1.1). These cellular associations are conserved amongst mammals and relate closely to the functions of Sertoli cells (Sharpe, 1993).

Stem-cell spermatogonia initially divide into two daughter cells (Amman, 1981). One of the cells prevails as a stem cell, called proliferative spermatogonium, while the other, differentiates into a Type B spermatogonium. The nomenclature for stem cells is $A_{isolated}$ (A_{is}) spermatogonia, proliferative cells are, A_{paired} (A_{pr}) and $A_{aligned}$ (A_{al}) spermatogonia, whereas differentiated cells are known at various stages of development to be A_1, A_2, A_3, A_4, Intermediate (In), and Type B (B) spermatogonia. Spermatogonia can be distinguished in histological sections by the amount of chromatin lying along the inner aspect of the nuclear envelope; Type A has essentially none, and Type B contains a large amount (Parvinen et al., 1991).

Type B spermatogonia undergo a final mitotic division to give rise to two daughter cells that enter a prolonged meiotic phase as preleptotene spermatocytes. Preleptotene spermatocytes are very similar to B cells but are slightly smaller. These cells are at an active stage of DNA synthesis (Parvinen et al., 1991).

Leptotene signals the initiation of the meiotic prophase, which is long-lasting and may extend for up to three weeks. The nuclei of leptotene cells lack peripheral chromatin but condensed chromosomes are apparent in the form of chromatin threads. During zygotene, homologous chromosomes become paired with the aid of the pairing apparatus or synaptonemal complex, and the chromosomes have a thicker appearance.

At pachytene, genetic recombination or crossing over occurs in the fully paired chromosomes. During mid- to late pachytene stage, there is prolific RNA synthesis (Tres and Kierszenbaum, 1977). The cells grow rapidly in size and the chromosomes become more widely dispersed within the nuclei. Diplotene is a

brief phase and the remainder of the cell division occurs rapidly to produce secondary spermatocytes.

The second meiotic division, or meiosis II, soon follows and results in four haploid spermatids for every pachytene spermatocyte (Sharpe, 1994). Meiosis II cells are considerably smaller than their meiosis I counterparts. Both secondary spermatocytes and Step 1 spermatids are similar in having very little heterochromatin but the spermatids are distinguishable by their smaller size. At this stage they are known as 'round spermatids' as the shape of the cells and the nuclei is roughly spherical. During spermiogenesis, each round spermatid differentiates into a spermatozoon whilst undergoing profound physiological, biochemical and morphological transformations.

Spermiogenesis in mammals is subdivided into three phases; these overlap in the commencement and completion of the morphological changes that occur in the spermatid. The acrosomal phase involves the development of the acrosome in early spermatids. The acrosome, however, continues to change and mature well into the later stages of spermiogenesis.

During the second phase, elongation of the flagellum, accompanied by the accumulation of mitochondria at the mid-piece, take place. At the same time, nuclear condensation and a progressive reduction in cytoplasmic volume occur (Sprando and Russell, 1987).

The final phase involves the elimination of the remaining cytoplasm and the release of the spermatozoon into the lumen of the seminiferous tubules (Fig. 1.1). The gradual reduction in cytoplasmic volume occurs through specialised structures, the tubulobulbar complexes, that form between the Sertoli cell and the head region of the spermatid. The release of the mature spermatozoon into the tubular lumen is partly mediated by severing links with the tubulobulbar complexes (Russell, 1990).

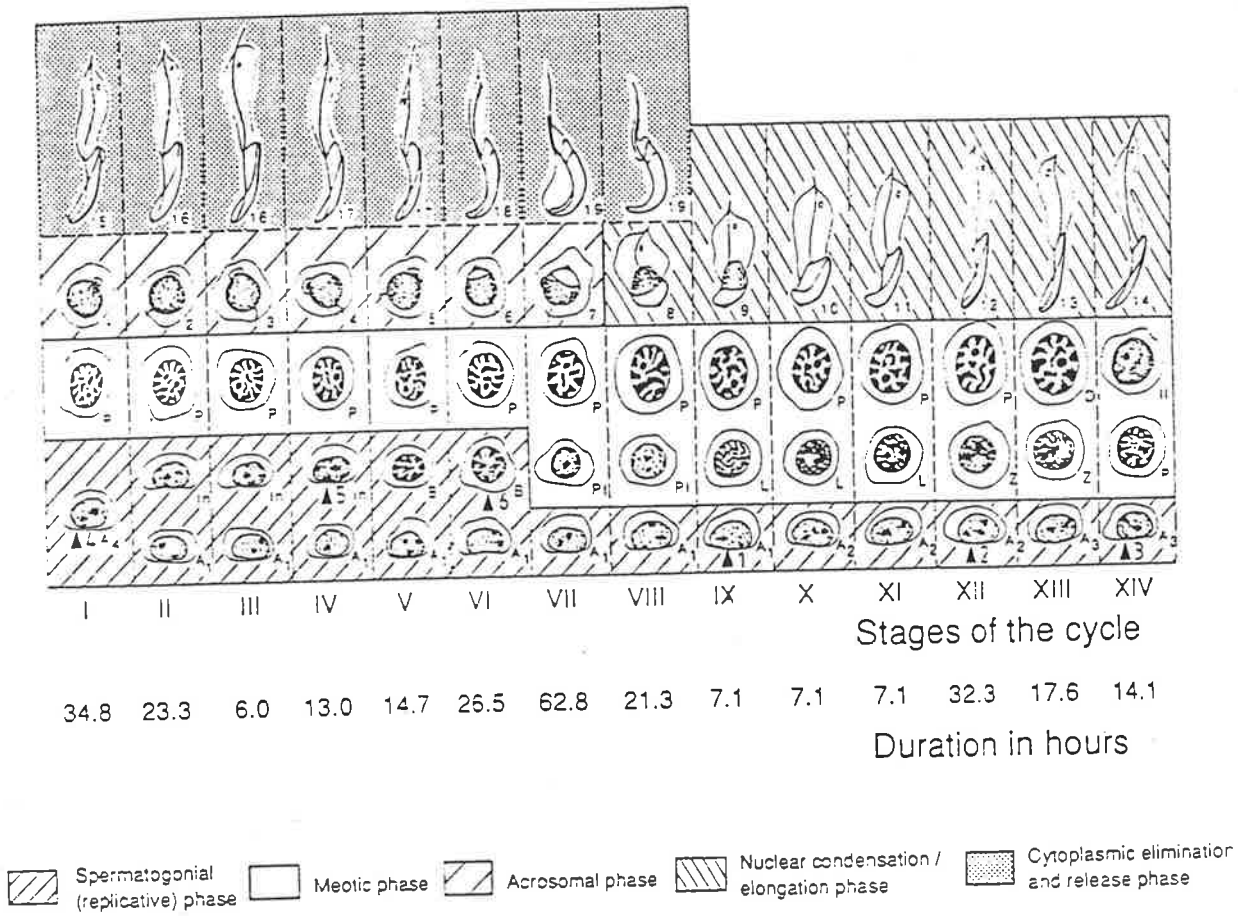

Fig. 1.1. Germ cell associations at the different stages of the spermatogenic cycle in the rat. Each stage is represented by a complement of germ cells that are in association with Sertoli cells at that particular stage. The lumen of the tubule is located to the top of the diagram and the basement membrane is to the bottom (Sharpe, 1993).

1.2.1. Nuclear changes during spermatogenesis

At the onset of spermiogenesis, the round spermatid is still capable of mRNA synthesis and is active in the production of heterogeneous nuclear RNA (hnRNA) (Kierszenbaum and Tres, 1975), and protamine RNAs (Hecht, 1990). However, during the elongation phase, the nucleus becomes transcriptionally inert as nuclear condensation progresses. At this time in eutherian mammals, histones become replaced by transition proteins, which in turn become displaced, and substituted with protamines (Hecht, 1990). Thus, the bulky nucleosomal (histone octamer and associated DNA) type of DNA packaging becomes

transformed into a highly compact nucleoprotamine structure (Ward and Coffey, 1991). Concomitantly, the nucleus becomes greatly reduced in size and adopts the species-specific shape.

Fawcett et al., (1971) suggested that the generation of the nucleoprotein complex may be an intrinsic factor that is responsible for the shaping of the spermatozoa nuclei. Other structures believed to be extrinsic determinants of nuclear shaping are the manchette (Russell et al., 1983), and perinuclear theca components such as the subacrosomal layer (Bellvé et al., 1992), and the postacrosomal nuclear sheath (calyx) (Longo and Cook, 1991). Given the lack of available evidence, none of these factors can be ascribed a predominant role in the shaping of the nuclei of spermatozoa.

The manchette is an organelle that appears around the caudal region of the nucleus during early spermiogenesis and disappears just before spermiation. It consists of an array of microtubules linked to the nuclear ring (Holstein and Roosen-Runge, 1981). The microtubules occur close to the nuclear envelope and form attachments to the fibrils of the condensing chromatin. During the elongation phase, the nuclear ring and the associated manchette move towards the posterior of the nucleus and may thus have a subsidiary role in nuclear shaping in eutherians (Russell et al., 1991).

The subacrosomal layer labels with antibodies to actin and this labelling is high during the elongation phase and subsequently disappears prior to sperm release (Fouquet et al., 1989). Actin may form a temporary framework that guides the assemblage of other proteins of the perinuclear cytoskeleton (Fouquet et al., 1992).

In young spermatids, the perinuclear substance (PNS), appears between the developing acrosome and the nuclear envelope. As the development of the PNS progresses to the postacrosomal region, the postacrosomal dense lamina appears in elongating spermatids. Cytochemical studies indicate that these thecal components are rich in basic proteins (Dadoune and Alfonsi, 1986; Dadoune, 1995). The proteins that have been isolated include the 60 kDa calicin, which may be related to keratin (Longo et al., 1987), and the thecin family of high molecular weight proteins (Bellvé et al., 1990). The perinuclear theca has been suggested as forming a dense mesh that interconnects the acrosome, nucleus and postacrosomal material, thereby providing consistency to the overall shape of the spermatozoon head. This view is supported by the finding that following the

extraction of protamines and DNA from the mouse sperm nucleus, the original shape of the nucleus is retained and is maintained by the perinuclear matrix, consisting of the perinuclear theca and a network of fibres (Bellvé et al., 1992).

1.3. VERTEBRATE PROTAMINES

During spermatogenesis in species from the different taxonomic groups, there is a high degree of compositional and structural variability in the spermatozoa nuclear basic proteins (SNBPs) that eventually become associated with DNA. There are several categories of SNBPs, classified according to their cytochemical and biochemical properties (Bloch, 1969). Type 1 proteins are the true protamines that are rich in arginines and found in many vertebrate groups such as fish, marsupials and birds. Type 2 are the keratinous protamines that contain cysteine residues and found in eutherian and cartilaginous fish spermatozoa. Type 3 are the intermediate protamines, which contain lysine and histidine amino acids as well as arginines and they occur in the spermatozoa of *Xenopus, Mytilus* and others. Type 4 are the somatic-like histones retained in the spermatozoa of *Rana,* echinoderms and goldfish. Type 5 are unknown entities that are not basic proteins, found in the non-motile spermatozoa of crabs (Bloch, 1969).

Bony fish, cartilaginous fish, mammals and birds represent the various vertebrate groups that incorporate protamines. These proteins are small in molecular weight and arginine-rich. Cysteine residues occur in the keratinous protamines of eutherians, cartilaginous fish, and one species of marsupial (Retief et al., 1995a), but not in the protamines of birds (Chiva et al., 1987), reptiles and other marsupials (Balhorn, 1989). Despite these similarities, there appear to be several lines of evolution leading to the various protamines, for example, the protamines of bony fish are likely to have evolved separately to those of birds, and mammals. Amongst the mammals, the P2 protamine family is restricted to a few species, mainly rodents and primates, and differs significantly from the P1 family of protamines. Therefore, the categorisation of SNBPs according to Bloch (1969) is strictly according to their biochemical properties. The classification does not necessarily reflect the phylogenetic relationship of the sperm proteins. The following sections describe the characteristics of the various protamines in terms of their gene and amino acid sequences and their evolutionary associations with one another.

1.3.1. Protamine genes

Amongst eutherians, there exist two families of protamines called P1 and P2. The protamines of both families are keratinous and the genes code for up to

six cysteine amino acids. Unlike that of P1, however, the P2 gene also code for several histidine residues (Kleene et al., 1985).

Most mammalian genomes appear to have genes for the P1 protamine, but the distribution of the P2 gene is more limited and has only been found in humans, mice, guinea pigs, and stallions (McKay et al., 1986; Bellvé et al., 1988; Belaiche et al., 1987). However, the genomes of diverse eutherians, marsupials and the platypus, a monotreme, appear to contain sequences that hybridise to cDNAs that code for mouse protamine 1 and protamine 2 under low stringency conditions in Southern blots (Johnson et al., 1988b). The P1 and P2 probes used did not cross-hybridise under similar conditions. Therefore, the positive signals detected for the various species could not be due to exclusive hybridisation to stretches of arginine codons. The hybridisation signals of mouse P2 probes, although reproducible, were much weaker in the genomic DNA of human, boar, dog, bull, insectivorous bat, wallaby, and platypus compared to that in the rat and hamster (Johnson et al., 1988b). In the same study, no hybridisation signal has been detected for the stallion spermatozoa, however Pirhonen et al., (1990), have subsequently isolated two P2 variants and a single P1 protamine. Sequence analysis of the P2 variants in the stallion, indicates that not only is there a difference in the amino terminal length, but also in several amino acid residues present. The P2 variants may be coded by two homologous P2 genes which may have resulted from gene duplication followed by point mutations (Pirhonen et al., 1990).

Although P2 protamine is absent in the rat sperm, its mRNA is detected, albeit at a level of only 1-2% of that in the mouse (Bower et al., 1987). A genomic DNA fragment of protamine P2 from the rat demonstrates >90% nucleotide sequence homology with the mouse P2 (Tanhauser et al., 1989). The low expression of the P2 gene in the rat, may be due to an alteration in the regulatory sequences leading to reduced transcription of the P2 genes (Johnson et al., 1988a).

The cDNAs for the mouse P1 and P2 protamines share little homology and do not cross-hybridise (Johnson et al., 1988a). The mammalian P1 gene, contains a single intron (Kleene et al., 1985; Retief et al., 1995a) and in eutherians, the gene codes for six to nine cysteines. P1 and P2 mouse protamine genes are present on chromosome 16 as single copy genes (Hecht et al., 1986). They are transcribed only in the testis and are translationally regulated (Kleene et al., 1984). Northern hybridisation studies show that mRNAs for both genes are first detectable in round spermatids, the first haploid precursors. These stable and

very abundant mRNAs are stored for up to 8 days prior to translation in the elongating spermatids during which nuclear condensation occurs (Kleene et al., 1983).

PI protamine is synthesised as the mature protein (Kleene et al., 1985) whereas P2 is synthesised as a precursor protein (Elsevier, 1982; Yelick et al., 1987). The P2 precursor binds to the condensing DNA before subsequent post-translational processing into the mature P2 protein (Yelick et al., 1987). Cleavage at a His-Arg bond at positions 43-44 removes from the precursor, a 43-amino acid sequence at the amino terminus (Yelick et al., 1987).

1.3.2. Amino acid sequence of protamines

In *Osteichthyes* or bony fish, the protamines invariably contain a neutral amino-terminal residue which tends to be either a proline (24 out of 28 species) or an alanine (4 out of 28 species) (Oliva and Dixon, 1991). A tetra-arginine cluster follows the amino-terminal residue and all has a serine residue at position 9 or 10. This serine residue forms part of a di-serine or tri-serine motif in the protamine of many species from this group. At position 12, a proline is usually present followed by either a valine or isoleucine at position 13. A penta-arginine cluster then occurs. The carboxy-terminal portion is also well conserved with the consensus sequence being $PRVSR_6GGR_4$ (Oliva and Dixon, 1991).

In the rainbow trout, six protamines have been isolated and are grouped into three families, family-1, -2 and -3. There is, however, some uncertainty whether all rainbow trout contain the same six protamines (Christensen and Dixon 1982). There also appears to be some developmental regulation of the level of expression in particular protamines (Ling et al., 1971). Protamine 1a of rainbow trout has two fewer amino acids than protamine 2b due to loss of codons 6 or 7 and 22 or 23 (to remove one serine and one arginine residue respectively). Protamine 3a is different from the family-2 sequences because it has an apparent frame-shift in the centre of its sequence resulting in differences in the lengths of two arginine tracts (Iwai and Ando, 1967).

The two dogfish protamines Z1 and Z2 are similar in having a high lysine content (Berlot-Picard, et al., 1986). As in all other protamines, they contain clusters of positive residues separated by neutral amino acids. The cysteines are evenly spaced along the molecule, similar to those of the eutherian P1 protamine (Berlot-Picard, et al., 1986).

Protamine 1 of eutherians, marsupials and birds (Balhorn 1989) shares a characteristic amino-terminal tetrapeptide sequence ARYR (alanine, arginine, tyrosine, arginine). One exception is the rabbit protamine (Ammer and Henschen, 1988), which has a valine at the first residue instead of alanine. This difference is unlikely to affect the overall nucleoprotamine structure as the amino acids have similar chemical properties. Following the ARYR tetrapeptide, is a conserved SRSR (serine, arginine, serine, arginine) sequence and a cluster of five to seven arginines. At position 8, there is either a serine or a threonine; both are polar hydroxyl amino acids susceptible to phosphorylation. The carboxy-terminus seems less conserved than the amino terminus. There are, however, certain identifiable trends such as the arginine clustering, the presence of valine at position 44, tyrosine at position 52, and the carboxy-terminal tyrosine.

There are also a number of cysteine residues in the P1 of eutherians and they occur between clusters of positive amino acids. Cysteine is generally lacking in the P1 of birds and marsupials (Chiva et al., 1987; Retief et al., 1995a; 1995b), and this may reflect a less crucial function of the cysteines compared to the conserved amino acid clusters. In one genus of marsupials, the planigales, the protamines appear to be contain cysteine residues. This occurrence, however, is likely be the result of convergent evolution of protamine 1 of the planigales to resemble that of eutherians (Retief et al., 1995a). Cysteines may participate in the final stabilisation of the already condensed nucleoprotamine, but are not involved in the actual condensation process.

P2 differs mainly from the mammalian-P1 or avian protamine family by the presence of histidines, replacing 25-30% of the arginines. In humans, protamine HP1 (P1 family) has only a single histidine residue compared to nine in HP2 (P2 family) and eight in HP3 (P2 family) (McKay et al., 1986). In the mouse, mP2 (P2 family) contains 13 histidines while mP1 (P1 family) lacks this amino acid. Although both contain high levels of arginine, the arginine residues of mP2 are scattered throughout the entire molecule and are not clustered in the central region of the protein as in P1 vertebrate protamines (Kleene et al., 1985). In both P1 and P2 protamines, the location of cysteine residues and their spacing along the molecules are very similar. It is likely that alignment of cysteine residues may be important for proper interaction, cross-linking, and deposition of mP1 and the mP2 precursor onto the DNA during nuclear condensation (Yelick et al., 1987). Cysteine, serine and glycine frequently separate the positive amino acid clusters in the protamine P2 molecule. As in P1, the motif SC (serine, cysteine) is

repeated three times. In addition, GC (glycine, cysteine) and T/YC (tyrosine, cysteine) usually split the positive amino acid clusters (McKay et al., 1986).

In primates and rodents, protamine P2 comprises 50-60% of the total protamine content (Hecht, 1989). Human P1 shares a 68.8% amino acid homology with that of mice and their respective P2 sequences share a 75.5% homology. However, comparison between P1 and P2 protamines reveal a lower homology. For example, in the mouse there is 56% homology between P1 and P2, and for human P1 and P2, there is a 56.3% identity (Bellvé et al., 1988; McKay et al., 1986).

1.3.3. Evolution of protamines

The existence of multiple protamine variants makes it difficult to develop a formal molecular model for the evolutionary relationship of protamines. It remains unresolved whether these variants reflect a common origin or whether they are the result of convergent evolution to serve a common function. Although fish and mammalian protamines have similar chemical properties and are repetitive in terms of the distribution of arginines, there is no apparent conserved amino acid sequence to show that they share a common predecessor. Similarly, this situation applies to the P1 and P2 protamines. By contrast, the avian and mammalian P1 protamines appear to share a common ancestor. There may be two major evolutionary lines for protamines; the first describes for that of fish and the second, for the protamines of mammals, birds and possibly reptiles.

1.3.3.1. Bony fish

The *Osteichthyes* are a vertebrate group that incorporates a range of proteins from histone-like to arginine-rich protamines in the mature sperm and offers an interesting insight into the evolution and function of these sperm nuclear basic proteins.

All protamines including those of fish have a core element that is arginine-rich. This has led to the suggestion that an ancestral "basic pentapeptide core" ARRRR, may have evolved into fish protamines through successive partial gene duplications and a few amino acid mutations (Krawetz and Dixon, 1988).

There are two hypotheses for the origin of the basic pentapeptide core. The first hypothesis suggests that protamines may have evolved from a histone or a histone-like protein (von Holt et al., 1984) and has stemmed from studies of SNBPs from echinoderms. In the echinoderms, the sperm basic proteins consist of histones (type H) and in some cases, highly specialised or sperm-specific histone H1 and H2B variants, such as types H+H1 and H+A. The N-terminal regions of these histone variants differ from their somatic counterparts due primarily to the presence of repetitive tetrapeptides (von Holt et al., 1984). The consensus sequence of the tetrapeptide is Ser-Pro-basic-basic, known as the SPKK motif, where the basic residue could either be lysine or arginine (Poccia, 1991; Poccia and Green, 1992). It is conceivable that protamines could be an assembly of tetra-or pentapeptides that resemble the clusters of amino acids

within the echinoderm sperm variants of histone H1 and H2B (von Holt et al., 1984). Accordingly, the evolutionary pathway for protamines could be described as stemming from histones (somatic-like) → specialised sperm histones (echinoderms) → protamines (fish).

A second hypothesis suggests that the basic repetitive unit could have an original and intrinsic function as a nuclear targeting sequence. Such a sequence is essential for transporting proteins from the cytoplasm to the nucleus. A consensus sequence may consist of a cluster of two basic residues, a spacer region, and a basic cluster consisting at least three basic amino acids (Dingwall and Laskey, 1991; Hanover 1992). Some of these basic clusters are similar to those proposed by Krawetz et al., (1987).

The divergence between protamines and histones may have occurred several times during the evolution of the bony fish. Although the relative frequency of this divergence is quite significant between orders, it is remarkably small during the differentiation of genera and species (intrafamily variation) and during the differentiation of families (interfamily variation) (Saperas et al., 1993). A model by Saperas et al., 1994, suggests that the origin of protamines in fish is likely to be due to a retroviral transmission. The subsequent heterogeneous distribution of sperm basic proteins may be caused by either loss of expression of the protamine gene or loss of the gene itself such that histones become as prevalent as protamines in the bony fish sperm.

1.3.3.2 Mammalian and avian

In mammals and birds, the "basic pentapeptide core" Ala-Arg-Arg-Arg-Arg of protamines may have originated from one or more retroviral transmission events, and could have evolved into modern protamines through a series of duplications and some point mutations (Black and Dixon, 1967; Krawetz et al., 1987). This hypothesis is partly supported by protamine sequences from trout, bull, and mouse that demonstrate homology to certain viral arginine-rich core protein sequences (Krawetz and Dixon, 1988; Jankowski et al., 1986).

Evidence to support a duplication mechanism comes from the presence of an oligonucleotide stretch that occurs in multiple copies in both chicken and mammalian P1 genes. This oligonucleotide sequence contains an overlap of the actual termination codon with a sequence that codes for an additional arginine cluster (Oliva et al., 1989). Another possible view, however, is that the modern

chicken protamine gene might have evolved from a longer avian protamine sequence through the mutation of an arginine codon (CGA) to a termination codon (TGA) (Oliva et al., 1989).

In the protamine P2 gene, the 5' precursor segment shares substantial nucleotide sequence homology with a segment of the Epstein-Barr viral genome. This observation suggests that the P2 ancestral gene may have originated from the integration of the viral sequence into an ancestral P1-like gene (Krawetz and Dixon, 1988). In addition, a 94-bp sequence at the 3'-untranslated region of the human P2 protamine gene is thought to have been duplicated with minimal sequence deviation (Oliva et al., 1989).

The eutherian and bird protamine gene lines may have diversified following species differentiation, perhaps around 300 million years ago (Oliva and Dixon, 1990). Diversification of protamines may have occurred through either the appearance of cysteine residues in the mammalian protamines or the loss of cysteines in those of birds. Since marsupials which separated from eutherians about 150 million years ago, do not generally have cysteine residues in the protamines, it is likely that these residues have evolved separately in the eutherian protamines. A possible mechanism is the mutation from a CGC or CGT arginine codon to the TGC and TGT codons for cysteine present in the modern eutherian protamines (Oliva and Dixon, 1990).

1.4. CHROMATIN STRUCTURES

The term chromatin used within the context of this thesis means the large scale packaging of DNA by proteins that are usually histones in somatic cells and SNBPs in spermatozoa of eukaryotes. The resultant DNA-protein complex economises the nuclear volume required to contain the genome which measures approximately one metre in the fully extended DNA. The level of DNA compaction in spermatozoa is almost six times higher compared to DNA in mitotic chromosomes (Ward and Coffey, 1991).

1.4.1. Nucleohistones

1.4.1.1. Somatic cell nucleohistones

The bulk of DNA in most eukaryotic cells is organised into nucleosomes at a first level chromatin folding (Finch and Klug, 1976). Approximately 146 bp of DNA wraps around a histone octet in a linear beads-on-a-string 11 nm nucleosomal filament. The histone cores do not bind randomly to the DNA, but are positioned preferentially at certain locations (Wolffe, 1994; Englander and Howard, 1995). For example, regions rich in A-T base pairs have naturally narrow minor grooves and wide major grooves in the DNA helix and are ideally suited to contact the nucleosome core. This is because the tight wrapping of the DNA around the protein core requires compression of the minor grooves and this is facilitated by clusters of two or three A-T base pairs (Wolffe, 1994).

Linear arrays of the 11 nm nucleosomes appear to be further coiled into 30 nm fibres often observed by electron microscopy (Finch and Klug, 1976). Earlier symmetrical models of higher chromatin structures such as the 30 nm solenoidal coils, assume that the length of the linker DNA is invariant and thus results in regular conformations. It is however, widely accepted that the internucleosomal linker length is not constant, but varies about a mean value (van Holde, 1988; Leonardson and Levy, 1989). The length of linker DNA and the pitch of the DNA helix are important determinants of the chromatin structures that may result from nucleosomal folding (Widom, 1992). When an appropriate variation in linker length is taken into consideration in computer simulations of chromatin folding, the outcomes are irregular 'fibres' (Woodcock et al., 1993). These simulated folding patterns correspond closely to *in situ* and *in vitro* observations

of non-symmetrical fibres (Leuba et al., 1994) resolved from scanning force microscopy.

In somatic cells, nucleosomal fibres of both interphase chromatin (Vogelstein, 1980; Lebkowski and Laemmli, 1982) and metaphase chromosomes (Lewis and Laemmli, 1982) are organised into loops. Non-histone proteins of the nuclear matrix (Vogelstein et al., 1980) and the metaphase scaffold (Lewis and Laemmli, 1982) confer topological constraints to each loop which forms an independent domain of supercoiling (Cook and Brazell, 1976). The DNA attached to the matrix appears to be sequence-specific and occurs at specific sites (Mirkovitch et al., 1987; Cockerill and Garrard, 1986). These attachment sites relate to gene function and contain replication origins (Vaughn et al., 1990; Pardoll et al., 1980) and active genes (Mirkovitch et al., 1987; Cockerill and Garrard, 1986).

1.4.1.2. Spermatozoa nucleohistones

There two main circumstances under which nucleohistones occur in the spermatozoa. In the first case, histones are the exclusive basic proteins that interact with DNA such as in the spermatozoa nuclei from echinoderms (Brandt et al., 1979; Poccia and Green, 1992) and some species of fish (Muñoz-Guerra et al., 1982). In the second group, histones comprise a small percentage of the basic nuclear proteins, the majority consisting of protamines or protamine-like proteins such as in the spermatozoa of bivalve molluscs (Ausio, 1986; Olivares et al., 1986) and in some eutherians (Moss et al., 1989; Gatewood et al., 1987; Gusse et al., 1986).

Nucleohistone structures of the spermatozoa from the mature sea urchin, *Arbacia lixula,* have been well studied in the past. Each core nucleosomes consists of 146 base pairs of DNA and an octamer of histone proteins (H2A-H2B-H3-H4) (Brandt et al., 1979). There are, however, several significant differences in the spermatozoa chromatin from the somatic counterpart. The spermatozoa nucleosomal structures contain 100-110 base pairs of linker DNA, and these 'repeats' are the longest ever reported. The sea urchin spermatozoa histones (Sp H1 and Sp H2B) are restricted to the male germ line and are larger than their somatic equivalents. The amino-terminal regions of Sp H1 and Sp H2B contain a set of tandemly repeated, basic, tetrapeptide elements with two basic residues flanking the Serine-Proline residues ('SPKK' motifs). The spermatozoon chromatin is exceptionally stable to thermal or ionic denaturation. Its chromatin

is also more resistant to linker digestion by micrococcal nuclease and more densely packed compared to mitotic chromosomes (Poccia and Green, 1992).

However, not all spermatozoa nucleohistones are specialised such as those of *A lixula*. For example, in the goldfish *C auratus*, the five histones present in the spermatozoa nuclei, H1, H2A, H2B, H3 and H4, are no different biochemically from the somatic histone counterparts (Muñoz-Guerra et al., 1982). The length of the chromatin repeats (205 bp) is shorter than that in the spermatozoa of the echinoderm, *A lixula* (241 bp). The variability in the length of these repeats is attributed to differences in the content of basic residues such as lysine and arginine in the histones, in particular that of histone H1. Consequently, although the length of the nucleosomal repeats is consistently 146 bp long, the linker length is variable and range from 110 bp in *A lixula* to 56 bp in *C auratus*.

Within the spermatozoa of humans, histone H1 is absent and of the other histones, H2A and H4 are in the acetylated forms (Gatewood et al., 1990). Acetylation of histones is a post-translational mechanism that causes a relaxation in the protein-DNA bonds and has a role in facilitating histone removal from the chromatin. The histones from the mature spermatozoa of humans may therefore be residual from the testicular variety that undergo post-translational changes during the period of nucleohistone-nucleoprotamine transition.

1.4.2. Nucleoprotamines

Balhorn in 1982, proposed a model for DNA-protamine interaction which has since been widely accepted. In the model, the central polyarginine segment of protamines binds to DNA such that each arginine residue neutralises a negative charge on the phosphodiester backbone of DNA. Each turn of the DNA double helix accommodates an individual protamine molecule. In eutherians, protamines are cross-linked around DNA by inter- and intraprotamine disulphide bridges that form at the C- and N-terminal ends of the molecule. Balhorn (1982) suggests that the DNA-protamine complex may align linearly along the length of the nucleus to produce a compact chromatin structure.

Two separate studies, however, indicate that nucleoprotamines may have tertiary coiled structures. Firstly, linear dichroism measurements of native chromatin from equine sperm, reveal that the DNA helix axis is perpendicular to the fibre length (Sipski and Wagner, 1977). This suggests that DNA-protamine complex may coil into superhelical structures and is not arranged in a linear

complex may coil into superhelical structures and is not arranged in a linear mode. Secondly, recent atomic force microscopical (AFM) studies demonstrate the existence of 60-100 nm nodules in the chromatin of both bull and mouse spermatozoa (Allen et al., 1993). These results, therefore, suggest that the nucleoprotamine complex folds into larger fibres that contain higher order sub-spherical units of an average of 70 nm in diameter. On the basis of computer simulation results, Hud et al., (1993) proposed that the basic packaging unit of nucleoprotamines may be a toroid (sphere with a central indentation or doughnut shape), and this may account for the variation in size of the AFM chromatin nodules. These spherical units or toroids may further align in either a linear (Koehler et al., 1983) or random array.

Chromatin fibres composed of spherical units are topologically constrained in loop domains by anchorage to both the nuclear matrix and the nuclear annulus (Ward et al., 1989; Ward, 1993). The latter structure abuts the internal nuclear membrane and occurs at the implantation fossa in hamster spermatozoa. The nuclear annulus anchors a small percentage of DNA that forms mini-loops of approximately 5 to 10 kb in length (Ward and Coffey, 1989). The rest of the genome radiates outwards from the annulus and adheres to the nuclear matrix. From the matrix, the DNA forms larger loops of about 46 kb long (Ward et al., 1989). Southern blot hybridisation studies show that probes made from genes isolated from both matrix attachment sites and the outer loops associate exclusively with their respective regions of isolation (Ward and Coffey, 1990). Therefore, it is possible that genes are spatially organised and have specific locations within spermatozoa nuclei.

1.4.2.1. Spermatozoa localisation of DNA sequences

In many cases, the localisation of genes and especially DNA repeat sequences within spermatozoa nuclei is contradictory in the published literature.

In the spermatozoa of a salamander (*Plethodontid cinereus*), *in situ* hybridisation studies using tritiated satellite RNA as probes, showed that the centromeres cluster at the base of the nucleus. Tritiated ribosomal RNA probes localised the ribosomal genes to a region anterior to the centromere cluster in the caudal half of the nucleus (Macgregor and Walker, 1973). The ribosomal RNA probes used are known to anneal specifically to the nucleolar organisers which are located at two loci near the centromeres in the chromosomes of *P cinereus*. These observations indicate that the nucleolar organisers are compacted into a

relatively short length of the nucleus and that in *P cinereus* they are located near to the cluster of centromeres. A model for the *Plethodontid* sperm nucleus suggests that the chromosomes organise into a U formation with the centromeres at the caudal end, and the chromosomal arms aligned along the long axis of the nucleus.

The nuclei of fresh *Plethodontid* sperm examined between crossed polaroids revealed a negative birefringence with respect to length which is likely to reflect a lengthwise orientation of nucleoprotein fibres. However, the authors could not reconcile this type of orientation with the granular condensation of the nucleoprotein, nor does the orientation reconcile with the scheme in which each chromosome arm extends forwards no further than the length of the spermatid nucleus and does not double back on itself. They conclude that the "chromatin fibres in all the chromosomes' arms must be extensively coiled, folded, or bunched and are yet aligned along the length of the sperm nucleus" (Macgregor and Walker, 1973).

In the rat, Moens and Pearlman (1989), using *in situ* hybridisation of biotinylated rat satellite DNA probes, showed that there is no specific distribution of centromeric DNA in the sperm nuclei. This is supported by immunofluorescence studies by Palmer et al., (1990) who showed that whole CREST[1] antisera localised to mature bovine spermatozoa in dispersed foci. To identify the centromeric protein detected by the antisera, immunoblotting of nuclear proteins resolved on SDS-polyacrylamide gels was carried out. These experiments showed that CENP-A and not CENP-B is present in the bull sperm head. CENP-A appears quantitatively retained in discrete foci in bull sperm nuclei but without a clear pattern of distribution.

In contrast, similar studies in bovine and murine sperm (Powell et al., 1992), revealed preferential localisation of centromeric DNA to the posterior region of the head, and predominantly on the dorsal side (convex surface underlying the acrosomal crescent).

Zalensky et al., (1995), using *in situ* hybridisation of biotinylated α-satellite (centromeric DNA) probes and three-dimensional reconstructions of confocal images, showed that all 23 centromeres cluster into a compact chromocenter

[1] Apart from histones, other somatic cell proteins that have been identified in spermatozoa include a class of proteins which organizes the centromeric regions of chromosomes. The antisera used came from patients with CREST scleroderma (Guldner et al., 1984; Earnshaw et al., 1984; 1985). CENP-A, CENP-B and CENP-C are the human CREST antoantigens with Mw of 17000, 80 000, and 140 000, respectively (Earnshaw and Rothfield 1985).

positioned within the interior of the nucleus of the human spermatozoon. The consensus telomeric repeat (TTAGGG)n used to probe the sperm nuclei showed that the telomeric ends of the chromosomes are localised to the periphery of the sperm nuclei. Localisation of unique subtelomeric sequences of the p and q arms of chromosome 3 indicates that the telomere sequences of the chromosome arms occur as dimers at the nuclear periphery.

The results of both the centromere and telomere studies by Zalensky et al., (1995) suggest that the chromosomes in the human sperm nucleus form a hairpin-like configuration by looping from the periphery to the interior and back to the periphery.

The discrepancy between the localities of centromeric proteins and DNA discussed above may be due to differences in the sample preparations. For example, 0.2 M NaCl, 2.5 M urea, and 10 mM dithiothreitol were used by Palmer et al., (1990) to decondense the bovine sperm heads, whereas, sonication and partial decondensation with 2-mercaptoethanol and 0.1-0.2 mg/ml trypsin have been used in the *in situ* hybridisation studies by Powell et al., (1992). In addition, the specificity of the probes and antibodies used to localise the anticipated target may not be accurate. The rat satellite DNA I probe used by Moens and Pearlman, (1989) labelled centromeres and telomeres of many chromosomes as well as some interstitial regions (Sealy et al., 1981). Similarly, a 93-amino acid COOH-terminal domain of the 140 amino acid CENP-A polypeptides share a 62% identity with the nucleosomal core protein, histone H3 (Sullivan et al., 1994).

Zalensky et al., (1995) used a relatively gentle method of spermatozoa nuclei preparation for *in situ* hybridisation that preserved the shape of the spermatozoa. In contrast to the previous two-dimensional images obtained from fluorescence microscopy, they have reconstructed three-dimensional images using confocal optical sections. The added depth of view has allowed the deduction of the DNA sequence location in three-dimensional space within spermatozoa nuclei.

1.5. TRANSFORMATIONS OF SPERMATOZOA CHROMATIN

1.5.1. Nucleohistone-nucleoprotamine transition during spermatogenesis

The chromatin of spermatogonia, spermatocytes, and round spermatids consists of the nucleosomal structure such as found in chromatin of somatic cells. During spermiogenesis this structure becomes lost in most species and is replaced by a highly compact, genetically inactive, nucleoprotamine complex.

Nuclear condensation during spermiogenesis studied at the ultrastructural level in various organisms indicate that there is great interspecific variability. The chromatin may align into fibres and then gradually condense, as in the pond snail *Cipangopaludina* (Yasuzumi and Tanaka, 1985). In *Nucella lapillus*, the dog whelk, chromatin fibres condense into sheets which subsequently fuse (Walker and Macgregor, 1968). In most eutherians, however, the fibres coalesce into a homogenous mass, as in *Felis domestica* (Burgos and Fawcett, 1955).

Sperm nuclear condensation in mammals (Balhorn, 1989), birds (Nakano, 1976) and reptiles (Kasinsky, 1987) is accompanied by the replacement of histones with protamines (Fig. 1.2). Several processes have been implicated in a sequential and regulated mechanism to coordinate histone removal and subsequent repackaging of DNA into nucleoprotamines under physiological ionic conditions.

During spermiogenesis, histone acetylation, especially the hyperacetylation of H4, induces a localised decondensation of chromatin which aids in the displacement of histones (Christensen et al., 1984). Topoisomerase activity induces local nicks in the DNA and this changes the topology of DNA by removing the negative supercoils associated with nucleosomes (Risley et al., 1986; McPherson and Longo, 1993). Transition proteins precede the actual binding of protamine molecules and disappear from the chromatin during spermatid maturation in the testis (Balhorn et al., 1984). These proteins may represent a form of precursor protamine and/or have a role in facilitating protamine deposition onto DNA (Balhorn et al., 1984).

During the incorporation of protamines, the chromatin begins condensation into the nucleoprotamine configuration. The final step is the dephosphorylation of protamines that are phosphorylated at the time of initial

binding to the DNA. The process of phosphorylation-dephosphorylation facilitates the binding of protamines to DNA and is mediated through the primary hydroxyl group of serine and threonine (Marushige et al., 1969). It is speculated that upon phosphorylation, serine and threonine which are susceptible to phosphorylation, acquire additional negative charges from the phosphates. The phosphorylated amino acids can then form electrostatic links with neighbouring cationic amino acids and therefore function like disulphide bonds. In birds, serine or threonine residues seem to occur at the cysteine positions in eutherian protamines (Oliva and Dixon, 1990).

The process of nucleohistone-nucleoprotamine transition occurs only after the spermatid has adopted its characteristic head shape and hence is independent of nuclear flattening (Fig. 1.2) (Courtens et al., 1983). However, morphological changes of the chromatin from course fibres to a homogenous appearance are still evident during the incorporation of protamines which occurs in the nuclei of Step 12 spermatids in the mouse (Biggiogera et al., 1992) and ram (Courtens et al., 1983). Therefore, there appears to be a correlation between the condensing effect of protamines, and the morphological changes observed during protamine incorporation *in vivo*. During spermatozoa transit in the epididymidis of eutherian species, further cross-linking and stabilisation of the chromatin occur by the formation of inter- and intra-protamine disulphide bonds.

In vitro attempts to establish the transition from nucleohistone to nucleoprotamine structures have not been successful to date. This may be due to incomplete removal of the histones, and/or a different order in the removal of each class of histone from the *in vivo* situation (Marushige et al., 1978). The mechanism of exchange is not simply an electrostatic competition process, whereby the small and highly basic protamines have a stronger affinity for DNA and displace the histones competitively. *In vivo*, the mechanism is more complex; the least tightly bound histone, H1, is the last to be removed while the most tightly bound core histone, H4, is the first to be displaced (Christensen et al., 1984).

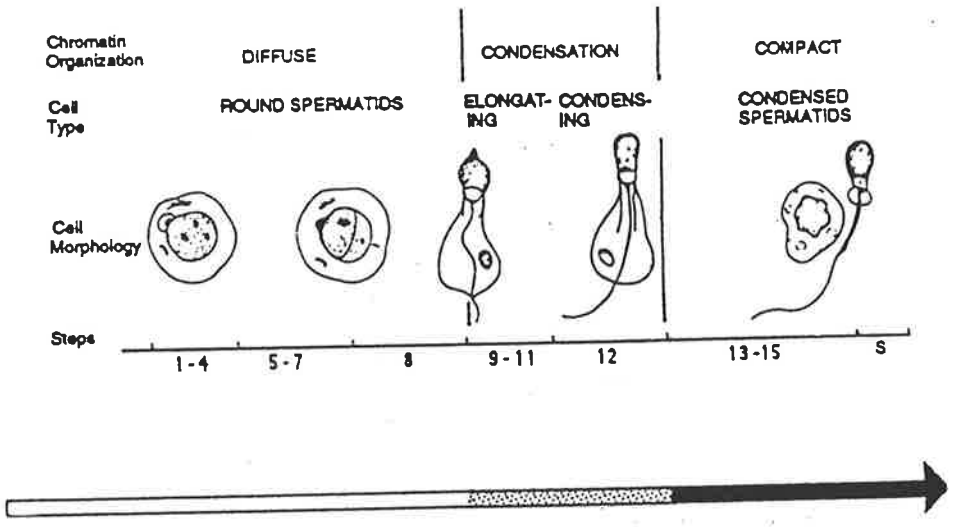

Fig. 1.2. Schematic representation of the changes that take place within the nucleus of the ram during spermiogenesis. The arrow indicates the transitional changes in the protein complement of the chromatin. Blank region of the arrow equates to the somatic histone complement, stippled region represents the transition proteins and the dark region represents the protamines (modified from Loir et al., 1985).

1.5.2. Methylation of spermatozoa DNA

Maternal and paternal genomic imprinting in mammals is a mechanism that generates differential expression of genes in relation to their parental origin. The molecular mechanism for this epigenetic inheritance is not well defined but should meet the following criteria: (1) the imprinting pattern should be transmitted through ensuing rounds of DNA replication, and (2) the imprint should be reversible during gametogenesis (Sapienza et al., 1989). Methylation of DNA at the cytosine residues appears to meet the requisites of both heritability and reversibility, and is considered a basis for imprinting (Razin et al., 1984).

In both the male (Mazo et al., 1994) and female germ cells (Driscoll and Migeon, 1990), a demethylation process occurs during meiosis. Demethylation of the DNA begins in meiotic cells and culminates in the haploid round spermatids which have the lowest level of methylation. During spermatid differentiation, *de*

novo methylation of specific genomic regions occurs which may promote differential imprinting of the paternal genome from the maternal genome.

One model which explains the selective methylation of DNA sequences suggests that steric hindrance by protein factors excludes the enzyme, DNA methyltransferase from binding to target DNA regions. In vertebrates, these regions consist of CpG islands where methylation by DNA methyltransferase occurs at the cytosine residue of the CpG dinucleotide (Razin et al., 1984). However, binding of the enzyme and hence, methylation of the CpG islands can be prevented by specific proteins that affix themselves to the same site.

In the mouse or hamster housekeeping gene, adenine phosphoribosyltransferase (aprt), the binding sites for a protein, Sp1, required to protect a flanking CpG island from *de novo* methylation, are located within the promoter (Macleod et al., 1994). *In vivo* footprinting studies using the island as a template show that three GC boxes clustered at the 5' edge of the CpG island are bound to proteins which are likely to be Sp1. In a transgenic mouse assay, deletion or mutagenesis of the Sp1 sites results in *de novo* methylation of the CpG island. This shows that the peripheral Sp1 sites are necessary to prevent methylation of the aprt island (Macleod et al., 1994).

A protein isolated from human spermatozoa nuclei called, sperm Alu binding protein (SABP), selectively protects Alu elements from methylation *in vitro* (Chesnokov and Schmid, 1995) and is consistent with the model suggested earlier. Alu sequences are short repeats that are widely distributed throughout the human genome and are unusually rich in CpG dinucleotides (Schmid and Maraia, 1992). Although they are entirely methylated in somatic tissue and oocytes, Alu repeats are hypomethylated in the male germ line (Schmid, 1991). This differential methylation may be pertinent to genomic imprinting in germ line cells or reflect differences in Alu transcriptional activity between these cell types.

In vitro essays show that the activity of SABP is specific to the Alu CpGs in preventing methylation and may explain the unmethylated state of Alu sequences in the male germ line (Chesnokov and Schmid, 1995). There are, however, some Alu sequences that are fully methylated. A hypothesis suggests that the heterogeneity in the methylation of Alu sequences may be explained by the presence of SABP in one of either the nucleoprotamine or nucleohistone compartment of sperm DNA (Chesnokov and Schmid, 1995). Alternatively, some

Alu sequences may have dysfunctional SABP binding sites that prevent the protein from binding to the sequence, and are consequently unable to protect the methylation of CpG islands.

1.5.3. Sperm nuclear decondensation in oocytes

In mammals, one of the first morphological events following spermatozoa incorporation into the oocyte is the disintegration of the sperm nuclear membrane. The perinuclear material then becomes dispersed in the ooplasm and the nucleus starts to decondense (Yanagimachi and Noda, 1970). In eutherians, nuclear decondensation requires the presence of reduced glutathione (GSH) which is synthesised by the mature oocyte (Calvin et al., 1986). GSH functions to reduce the disulphide bonds of protamines that stabilise the nucleoprotamine complex. Protamines are eventually removed from the nucleus by molecular chaperones (Dingwall and Laskey, 1991) such as nucleoplasmin.

In Xenopus oocytes, hyperphosphorylation of nucleoplasmin enables these molecules to compete successfully with DNA for the binding and subsequent removal of protamines (Ohsumi et al., 1995; Leno et al., 1996). On exposure to toad nucleoplasmin in vitro, protamines become removed from human spermatozoa resulting in the decondensation of the nucleus (Itoh et al., 1993). Although nucleoplasmin has not been isolated from eutherian oocytes, the male pronucleus growth factor (MPGF) required for the decondensation of the spermatozoa nucleus has been implicated to have a similar function to nucleoplasmin (Thibault and Gerard, 1973; Yanagimachi, 1994). Following the removal of protamines, there is a period where sperm DNA is bound to neither protamines nor histones. The naked DNA then binds to histones that are abundant in the ooplasm and the chromatin subsequently develops into the pronucleus.

The ovulated oocyte which is arrested at second meiotic metaphase becomes activated upon sperm-egg binding, and eventually completes meiosis. Both spermatozoa and egg nuclei compete for the pronucleus formative material (PFM) (Austin and Braden, 1955). In the mouse, the male pronucleus has a much greater affinity for PFM than the egg pronucleus, resulting in a larger pronucleus of the sperm compared to that of the egg (Austin and Walton, 1960).

Approximately 8 h following fertilisation in the mouse, both male and female pronuclei begins DNA synthesis (Howlett and Bolton, 1985). In the mouse,

maternal control of DNA transcription is relinquished to the zygote during the early or mid-two-cell stage. Pronuclear eggs also synthesise proteins using stored mRNAs and these proteins are thought to have a role in initiating mitosis (Howlett, 1986).

The sperm and oocyte pronuclei migrate to the center of the oocyte aided by the cytoskeletal machinery such as actin (Karasiewicz and Soltynska, 1985) and microtubules (Maro et al., 1986). The pronuclei approach one another, and at close proximity, form complex processes that eventually interdigitate. Vesiculation of the pronuclear envelope occurs followed by the disappearance of the membranes and formation of mitotic spindles in preparation for cell division (Longo, 1973).

1.6. CONSEQUENCES OF SPERMATOZOA NUCLEAR PACKAGING

Protamines, unlike histones, do not appear to have any specific roles in gene activity. The variability in the types of protamine expressed and the high divergence of the amino acid sequences may suggest a role in DNA condensation rather than involvement in specific gene functions. These conjectures have been recently supported by transgenic mouse studies that showed undiminished fertility rates in mice that express *gallus* protamine (galline) transgenes (Rhim et al., 1995). This elegant study indicates that DNA interacts indiscriminately with mouse protamines and galline, which is however, not that surprising given the very basic (positively charged) nature of all protamine types.

It is, however, premature to rule out the significance of protamines in determining functional chromatin structures in view of the determination that the spermatozoa of infertile men have abnormal protamine ratios with selective absence of certain protamine subtypes, in particular those from the protamine 2 family (Balhorn et al., 1988; Belokopytova et al., 1993; DeYebra et al., 1993). In addition, the two mouse protamines Prm 1 and Prm 2 have been shown to bind DNA in approximately 1:2 stoichiometry, a ratio that persists in transgenic mice that have over threefold increase in expression of Prm 1 protein (Peschon et al., 1987). This observation implies that the two protamines are assembled into chromatin in a very specific manner. Transgenic studies that aim to diminish the ratios or amounts of protamines subtypes, are required to carefully screen the various possibilities of the roles that protamines may have in causing male infertility.

Abnormal spermatozoa chromatin may cause embryonic genetic defects, which are the most prevalent contributor to early spontaneous abortion (Wilcox et al., 1988). Chromatin structural abnormalities have been found in the spermatozoa of infertile males in several eutherian species including humans (Wilcox et al., 1988; Jager 1990; Evenson et al., 1994). It is however, uncertain whether abnormal chromatin is a direct cause of infertility or embryonic defects. It is difficult to gauge the level of disruption to mouse spermatozoa chromatin caused by transgenic *gallus* protamines constructed by Rhim et al., (1995), for example, there is no evidence to suggest that the spatial distribution of DNA has been either altered or preserved. The consequences of abnormal chromatin structure in spermatozoa function in terms of DNA configuration and organisation, remain to be determined.

The study of spermatozoa chromatin would be incomplete unless more is known about the structural organisation of DNA in spermatozoa. This is important in view of recent in situ hybridisation studies by Zalensky et al., (1995) that demonstrate precise location of telomeric and centromeric DNA in the nuclei of human spermatozoa. The observations suggest that the nucleus may be spatially organised and may thus have important consequences in the manner in which spermatozoa DNA later translates into genetically active chromatin in the zygote (Zalensky et al., 1995). It remains to be seen whether disruption in the ordered distribution of DNA in spermatozoa is linked in any way to male infertility and/or embryonic abnormalities.

Studies on spermatozoa chromatin remain at an incipient stage even though there is a wealth of knowledge about the amino acid and gene sequences of the packaging proteins. This is partly due to difficulties associated with studying a highly condensed nucleus. There are still many gaps in the science of spermatozoa chromatin structure. Some further questions that remain to be answered include (1) what are the evolutionary history and consequences of the different protamine types? (2) how does DNA interact with protamines? (3) do specific DNA sequences influence the organisation of the genome in spermatozoa? (4) how does spermatozoa chromatin structure influence the imprinting of the male eukaryotic genome? (5) what is the link between spermatozoa nuclear basic proteins including sperm-specific histones, and male infertility?

1.7. SUMMARY

In vertebrates, the transformation of the germ cell into a specialised male gamete involves fundamental chromatin changes such as the formation of the haploid genome during meiosis, elimination of imprinting and the development of a new imprinted genome, and the removal of somatic cell packaging proteins (histones) and their replacement with the smaller molecular weight protamines. Although these processes are highly complex dynamic systems, much can be learnt from the final existing structure that can help us understand the underlying mechanisms that drive each system and identify how they relate to one another. For example, the specific localisation of telomeres and centromeres and the identification of loop domains, indicate some level of DNA spatial organisation in spermatozoa. This may be the consequence of an ordered mechanism of DNA condensation that is partly reliant upon the architecture of the nuclear matrix.

A major change in the chromatin that takes effect during DNA condensation is the replacement of a set of histones with protamines. The mechanism appears to preserve the topology of the chromatin as deduced from structural studies of higher order chromatin organisation. However, at the primary level of DNA-protein interaction, there is a vast difference between nucleohistones and nucleoprotamines. The former occurs in the form of nucleosomes where DNA winds in approximately 1.7 turns around a histone octamer, whereas protamines may bind to either the major or minor groove of the DNA molecule. There are, however, some similarities between nucleohistone and nucleoprotamine higher order structures. For example, the primary fibres of both chromatin types are likely to fold into larger fibres that are approximately 30 nm for nucleohistones, at least in extracted chromatin, and 50-100 nm for nucleoprotamines. In addition, the anchorage of DNA to the nuclear matrix, the formation of DNA loops and the specific location of DNA sequences are common for both somatic and sperm cell nuclei.

A fraction of Alu repeats in humans remain unmethylated in spermatozoa. Methylation appears to be dependent on the accessibility of chromatin to specific DNA-binding proteins that protect the DNA from methyltransferase enzymes. A point of speculation is whether the hypomethylated and hypermethylated Alu sequences may belong to different structural fractions of spermatozoa chromatin such as nucleohistones and nucleoprotamines.

In addition, the primary structures or the amino acid sequences of protamines and histones have given insight into the evolution of protamines which stemmed from retroviral transmission and duplication events. This, however, begs further questions on why protamines have evolved, what their function is and how their evolution relates to genome size and metabolic rates of individual species.

Although much is known about the amino acid and gene sequences of protamines there is either a great paucity or confusion of data in relation to chromatin organisation in spermatozoa that include: (1) physical data such as those obtained from X-ray crystallographic studies on DNA-protamine interactions, (2) the relative distribution of the different protamines (for example P1 and P2) as well as histones in the mature spermatozoa nuclei, (3) the localisation of specific DNA sequences such as telomeres, centromeres and single-copy genes in the spermatozoa nuclei.

Chapter 2. RESEARCH PROJECT

2.1. INTRODUCTION

The theme of this project is on the chromatin organisation of *Sminthopsis crassicaudata,* an Australian marsupial which belongs to the family, Dasyuridae. The spermatozoa of species from Dasyuridae and Peramelidae, contain two distinct regions in the nucleus (Sapsford et al., 1969; Harding et al., 1982; Breed et al., 1989). This peculiarity is especially prominent in the dasyurids where the sperm nucleus comprises a central region with a homogeneous electron-dense appearance (C1), and a peripheral region that appears deeply grooved or indented (C2) (Breed et al., 1994).

We have previously shown that these two nuclear regions have a different substructural organisation (Breed et al., 1994). In addition, the C2 region appears faintly fluorescent when stained with DNA fluorochromes such as DAPI, ethidium bromide or propidium iodide, whereas the C1 region is brightly fluorescent and it has thus, been unclear whether DNA is present within the C2 region.

In some other species of mammals, the spermatozoon nucleus is also not completely electron-dense and homogenous. For example, in humans and the Asian rodent, *Bandicota*, there are numerous vacuoles with no fixed location, present within the mature sperm nucleus (Tanphaichitr et al., 1982; Breed, 1983). *Plethodontid* salamanders have an electron-opaque concentric lamellar structure located anteriorly in the mature spermatozoon (Macgregor and Walker, 1973). In another Urodele, *Notophthalmus viridescens* (Fawcett, 1970) a structure, called the nuclear "cote", surrounds the chromatin in the postacrosomal region and tapers to a thin rod anteriorly. The internal structure of the cote consists of minute tubular subunits packed in hexagonal array and the tubules align parallel to the long axis of the nucleus (Picheral, 1971). The composition of the cote may be proteinaceous. Its function however, is unknown.

Unlike that of the nuclear inclusion (cote) of the urodele species, the internal organisation of the peripheral indented (C2) nuclear region in the sperm of *Sminthopsis* cannot be resolved into any detailed structural organisation at

high magnification. At present, the composition and function of the C2 region is still unknown.

A further unusual aspect of the dasyurid caput epididymal spermatozoon is the presence of an expanded nuclear envelope (ENE) which surrounds the caudal extremity of the nucleus (Breed et al., 1994). Within the ENE, flocculent material and electron-dense inclusions are present. Although the occurrence of redundant nuclear envelope has been reported in the bandicoot (peramelid) sperm (Sapsford et al., 1969), the electron-dense inclusions appear to be unique to the dasyurids (Harding et al., 1982).

2.2. AIMS

This project aimed to determine the organisation of the chromatin in the spermatozoa nuclei of *Sminthopsis crassicaudata*. For this, a systematic series of investigations was carried out. These included (1) a study on the ultrastructure of spermiogenesis to determine the morphogenesis of nuclear condensation and to compare the timing of chromatin condensation in both nuclear regions, (2) a qualitative evaluation of the distribution of DNA within the nucleus including the electron-lucent areas surrounded by the ENE, (3) isolation of spermatozoa nuclear basic proteins (SNBPs) and, whenever possible, immunolocalisation of the SNBPs within the spermatozoa nuclei, (4) determination of the higher order chromatin structures using transmission electron microscopy (TEM) and atomic force microscopy (AFM), and (5) molecular cloning and localisation by fluorescence *in situ* hybridisation of DNA from the two chromatin fractions, (C1) and (C2).

2.3. ANIMALS

To avoid repetition in the following chapters, details on the sacrifice of animals and on how spermatozoa were obtained will be described below.

Sminthopsis crassicaudata (or fat-tailed dunnarts) were obtained in the years 1993 and 1994, from the Department of Genetics, University of Adelaide. In subsequent years, from 1995 to 1996, they were purchased from Department

of Animal Services, University of Adelaide. Adult *Sminthopsis crassicaudata* males (10 to 12 months old), were used in all studies and were sacrificed by peritoneal injection with sodium pentobarbitone (Nembutal, Boehringer) at a dose of 0.5 ml/kg body weight.

All animals were caged in a room with a lighting regime of 16h of light and 8h of darkness. They were maintained on a diet of cat food supplemented with mealy worms, and water *ad libitum* (Bennett et al., 1990).

Chapter 3. ULTRASTRUCTURE OF NUCLEAR CONDENSATION AND LOCALISATION OF DNA AND PROTEINS[2]

3.1. INTRODUCTION

As described in Chapter 2, the spermatozoa of *Sminthopsis* have two distinct nuclear regions; one which has a homogeneous and amorphous appearance (C1), and the other which occurs at the periphery and has deep grooves or fissures (C2). In addition, there is an expanded nuclear envelope (ENE) in caput epididymal spermatozoa which eventually disappears in the cauda epididymidis, indicating that further development of the sperm nucleus may occur during epididymal transit.

The aim of this investigation was to determine, by ultrastructural studies, the morphogenesis of the nucleus during spermiogenesis, and whether DNA condensation continues within the epididymis. The presence or absence of DNA and protein within the two nuclear regions and within the ENE was investigated using (1) DNAase-gold labelling (Zini et al., 1989), and (2) cytochemical staining for lysine-rich proteins (Courtens and Loir, 1981a).

---

[2]This chapter has been published as a paper in Mol Reprod Dev 43:217-227 (1995).

3.2. MATERIALS AND METHODS

3.2.1. Transmission electron microscopy

Testes from a total of six mature *Sminthopsis crassicaudata* males were cut into 1-3 mm^3 cubes and fixed for 4-8 h. Each epididymidis was divided into five segments from the (1) caput, (2) junction of caput and corpus, (3) corpus, (4) junction of corpus and cauda, and, (5) cauda. The segments were then cut into small cubes and fixed with 3% glutaraldehyde (Appendix 2) for 4-8 h and prepared for transmission electron microscopy (TEM) (Appendix 3A and B).

3.2.2. Staining of lysine residues

Tissues from the epididymis and testis were obtained from four male *Sminthopsis* and cut into small pieces (1-3 mm^3). They were fixed for 4 hr at 20°C in 3% glutaraldehyde and dehydrated by passing through a graded series of ethanol. The tissues were then *en bloc* stained with 3% phosphotungstic acid in absolute ethanol for 16 hr (Courtens and Loir, 1981a), washed in ethanol and embedded in Spurr's resin. Ultrathin sections were observed without counterstaining.

3.2.3. DNAase-gold labelling

For DNAase-gold staining, epididymal and testicular tissues (1-3 mm^3) were fixed for 4 h in 0.25% glutaraldehyde (Appendix 2) and processed as described in Appendix 3C. The tissues were placed in gelatin capsules which were filled with LRWhite resin and capped. The resin was polymerised by incubating in the oven at 50°C for 48 h. Ultrathin sections were cut and placed on nickel grids. The sections were washed twice in PBS, blocked with 0.5% ovalbumin (Sigma) (Appendix 1) and washed again in PBS. To label the tissues, the grids were placed on drops of 10μg/ml DNAase-gold conjugates (10nm, ICN Biochemicals Icn., Aurora, Ohio) for 45 min, and washed in PBS followed by distilled water (Zini et al., 1989). The sections were finally stained with 2% uranyl acetate in water for 30 s, and 2% lead citrate for 1 min before visualization with the TEM. The specificity of labelling was determined by incubating DNAase-gold with 1mg/ml of the appropriate substrate DNA type I (from calf thymus, Sigma, St. Louis) before testing on tissue sections as above.

3.3. RESULTS

3.3.1. Steps of spermiogenesis in *Sminthopsis crassicaudata*

Spermiogenesis of *Sminthopsis* can be divided into 15 arbitrary steps based upon ultrastructural observations of spermatid differentiation. A summary of the steps is given below:

Step 1. The Golgi complex surrounds the acrosomal vacuole which lies close to the nucleus of the round spermatid.

Step 2. The acrosomal vacuole fuses with the nuclear envelope causing an indentation on the nuclear surface.

Step 3-4. The acrosomal vacuole enlarges and spreads over the nuclear surface. The nucleus rotates within the cytoplasm to orient the acrosome toward the basement membrane of the seminiferous tubule.

Step 5. The nucleus begins to protrude anteriorly as the acrosomal vacuole collapses. The basal plate of the implantation fossa and microtubules of the manchette become visible.

Step 6. A nuclear socket is present at the abacrosomal pole of the nucleus. Microtubules of the manchette insert into the nuclear rings and surround the nucleus extensively. Sertoli cell spurs are prominent at the periphery of the acrosome.

Step 7. The nucleus flattens so that its long axis lies perpendicular to that of the sperm tail. Chromatin condensation proceeds dorso-ventrally. The condensing chromatin appears granular and becomes increasingly electron-dense. The acrosome at this stage is finely granular and moderately electron-dense. Mitochondria accumulate within the cytoplasm just above the acrosome.

Step 8. The spermatid nucleus tapers caudally but the apical region continues to condense. The chromatin appears finely granular. In the apical and caudal regions, the nuclear envelope encloses electron-lucent areas that contain flocculent material.

Step 9. The spermatid rotates and the apical region of the sperm head becomes tapered. A subacrosomal space occurs above the dorsal surface of the sperm nucleus.

Step 10. The spermatid nucleus attains its distinctive spearhead shape. The acrosome lies above the dorsal nuclear surface and tapers into a thin segment caudally but folds upwards apically. Mitochondria migrate to the mid-piece of the sperm tail.

Step 11. An enlarged nuclear envelope is present around the caudal region of the nucleus. A layer of electron-dense material deposits on the surface of the C1 chromatin at the caudal extremity. This layer, the nuclear mantle, has an uneven surface at this stage. There is a cessation of nuclear condensation and mitochondria align at the mid-piece of the sperm tail. Microtubules of the manchette and the Sertoli cell spurs have become disorganised.

Step 12. The nuclear mantle region has acquired an even surface. The smooth surface of the condensed C1 chromatin becomes irregular as the C2 chromatin region begins to form.

Step 13. Development of the C2 region progresses with the aggregation of spherical chromatin bodies.

Step 14. The spermatid nucleus develops characteristic indentations in the apical region, and along the lateral and part of the ventral surface of the C1 chromatin. The spermatid head now lies perpendicular to the long axis of the tail.

Step 15. Some cytoplasm is discarded and phagocytosed by Sertoli cells but a cytoplasmic droplet remains around the neck of the spermatozoon. Spermiation occurs and testicular spermatozoa are released into the seminiferous tubule lumen.

3.3.2. Nuclear condensation

Steps 1 to 9 are similar to those described for other marsupial species (Sapsford et al., 1969; Harding et al., 1979). In *Sminthopsis*, Step 7 spermatids have begun to lose their uniform tetragonal shape to assume a more differentiated form and, by Step 10, they have attained the characteristic sperm head shape (Fig. 3.1A). By this time, the main nuclear region has a homogenous appearance and condensation of the C1 region appears complete. Nuclear spaces

at the apical and caudal regions are enclosed by the nuclear envelope and contain flocculent material (Figs. 3.1A and B). At the cauda of the nucleus, distal from the perinuclear ring, vesicles are present adjacent to the nuclear envelope (Fig. 3.1B). The spermatid has begun to shift the position of its head relative to the tail and mitochondria have started to migrate to the mid-piece of the tail (Fig. 3.1A).

In Step 11 spermatids, the nuclear envelope at the caudal nuclear region is greatly enlarged (Fig. 3.2A). Whorls of membranes are evident where the nuclear and plasma membranes converge near the distal acrosomal region. At this stage, mitochondria are aligned along the mid-piece of the tail (Fig. 3.2A).

In these spermatids, the C2 chromatin has not yet formed and at the apical region of the nucleus, the nuclear envelope surrounds an electron-lucent area (Figs. 3.2A and B). Strands of filamentous material intersect this space and connect the ventral surface of the C1 chromatin to the nuclear envelope. The dorsal surface of the C1 chromatin, however, is closely apposed to the nuclear envelope (Fig. 3.2B). At the cauda of the nucleus, spherical structures appear adjacent to the inner aspect of the expanded nuclear envelope (ENE). In addition, the tip of the condensed C1 chromatin is in contact with the ENE (Figs. 3.2A and C). A layer of material, the nuclear mantle, lies along the dorsal nuclear surface, posterior to the acrosome and appears to have an irregular surface (Fig. 3.2C).

In Step 12 spermatids, C2 chromatin has begun to form. Irregular regions of chromatin appear along the previously smooth surface of the C1 region in the lateral and ventral areas of the nucleus (Figs. 3.3 and 3.4). In Step 13 spermatids, the numerous globular structures that appear in the nucleoplasm adhere to the C1 region and appear to coalesce (Figs. 3.5 and 3.6).

Just prior to spermiation, Step 14 spermatids have the characteristic indentations of the C2 chromatin at the periphery of the nucleus (Fig. 3.7A). The nuclear mantle has adopted a levelled surface and is approximately 71.2 ± 5.4 nm thick. The ENE sometimes has a few spherical inclusions, and fragments of nuclear membranes containing flocculent material are present outside the nuclear pores (Figs. 3.7B and C). The ENE appears reduced from that of Step 11 spermatids and the long axis of the sperm head is now perpendicular to that of the tail in a T-configuration.

3.3.3. Nuclear changes in the epididymidis

Caput epididymal spermatozoa retain the ENE. It is however, no longer at the dorsal surface as in testicular spermatids, but has shifted to a ventral position, with a concomitant adherence of the nuclear envelope to the nuclear mantle (Fig. 3.8A). Within the ENE, electron-dense inclusions and flocculent material are apparent (Figs. 3.8A and B). The spermatozoa retain a T configuration, inherited from their testicular predecessors. The nuclear mantle is still present on the surface of the C1 chromatin but is thinner (42.6 ± 1.7 nm) than in spermatids (Fig. 3.8A).

At the caput-corpus junction, the spherical inclusions are no longer present, but a large accretion of electron-dense material lies adjacent to the nuclear envelope (Fig. 3.9). In the corpus region, the ENE appears smaller and large electron-dense structure(s) lies directly outside the nuclear pores (Fig. 3.10). The nuclear mantle has now disappeared, however, the nuclear membrane on the dorsal surface appears very electron-dense and may contain nuclear pores (Fig. 3.10).

At the corpus-cauda junction, small folds of nuclear membrane are visible in the now very reduced ENE (Fig. 3.11). In cauda epididymal spermatozoa, the ENE has completely disappeared and the caudal region of the nucleus has a concave shape which accommodates the proximal mid-piece of the sperm tail (Fig. 3.12).

3.3.4. Phosphotungstic acid staining for lysine-rich proteins

The nuclear mantle of Step 10 spermatids stains intensely following treatment with alcoholic phosphotungstic acid (Fig. 3.13). The C2 region stains lightly and the C1 region is generally unstained. Granular material within the ENE is electron-dense (Fig. 3.13).

In caput epididymal spermatozoa, similar staining properties of the nuclear structures are observed. The nuclear mantle is thinner in appearance. Within the ENE, spherical structures appear electron-dense (Figs. 3.14A and B).

In cauda epididymal spermatozoa, the ventral surface of the C1 chromatin does not stain with PTA confirming that the nuclear mantle is no longer present.

There are nuclear pores present in the nuclear envelope overlying the region where the nuclear mantle had previously occurred (Fig. 3.15).

3.3.5. DNAase-gold

In caput epididymal spermatozoon, the C1 and C2 nuclear regions bind to DNAase-gold (Figs. 3.16A and B). However, nuclear inclusions and flocculent material within the ENE (Figs. 3.16A and B) as well as the nuclear mantle (Fig. 3.16A) are not labelled. In control sections, the labelling is greatly reduced when DNA is added to the enzyme-gold complexes prior to the incubation (not shown), indicating that binding of the tissue sections with the complex is by way of DNA and DNAase interaction(s) (Bendayan, 1981).

3.4. DISCUSSION

The marsupial superfamilies, Perameloidea and Dasyuroidea are both members of the Polyprotodonta and they are considered to be more closely related to one another than to any other marsupial group (Clemens, 1968; Clemens et al., 1989). The spermatozoa of both groups are noted for their large size and their highly unusual flagella structures (Harding et al., 1979). In *Sminthopsis*, total sperm tail length is about 250 μm (Breed et al., 1994) which makes it one of the largest of mammalian spermatozoa. The peramelids and dasyurids also possess two chromatin regions in the spermatozoon. However, the extraneous nuclear regions in peramelids are less prominent compared to the C2 region of *Sminthopsis* and occur as small globular structures at the caudal extremity of the nucleus (Sapsford et al., 1969).

In *Sminthopsis,* the peripheral indented chromatin region (C2) occurs at the apex of the nucleus, along the lateral surface of the homogeneous region (C1), and over 1/3 of the posterior ventral surface. There are some regions where C2 chromatin is not found: (1) at the basal plate of the implantation fossa, and (2) beneath the acrosome (Breed et al., 1994). These structures are formed prior to chromatin condensation of the C2 region.

During spermiogenesis in *Sminthopsis*, condensation in the C1 region occurs dorso-ventrally and the chromatin changes uniformly from thread-like to slightly granular and finally to a homogeneous appearance. At this time in Step 10 spermatids, the distinctive tapered shape of the sperm head is apparent and the C1 chromatin region appears fully condensed. At the caudal extremity of the nucleus, the nuclear envelope encloses an area that is electron-lucent and contains flocculent material. Vesicles present in the close vicinity of the nuclear envelope at the periacrosomal ring, may supplement the existing nuclear envelope (Vigers and Lohka, 1991) so that it becomes very enlarged in Step 11 spermatids. In these spermatids, membranous whorls are present in the same region distal to the acrosome where the vesicles occurred in earlier spermatids. The appearance of spherical inclusions adjacent to the nuclear pores coincides with the formation of the nuclear mantle. This structure overlies the dorsal surface of the C1 region, from the periacrosomal ring to the tip of the nucleus.

Condensation of the C2 region commences in Step 12 spermatids and is observed as spherical chromatin structures along the surface of the C1 region.

Chromatin subunits also appear within the nucleoplasm and partially coalesce to complete the nuclear structure prior to spermatozoon release into the seminiferous tubule lumen.

The nuclear mantle is distinguishable from the C1 and C2 regions by not containing DNA, and by staining strongly with alcoholic phosphotungstic acid (PTA). The specificity of this method was discussed by Courtens and Loir, (1981a) who showed that alcoholic PTA (3%) stains preferentially for lysine-rich, but not arginine-rich, nucleoproteins.

The nuclear mantle may be the equivalent of the basal knobs in the mature spermatids of eutherians which occur at the posterior region of the nucleus and are surrounded by a 'nuclear pocket' consisting of 'redundant' nuclear envelope (Courtens and Loir, 1981b). The basal knobs stain strongly for alcoholic PTA in late spermatids and appear to contain histone-like proteins (Courtens and Loir, 1981b), as well as centromeric proteins (Courtens et al., 1992). In *Sminthopsis,* the existence of the nuclear mantle is transient and occurs from between the time of its appearance in Step 11 spermatids to the completion of spermatozoa migration to the corpus epididymidis. The material present in the nuclear mantle may consist of proteins such as histones that are not bound to DNA but are instead targeted for removal following nuclear condensation.

In the mature spermatid of dasyurids, and to some extent in peramelids (Sapsford et al., 1969) and eutherians (Courtens et al., 1981b), there is an electron-lucent region surrounded by the nuclear envelope. In the dasyurid spermatozoa, the nuclear envelope surrounds a much larger region and, within this enlarged nuclear envelope (ENE), electron-dense globular and ringed structures are present. We have previously suggested that in *Sminthopsis,* these inclusions may represent localised regions of condensed chromatin (Breed et al., 1994). We have also proposed that nuclear condensation and gene activity, may still occur within the ENE in caput epididymal spermatozoa (Breed et al., 1994). The present study demonstrates that the inclusions within the ENE do not contain DNA but proteins are present. There are also nuclear pores present in this region of the nuclear envelope which may indicate transfer of materials between the cytoplasm and nucleus.

As the spermatozoon travels down the epididymis, the spherical inclusions eventually disappear. However, a large accretion of electron-dense material appears near the nuclear pores and is subsequently removed from the nucleus.

Since the electron-dense inclusions in the caput sperm are not chromatin, we surmise that nuclear condensation occurs primarily in the testis and that, in the epididymis, redundant nuclear material is removed through the nuclear pores. The latter process may include the depolymerisation and elimination of nuclear mantle proteins.

In the study of *Sminthopsis* spermatozoon DNA, both C1 and C2 regions show positive labelling for DNAase-gold which indicate that DNA is present within these regions. The C2 region is therefore an integral part of the genome.

A possible clue to its unusual morphology is revealed by the process of nuclear condensation in the testis. Ultrastructural observations suggest that the final condensation event at the nuclear periphery is incomplete and may have resulted in the numerous grooves observed in the C2 region.

3.5. CONCLUSION

Both the nuclear regions, (C1) and (C2) in the spermatozoa of *Sminthopsis crassicaudata* contain DNA. The mode of condensation of the two regions appears to differ; the condensing C1 chromatin consists of fine granules that eventually form homogeneously electron-dense chromatin, whereas that of C2 consists of globular structures that appear to partially condense to result in chromatin that contains numerous electron-lucent grooves. A hitherto undescribed structure, the 'nuclear mantle', first appears in Step 11 spermatids and does not contain DNA, but is likely to contain lysine-rich proteins. This structure is not present in the mature spermatozoa. The expanded nuclear envelope at the caudal extremity, unlike similar structures in eutherians and other marsupials, persists in caput epididymal spermatozoa. Spherical inclusions within it do not bind to DNAase-gold conjugates but stain for lysine-rich proteins. As the sperm travel down the epididymis, these inclusions amass near the nuclear pores and become removed from the nucleus.

Fig. 3.1A. Longitudinal section of Step 10 spermatid. The chromatin appears homogeneously condensed (C1). Nuclear spaces containing flocculent material (f) occur below the apical region and around the caudal segment of the nucleus. Mitochondria (mt) migrate to the mid-piece region of the sperm tail. Bar = 2.0 μm.

Fig. 3.1B. Caudal nuclear segment of Step 10 spermatid. Nuclear pores (np) are present on the ventral surface of the nuclear envelope. Note the occurrence of vesicles (arrowheads) close to the dorsal aspect of the nuclear envelope distal to the periacrosomal ring (pr). Bar = 0.30 μm.

Fig. 3.2A. Step 11 spermatid. An enlarged nuclear envelope (ENE) is present at the cauda of the nucleus. Membranous whorls (w) at the nuclear envelope are visible at the region of overlap with the sperm plasma membrane. The acrosome (a) lies above the dorsal nuclear surface and folds upwards proximally and tapers into a thin segment distally. Mitochondria (mt) align at the mid-piece of the sperm tail. Bar = 0.70 μm.

Fig. 3.2B. Apical nuclear region of Step 11 spermatid. Nuclear envelope (arrowhead) is closely apposed to the dorsal surface of the nucleus above which lies the subacrosomal space (s). On the ventral nuclear surface there is a space between the condensed nucleus and the nuclear envelope (ne) which is intersected by filamentous material (f). Bar = 0.25 μm.

Fig. 3.2C. Caudal nuclear region of Step 11 spermatid. Spherical electron-dense structures are apparent just inside the nuclear envelope (arrowheads). A layer of electron-dense material (the nuclear mantle (NM)) lies on the ventral nuclear surface. Bar = 0.25 μm.

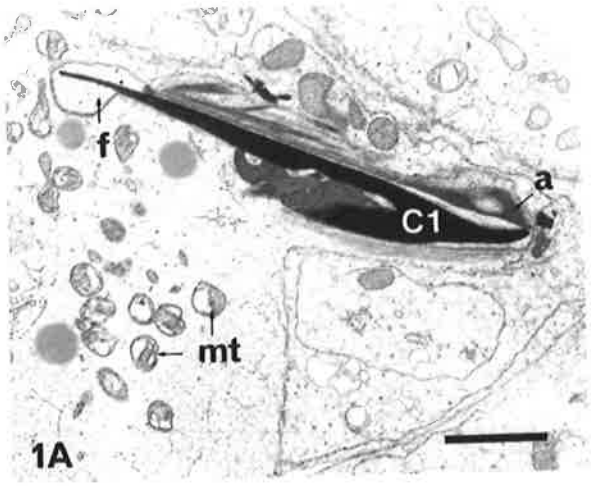
f
a
C1
mt
1A

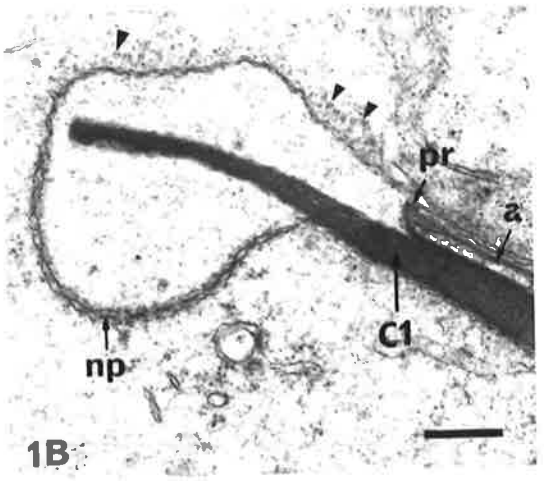
pr
a
C1
np
1B

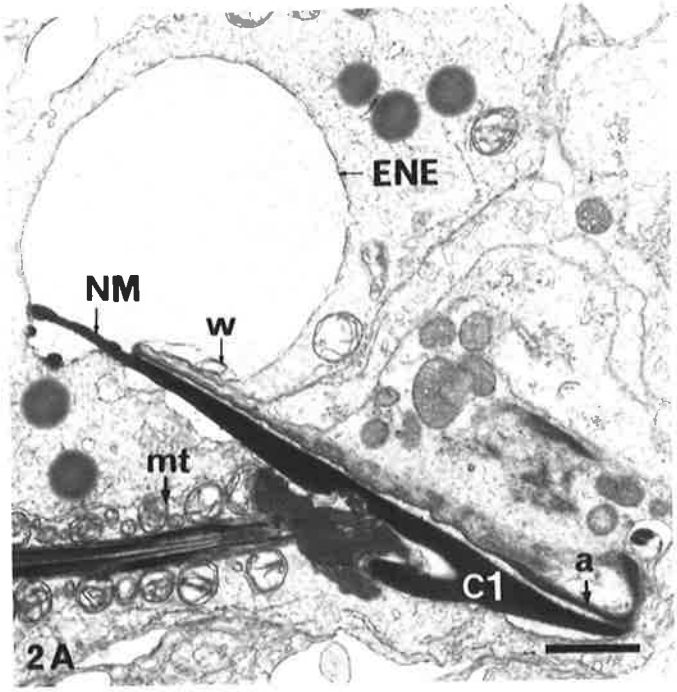
ENE
NM
w
mt
C1
a
2A

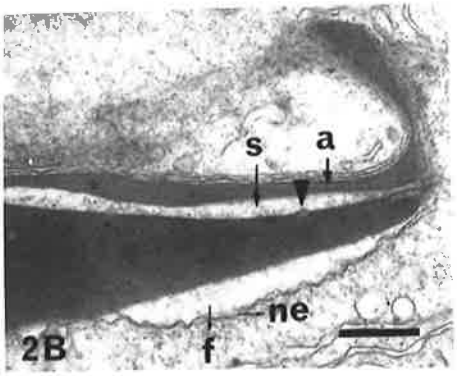
s
a
ne
f
2B

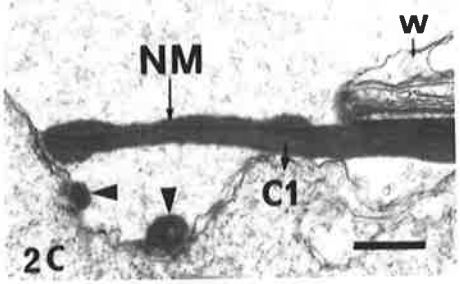
w
NM
C1
2C

Fig. 3.3. Parasaggital section of Step 12 spermatid showing spherical structures (arrowheads) at the periphery of the previously smooth chromatin (C1). Bar = 1 μm.

Fig. 3.4. Step 12 spermatid in frontal plane of section. C2 chromatin has formed on the surface of the C1 region. Small nuclear inclusions are visible (arrowheads). Bar = 0.3 μm.

Fig. 3.5. Step 13 spermatid. At the apical region of the nucleus, spherical chromatin structures form and aggregate (arrowheads). Bar = 1 μm.

Fig. 3.6. Oblique section of a Step 13 spermatid. Formation and aggregation of chromatin (arrowheads) are apparent. Bar = 0.3 μm.

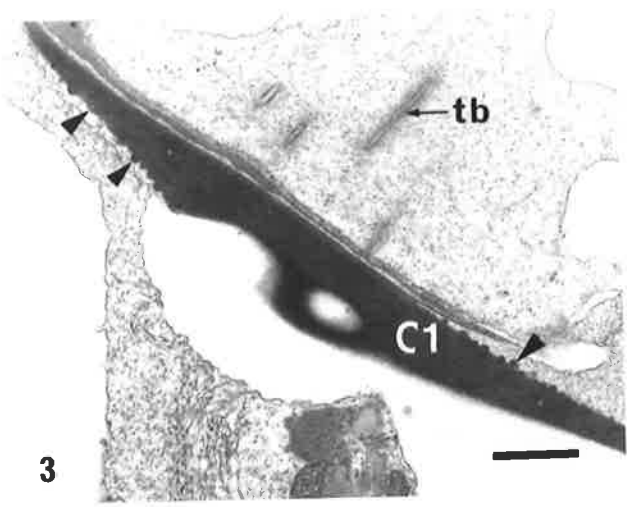

3

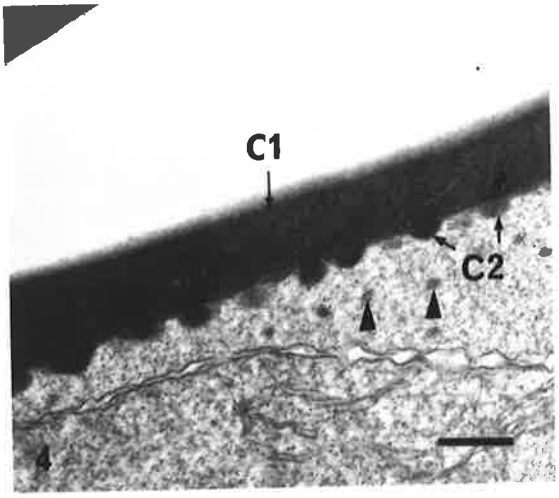

4

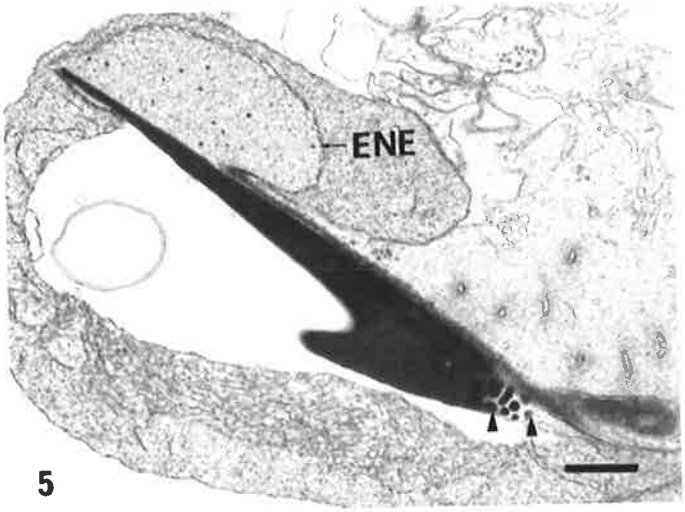

5

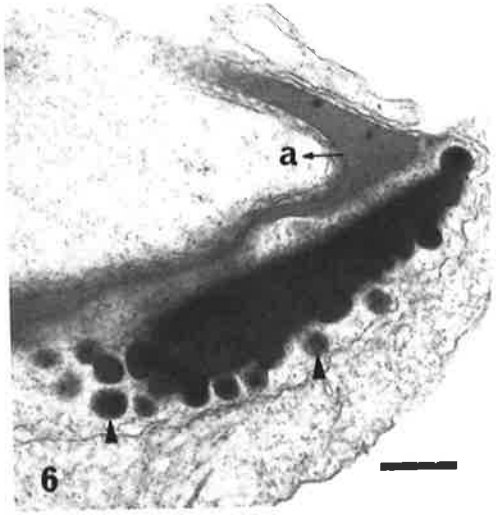

6

Fig. 3.7A. Step 14 spermatid prior to release into the lumen of the seminiferous tubule. The mature spermatid nucleus has characteristic indentations in the apical region (C2). From this section of view, the acrosome does not appear folded. Bar = 1.2 μm.

Fig. 3.7B. Caudal extremity of the nucleus of Step 14 spermatid. Fragments of membranes (arrowheads) containing flocculent material are present outside the nuclear pores. The surface of the nuclear mantle (NM) appears more even. Bar = 0.15 μm.

Fig. 3.7C. Step 14 spermatid. A double membrane (arrowhead) encloses flocculent material outside the nuclear pores. C2 chromatin is present on the ventral surface. Bar = 0.15 μm.

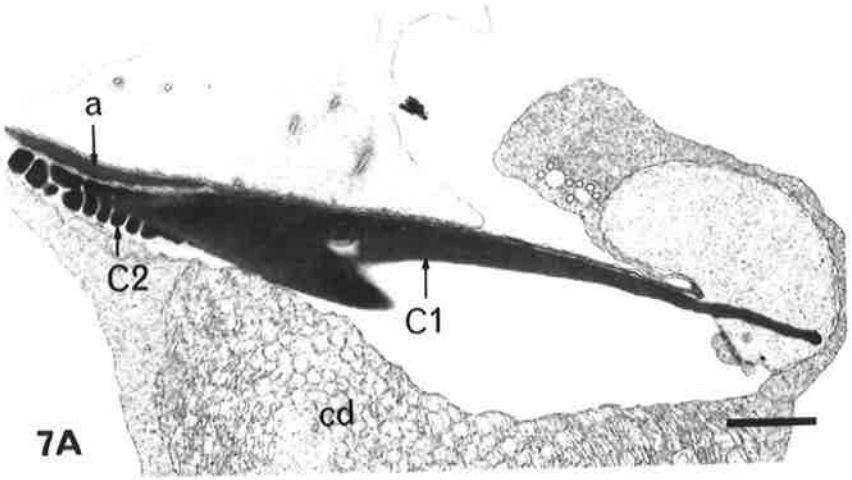

7A

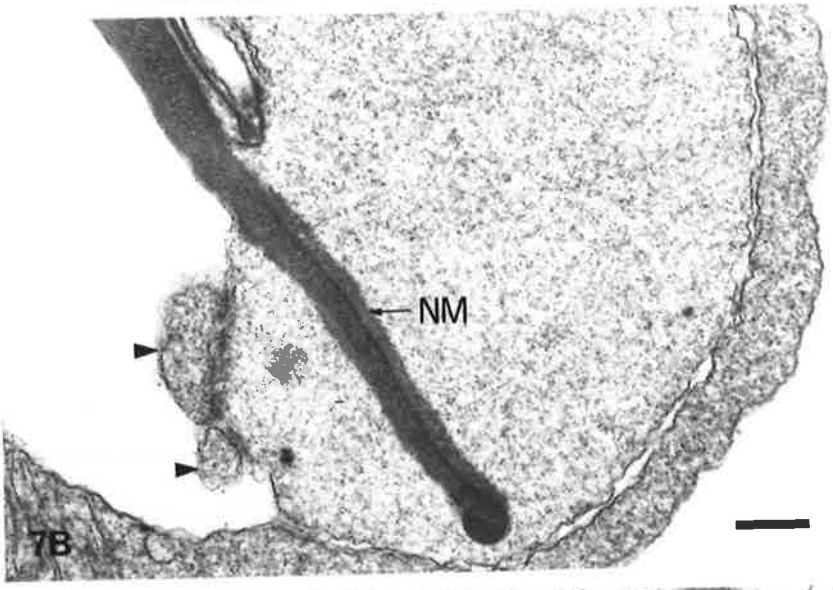

7B

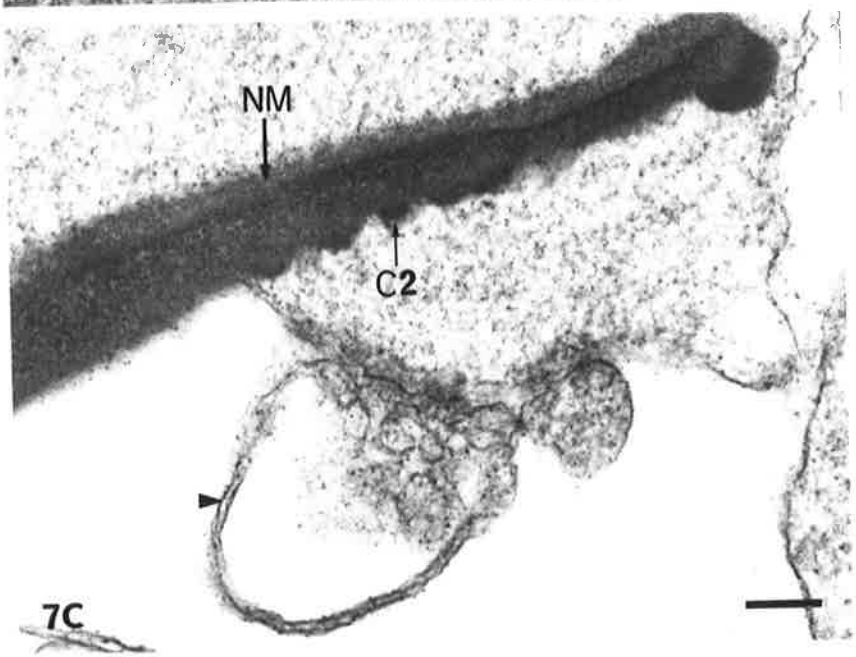

7C

Fig. 3.8A. Caput epididymal spermatozoon. The ENE is present on the ventral region of the sperm head and contains electron-dense inclusions (arrowheads). The nuclear mantle (NM) is still present at the caudal region of the nucleus. Bar = 0.5 μm.

Fig. 3.8B. Transverse section of caudal region of caput epididymal spermatozoa. Nuclear inclusions are present (arrowheads) within the ENE. Bar = 0.5 μm.

Fig. 3.9. Transverse section of spermatozoon from the caput-corpus junction. A large inclusion (arrowhead) is present at the edge of the nuclear envelope. Bar = 0.3 μm.

Fig. 3.10. Longitudinal section of spermatozoon from the corpus epididymidis. An electron-dense structure (small arrowheads) lies outside the nuclear pores (np) of the ENE. Part of the ENE has folded into membranous whorls (w). The nuclear mantle is no longer visible. The nuclear envelope is very electron-dense in the region where the nuclear mantle had previously laid (large arrowheads). Bar = 0.4 μm.

Fig. 3.11. Transverse section of spermatozoon from the corpus-cauda junction. The ENE has almost disappeared. Folds of nuclear membrane are present (arrowhead). Bar = 0.3 μm.

Fig. 3.12. Longitudinal section of spermatozoon from the cauda epididymidis. The sperm head has completed its rotation and is now closely apposed to the flagellum. The ENE is no longer present. Bar = 1.5 μm.

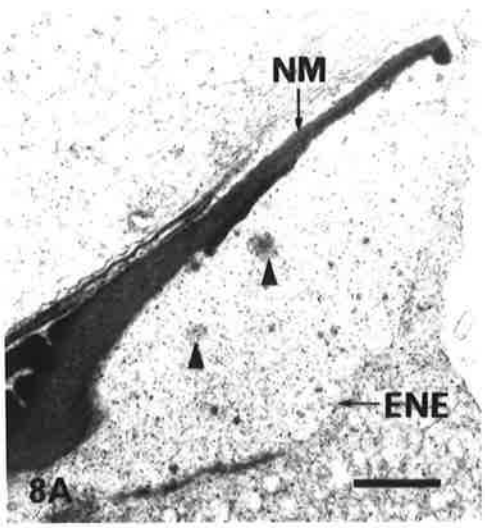
NM
ENE
8A

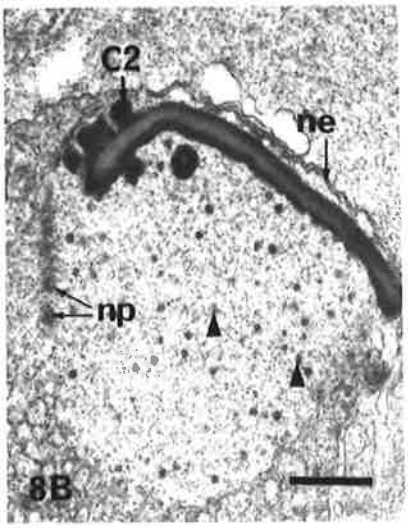
C2
ne
np
8B

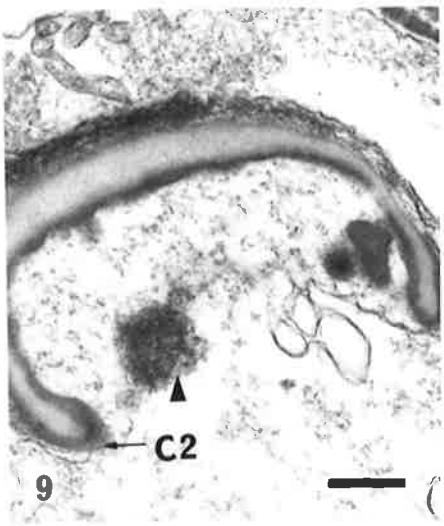
C2
9

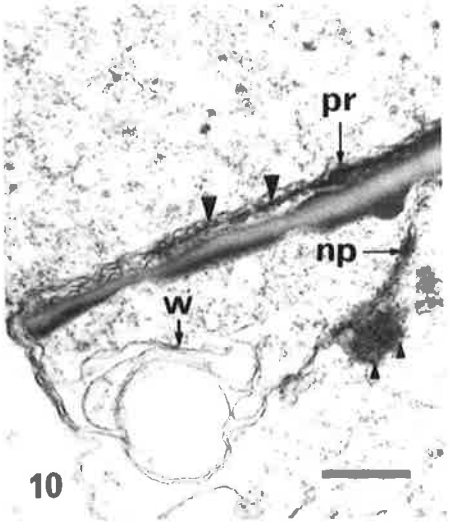
pr
np
w
10

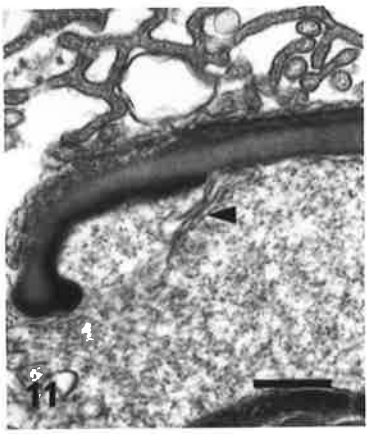
11

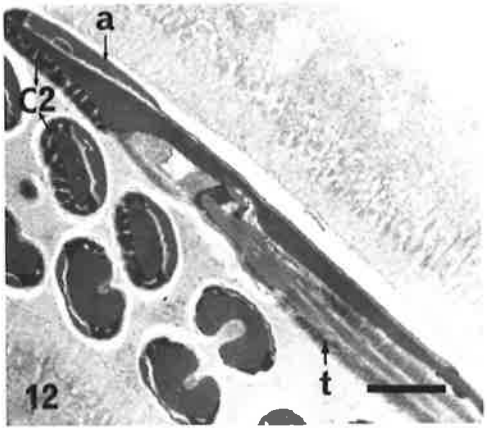
a
C2
t
12

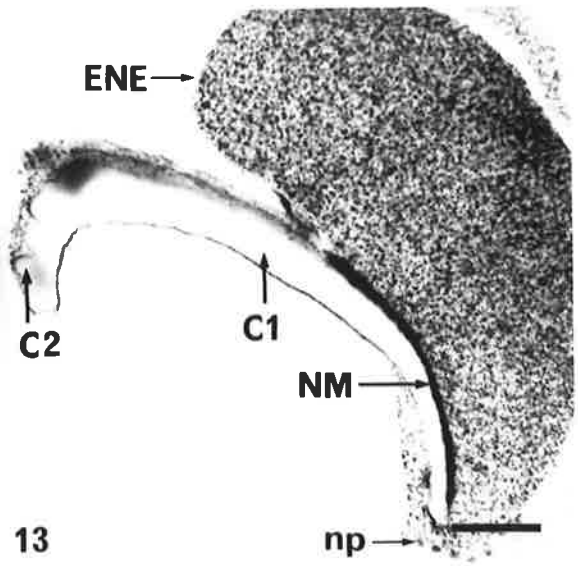

13

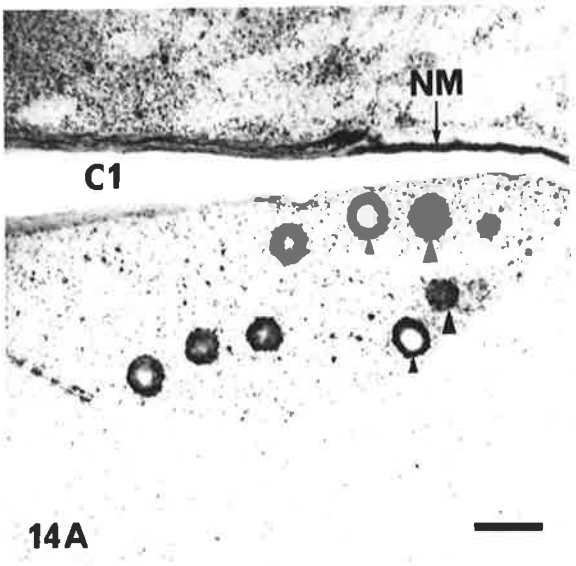

14A

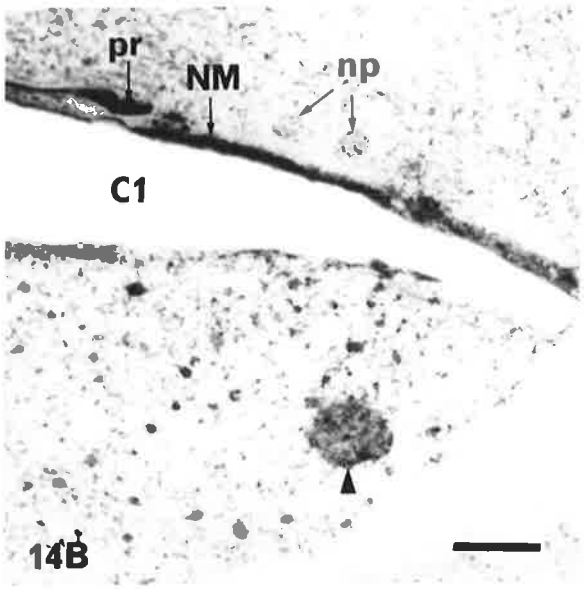

14B

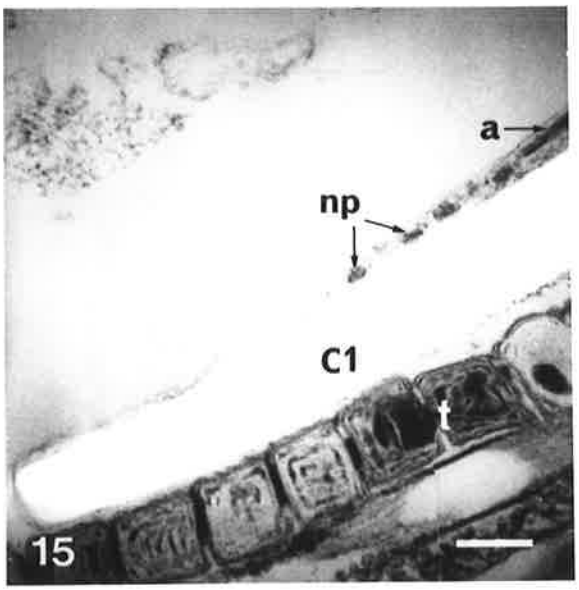

15

Fig. 3.16A. Longitudinal section of caput epididymal spermatozoon. DNase-gold labelling is visible over both C1 and C2 regions. The nuclear mantle region (NM) and inclusions (arrowheads) within the ENE are not labelled. Bar = 0.3 μm.

Fig. 3.16B. Transverse section of caput epididymal spermatozoon. Particles of DNase-gold conjugate (10 nm) label both C1 and C2 regions. Bar = 0.3 μm.

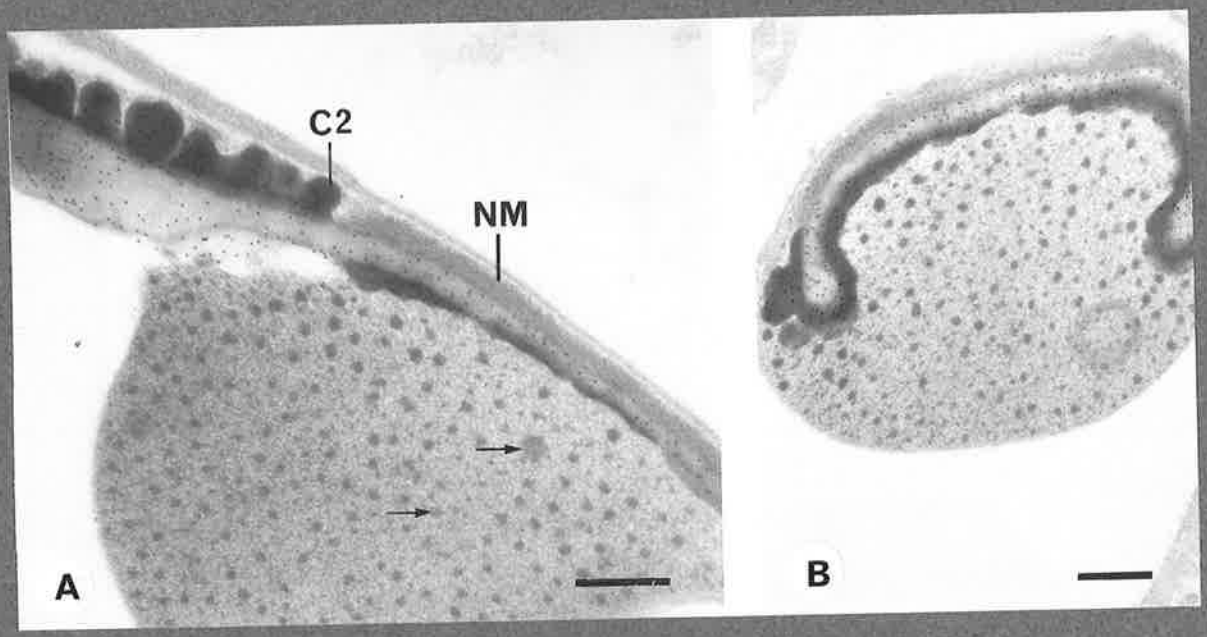
C2
NM
A
B

Chapter 4. CYTOCHEMICAL STUDIES ON THE DENSITY AND COMPACTION OF SPERMATOZOA CHROMATIN

4.1. INTRODUCTION

Two characteristics of the C2 chromatin, (1) its high electron-density and (2) the presence of fissures, were investigated by examining the staining and condensation properties of the spermatozoa chromatin.

Part A. Staining Properties of Spermatozoa Chromatin

Staining for electron microscopy utilises large cations such as uranyl, lead and osmium. These heavy metal stains impart a greater potential for electron scattering to specimens bombarded with a high density electron beam. In conventional thin sections, the C2 chromatin of *Sminthopsis* spermatozoa nuclei appears more electron-dense compared to the C1 chromatin. Therefore, in these sections, the chromatin of the C2 region demonstrates a greater potential for electron scattering compared to that of C1.

Two factors that influence the amount of electron scattering are (1) affinity of structures for heavy metal stains, and (2) the mass thickness of the biological material. The appearance of high electron-density in the C2 region may be due to either one or both of these factors. To determine why there is a difference in the electron-density between the two regions of the nuclei, the unstained spermatozoa of *Sminthopsis* were compared with those that were stained with various combinations of uranyl acetate, lead citrate and osmium tetroxide.

Part B. Induction of Chromatin Condensation in Spermatozoa

The presence of fissures or gaps in the C2 region of the spermatozoa is inconsistent with highly condensed, protamine-packaged DNA. These fissures may be caused by incomplete chromatin aggregation or partial DNA condensation in the C2 region. To test this hypothesis, *Sminthopsis* sperm nuclei were incubated with the basic proteins, herring and salmon protamines, and observed by both fluorescence and transmission electron microscopy to

determine whether the chromatin within the C2 region could be further condensed by the protamines.

Protamines are highly basic proteins that bind to the DNA double helix, possibly within the grooves, by electrostatic interactions (Balhorn, 1982). The positive charges of arginine residues, grouped in the central region of the protamine molecule, neutralise every phosphodiester negative charge in the backbone of the DNA helix (Balhorn, 1982). As a result, the repulsive forces between nucleoprotein fibres become greatly reduced causing a collapse or the aggregation of the fibres into an almost crystalline and homogeneous structure. The nuclei of spermatozoa that are packaged by more than one type of protein may have chromatin that appears heterogeneous. In the case of *Sminthopsis*, the highly indented C2 chromatin may be packaged by proteins that are less basic or less positively charged compared to protamines. Incubation of spermatozoa with protamines may therefore be informative on whether the chromatin could be further condensed using a presumably more basic protein than the one inherently present within the C2 region.

4.2. MATERIALS AND METHODS

4.2.1. Staining for transmission electron microscopy

Each cauda epididymidis from three mature *Sminthopsis* males was cut into approximately 1-3 mm^3 pieces that were fixed for 4-8 h. The tissues were washed twice in PBS, pH 7.5 and divided into two pools. The first sample was immersed in 1% osmium tetroxide for 1 h, whereas the other was left unosmicated. All tissues were dehydrated by passing through a graded series of ethanol, embedded in TAAB expoxy resin (TAAB Lab Equipment, Reading, Berks) or LRWhite (LRW) resin (Probing and Structure, Thuringowa Central, Queensland), and left to polymerise at 60°C in the oven. Two different resins were used to determine whether there may be varying degrees of penetration of stains. Thin sections were cut using an ultramicrotome and were left either unstained or stained with 2% uranyl acetate for 5 min and/or with 2% lead citrate (Appendix 4) for 10 min. LRW sections were stained for 1 min in 2% aqueous uranyl acetate for 1 min and/or with lead citrate for 20s. The sections were viewed with the transmission electron microscope (TEM) (Phillips CM100). To increase image contrast of the unstained specimens, the accelerating voltage was lowered from 80 kV to 60 kV and the objective aperture size was decreased from 50 μm to 20 μm.

Table 4.1 indicates the different staining and embedding methods used for the study of the effects of stains and resins on the electron-density of spermatozoa chromatin. Letters (a)-(j) refer to the different combinations of heavy metal stains and resins.

TABLE 4.1: COMBINATIONS OF EMBEDDING RESINS AND CATIONIC SALTS

	Heavy Metal Stains				
Resin	Osmium Tetroxide	Uranyl Acetate	Lead Citrate	All stains	Unstained
TAAB	(a)	(c)	(e)	(g)	(i)
LRWhite	(b)	(d)	(f)	(h)	(j)

4.2.2. Incubation with protamine sulphate

Spermatozoa from the cauda epididymidis from two mature *Sminthopsis* males were expressed into distilled water and were partially demembranated by sonication followed by treatment with 0.1% Triton X-100 for 20 min.

A subsample of demembranated sperm was left untreated and used as a control and the rest of the sample was incubated with 3 mg/ml protamine sulphate from herring or salmon (Sigma) for 3 h. The samples, including the controls, were washed three times with PBS, pH 7.5. Drops of sperm suspension were placed on slides and stained for 10 min with 50 μg/ml 4',6-diamidino-2-phenylindole (DAPI) (Sigma) and the slides were mounted with anti-fade solution (Molecular Probes, Eugene, USA). The samples were examined under a fluorescence microscope (BH-RFL) using a dichroic mirror (DM-455) and a filter combination, IF-490/530 nm.

The rest of the protamine treated- and control samples were centrifuged at 14 000 g for 2 min and the sperm pellet fixed with 3% glutaraldehyde, and prepared for conventional TEM (Appendix 3).

4.3. RESULTS

4.3.1. Transmission electron microscopy of sperm nuclei

The C2 chromatin consistently appeared more electron-dense than the C1 region (Fig. 4.1A and B) in specimens stained with osmium tetroxide (OsO_4), uranyl acetate and lead sulphate. The results were the same regardless of whether the stains were used alone or in combination with one another (Table 4.1: (a)-(h)).

The chromatin however, appeared more electron-dense in specimens embedded in LRW resin compared to those embedded in TAAB, even though specimens embedded in LRW were stained for a shorter period.

By contrast, the C2 region in the unstained specimens appeared more electron-translucent than the C1 region (Fig. 4.2A and B). The results were the same for different types of embedding resin used (Table 4.1: (i) and (j)).

4.3.2. Protamine incubation studies

In the control samples, both intact spermatozoa (not shown) and those treated with 0.1% Triton X-100, and stained with DAPI displayed a brighter fluorescence in the central region of the nuclei compared to the posterior and apical regions, where the C2 chromatin mainly occurs (Fig. 4.3A). Transmission electron microscopy revealed that treatment with 0.1% Triton X-100 partially removed spermatozoa membranes but left the chromatin intact (Fig. 4.3B). The characteristic indentations of the C2 chromatin were also apparent.

However, following partial demembranation and treatment with protamine sulphate, DAPI-stained spermatozoa displayed a more uniform fluorescence in the nuclei (Fig. 4.4A) where all regions including the apex and cauda of the nuclei appeared equally brightly fluorescent. Ultrastructurally, the grooves that interweaved the C2 chromatin appeared largely reduced. In most cases the grooves were completely lacking and the C2 chromatin had an almost uniform and amorphous appearance similar to the C1 region (Fig. 4.4B). Both herring and salmon protamines produced similar results.

4.4. DISCUSSION

Imaging in electron microscopy involves interactions between the electron beam with the nuclei of positively charged atoms. Image contrast is created by the extraction of electrons from the beam as a result of electron scattering.

On approaching the positively charged atomic nuclei, electrons of the beam become scattered so that the emergent beam is no longer homogenous. The voids in the emergent electron beam created by the scattered electrons, are imaged by the magnifying system as dark areas of so called high electron-density. Electrons of a certain velocity, at a given distance from the atomic nucleus, are more strongly deflected by a nucleus which has a high positive charge. Therefore, image contrast at any given voltage and aperture size is proportional to the atomic number. The atomic number is directly related to the size of the atomic nucleus hence, approximately to its density. Consequently, the greater the specimen density, the greater is the probability of scatter. By contrast, the less dense areas of the specimen scatter fewer electrons, therefore appearing brighter or electron-lucent.

Another factor influencing the degree of electron scattering is the thickness of the specimen. The number of atoms encountered by the electron beam as it passes through the specimen increases with specimen thickness. Hence the degree of scattering is dependent upon the product of specimen density and thickness, termed the mass thickness ($\mu g/cm^2$). Variations in mass thickness in the specimen result in differential electron scattering and thus creates image contrast.

Cations such as osmium, uranyl and lead are used in TEM staining to increase the contrast between biological structures. These cations have large atomic nuclei that confer a higher probability of electron scattering when the atoms are bombarded with an electron beam. The larger the number of atoms the imaging electrons encounter in their passage through the specimen, the greater will be the probability of scatter (Hayat, 1981).

Other factors that influence image contrast include the operating voltage and aperture size. Small apertures will enhance the image contrast, however, the ultimate resolving power will be reduced. At high voltages, the electrons scatter at large angles and fall outside the objective aperture. These electrons can no

longer participate in image formation. Therefore, to increase the retrieval of the scattered electrons, the operating voltage is lowered.

For this study, the aperture size and accelerating voltage were reduced to increase image contrast in the unstained specimen. These adjustments were not expected to have a negative impact on the experiments, since similar adjustments for the stained specimen would serve to enhance the effects of staining.

A variety of resins were used for embedding the tissues to determine whether there is a difference in the penetration of the stains allowed by the resins. The two types of resin, LRW and TAAB, produced similar results, although LRW, a water-miscible resin, has a relatively higher rate of impregnation of stains compared to TAAB, an epoxy resin.

In the unstained specimen, the C1 chromatin appears to be electron-dense when visualised at 60 kV and using a 20 μm objective aperture. This was consistent for all regions of the C1 chromatin, from the thin posterior part (approximately 1 μm in thickness) to the thickest areas at the anterior end of the nucleus (approximately 2.5 μm). Therefore variations in the thickness of the specimen do not appear to affect the electron-density. Since no cationic stains have been used to enhance image contrast, the electron-density of the C1 chromatin must be due to the inherent properties of its constituents. In the context of chromatin structures, these results reflect a very condensed state of the C1 chromatin.

By contrast, without the aid of stains, the C2 region appeared electron-lucent. This could be due to (1) a low density of material, which gives a low probability of electron scatter, or, (2) extraction of material during tissue processing. Extraction of nucleoproteins to any great extent is unlikely since the fixative used in all cases was glutaraldehyde at 3% which effectively crosslinks proteins. Therefore it appears that the low electron-density of the unstained C2 chromatin reflects either a low concentration of chromatin in the region or a relatively less dense packaging, or both.

When stained with cations and visualised at 80 kV using a larger, 50μm, objective aperture (conventional applications in TEM), the C1 chromatin did not appear any more electron-dense compared to the same region in the unstained specimen. Therefore, the C1 chromatin may have a low affinity for positively charged stains such as uranyl, lead and osmium and this may reflect a lack of available negative DNA charges that may bind the stains.

On the other hand the electron-density of the C2 chromatin becomes enhanced when stained with heavy metals so that it appears more electron-dense than the C1 region. This observation is invariable irrespective of the type of heavy metal stain used or whether the stains are used by themselves or in conjuction with one another. This indicates that the C2 region has a greater affinity for cationic metals which could reflect the presence of negatively charged residues such as free phosphodiester charges of DNA molecules within the chromatin.

At the ultrastructural level, the C2 region contains numerous fissures or grooves that may indicate partial chromatin aggregation (Soon and Breed, 1996). These fissures disappeared following incubation of spermatozoa with protamines from herring and salmon. The binding of the added protamines to free phosphodiester charges of DNA may have caused further chromatin compaction that removed the fissures in the C2 region. It is therefore *unlikely* that DNA within the C2 region is naturally packaged by protamines which tend to completely neutralise the negative charges of the DNA backbone and in essence prevent any further binding to proteins. However, the DNA may be packaged by proteins that are of a less basic nature or less arginine-rich compared to protamines.

This study also provides an explanation for the perplexing observation of differential fluorescence of *Sminthopsis* spermatozoa nucleus; when stained with fluorochromes, the apical and posterior regions of the spermatozoa nuclei appear less bright than the inner C1 region (Breed et al., 1994). The present study shows that the nuclei can be induced to fluoresce uniformly by incubating spermatozoa with protamine sulphate prior to staining with 50 μg/ml DAPI. Since the fish protamines are likely to have further condensed the chromatin in the C2 region, we can rationalise that the less bright fluorescence of the C2 chromatin in untreated samples, is due to a lower density of DNA compared to the C1 region.

4.5. CONCLUSION

C2 chromatin appears to have (1) excess negative charges as shown by its strong affinity for cations and the ability of protamines to bind and further compact the chromatin, and (2) a low density as suggested by its electron-translucence in the unstained spermatozoa, and the ability of protamines to elicit a qualitative increase in fluorochrome binding density within the region.

C1 chromatin on the other hand may have a high density as the structure appeared electron-dense in the unstained specimen. This region does not appear have a great affinity for cationic stains since the electron-density is not greatly enhanced following staining with cationic salts.

Fig. 4.1. Spermatozoa from cauda epididymidis of *Sminthopsis* stained with 1% osmium tetroxide, 2% uranyl acetate and lead citrate, and embedded in LRW resin (A); spermatozoa stained with 1% osmium tetroxide alone and embedded in TAAB resin (B). In both micrographs, C2 chromatin (small arrows) shows greater uptake of stain and appears more electron-dense compared to C1 chromatin (large arrows). (a, acrosome; t, tail). Bar (A) = 1.5 μm; Bar (B) = 1.0 μm.

Fig. 4.2. Unstained *Sminthopsis* spermatozoa from cauda epididymidis embedded in TAAB resin (A); embedded in LRW (B). C2 regions (small arrows) appear electron-lucent, whereas C1 chromatin (large arrows) is electron-dense. (a, acrosome; t, tail). Bar (A) = 1.0 μm; Bar (B) = 1.0 μm.

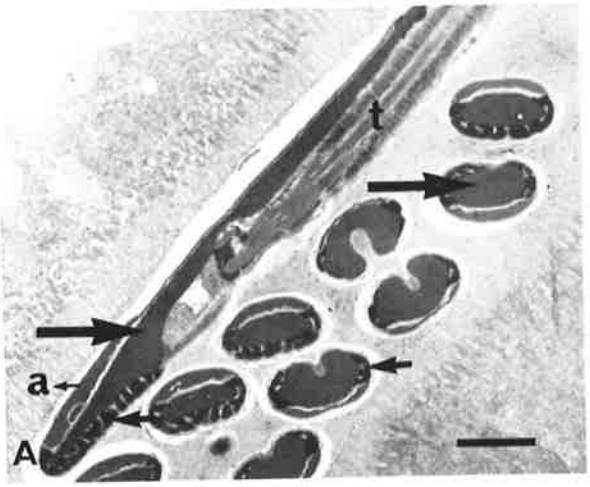
t
a
A

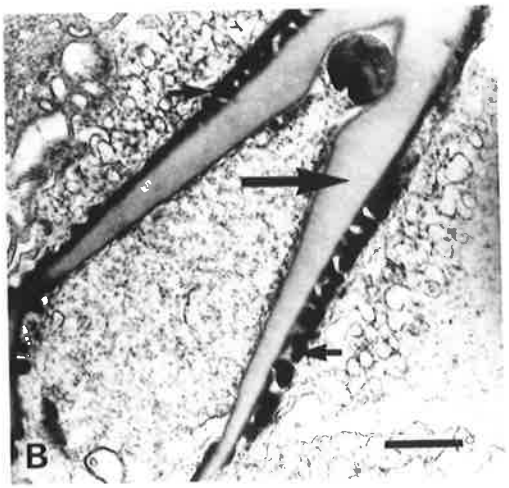
B

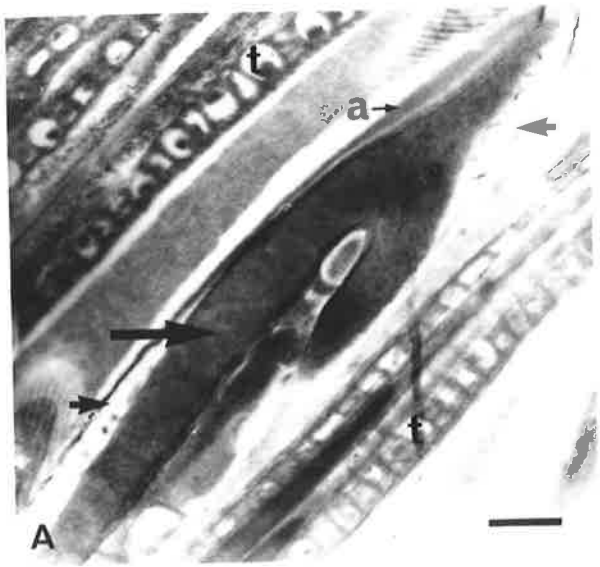
t
a
t
A

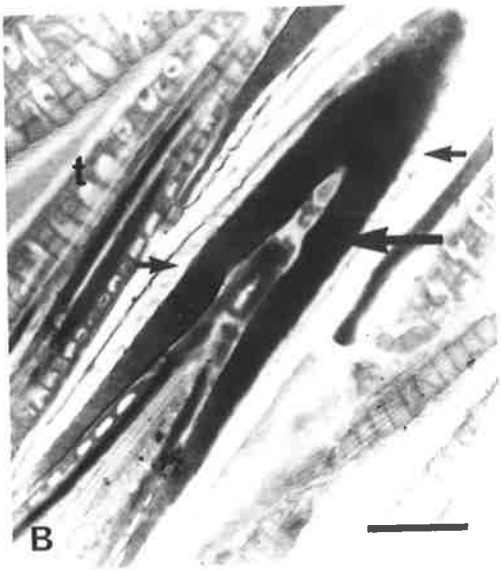
t
B

Fig. 4.3. Sperm partially demembranated by 0.1% Triton X-100. Fluorescence microscopy of DAPI stained spermatozoon displaying characteristic faint fluorescence at the apical and posterior regions (arrows) (A); ultrastructure of the apical nuclear region showing the presence of grooves within the C2 chromatin (arrowheads) (B). Bar (A) = 16 μm; Bar (B) = 294 nm.

Fig. 4.4. Partially demembranated sperm incubated with herring protamine. Fluorescence microscopy of DAPI stained spermatozoa no longer displaying the faint fluorescence at the apical and posterior regions (arrows) (A); ultrastructure of the apical nuclear region showing disappearance of fissures in the C2 chromatin (B). Bar (A) = 17 μm; Bar (B) = 360 nm.

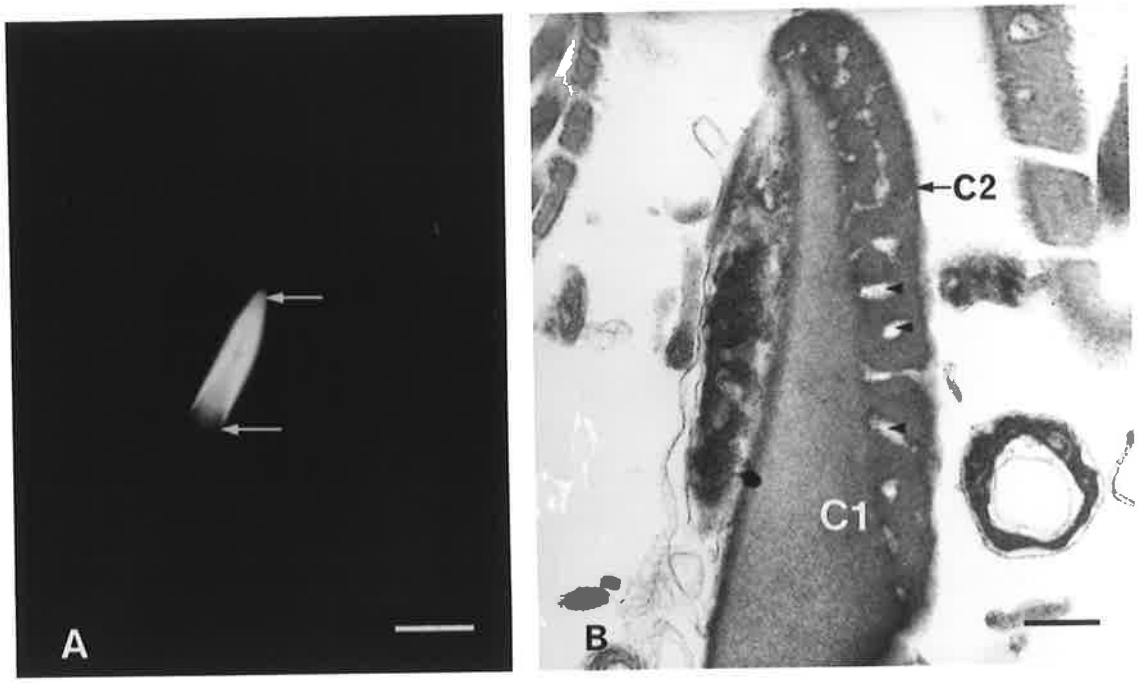
A
B
C2
C1

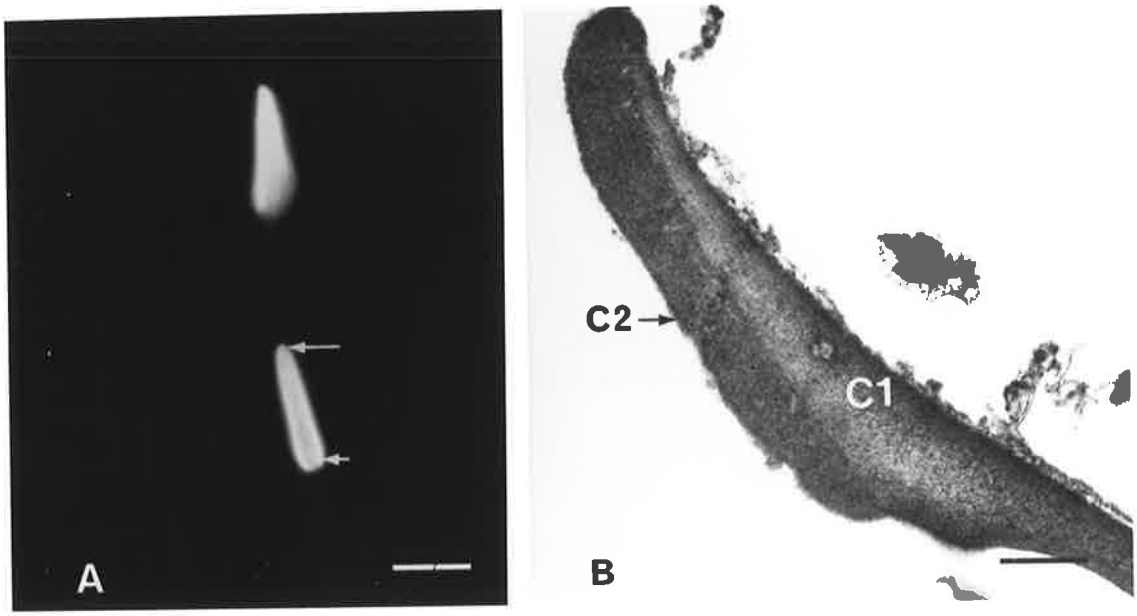
A
B
C2
C1

Chapter 5. ISOLATION OF SPERMATOZOA NUCLEAR BASIC PROTEINS[3]

5.1. INTRODUCTION

The pattern of DNA condensation of the C1 and C2 regions of *Sminthopsis* spermatozoa appears to be very different (Chapter 3). Chromatin C1 condensation occurs by gradual changes from a granular state to a highly compacted and homogenous structure. Condensation of the C2 region transpires by way of partial coalescence of chromatin subunits. The incomplete condensation of the chromatin produces the characteristic globular structures and associated grooves of the C2 region (Chapter 3 and 4). In addition, cytochemical studies indicate that DNA within the C2 region may be less condensed than that of C1 (Chapter 4).

The differences in the pattern of chromatin condensation of the two nuclear regions may be due to a shift in basic protein composition or in other factors that affect the ionic strength and the hydrophobic environment of the condensing chromatin. Therefore, there is a possibility that chromatin within the two nuclear regions may be organised by distinct proteins.

The objectives of this study were, to (1) isolate and identify the sperm nuclear basic proteins (SNBPs) from *Sminthopsis* by using reverse-phase HPLC and gel electrophoresis, and, (2) localise SNBPs to the sperm nucleus by immunocytochemistry (subject to the availability of antibodies).

---

[3]Work from this chapter has been included in a manuscript entitled "Isolation of histones, and related chromatin structures from spermatozoa nuclei of a dasyurid marsupial, *Sminthopsis crassicaudata*" submitted in July 1996 to J Exp Zool.

5.2. MATERIALS AND METHODS

Adult *Sminthopsis crassicaudata* males were used in all studies and they were sacrificed as described in Chapter 2. All steps were carried out at 4°C except where indicated.

5.2.1. Purification and identification of protamines

Cauda epididymal spermatozoa from ten *Sminthopsis* were expressed into Tris-HCl, pH 7.5 containing 1 mM PMSF, and washed three times with the buffer. SNBPs were extracted using a modified version of the method by Balhorn et al., (1977). Spermatozoa were decondensed by incubation in 5 M guanidine hydrochloride for 1 h and nuclear proteins were extracted in 8 M urea and 2 M NaCl, for another hour. Hydrochloric acid was added to 0.5 M and the sample was incubated for 1h and then centrifuged at 12 000 g for 10 min.

The supernatant containing SNBPs was run on reverse-phase HPLC (Varian 5000, Walnut Creek, USA) using a Vydac C-4 column (214TP54, Vydac Separation Group, Hesperia, CA) at a speed of 1 ml/min at room temperature and the proteins were eluted using a acetonitrile gradient from 10 to 30% in 0.1% trifluoroacetic acid (Ammer and Henschen, 1988). UV absorbance at 254 nm was recorded with an on-line detector and the protamine fraction was collected in an Eppendorf tube and dried in a speedvac. The HPLC purified protamines were electrophoresed in a mini-gel system (BioRad Laboratories, Pty Ltd, Richmond, CA) containing 15% polyacrylamide gel in 6.5 M urea at pH 3.2, and were also further characterised by subjecting the HPLC fraction to automated sequencing (Applied Biosystems 475, Victoria, Australia).

5.2.2. Extraction and fractionation of spermatozoa histones

Spermatozoa histones were extracted using a modified method of Ausio, (1992a). Caput and cauda epididymides from four *Sminthopsis*, were separated into two pools, cut into 3-4 mm^3 pieces and placed in distilled water. Spermatozoa exuded into the water without additional force applied to the tubules and were quickly collected, washed twice with PBS, and stored in 90% ethanol until further use. Sperm samples were also checked under phase contrast for somatic cell contamination.

The ethanol cell suspension was centrifuged at 16 000 g in a microfuge for 10 min and the pellets were dried immediately in a speedvac. For the removal of cytoplasmic membranes and tails, the pellets were resuspended in 150 mM NaCl, 20 mM Tris-HCl, pH 7.5 containing 0.5% Triton X-100, 0.4 mM PMSF and 10 μg/ml TLCK (approximately 100μl was used for a 0.5 x 10^6 cells pellet) and the homogenate was incubated for 20 min.

The suspension was centrifuged and the pellets obtained were resuspended and homogenised in 35% acetic acid and incubated for 1h at room temperature with occasional vortexing. The samples were centrifuged at 16 000 g for 10 min and hydrochloric acid was added to the acetic acid supernatants to a concentration of 0.25 M. The extracts were precipitated with 6 volumes of acetone at -20°C for 1 h, collected by centrifugation and dried in a speedvac. The precipitates containing *Sminthopsis* SNBPs were subjected to urea-acetic acid gel electrophoresis.

5.2.3. Gel electrophoresis and protein quantitation

Urea (2.5 M), acetic acid (5%) polyacrylamide gel electrophoresis of SNBPs was carried out using the method of Ausio, (1992a). A stock solution (40 ml) containing 30% acrylamide and 0.2% bisacrylamide was mixed with 10 ml of 43.2% acetic acid, 30 g of urea, and 70 mg of thiourea. Distilled water was added to 79.5 ml. At the solubilisation of the urea, 0.5 ml of 30% H_2O_2 were added to the mixture, and the resulting solution was immediately poured into gel tanks.

Protein markers used included chicken erythrocyte histones (Sigma), SNBPs from boar (from Dr. Zalensky) and salmon protamines (Sigma). The stained gels were scanned using a Molecular Dynamics personal densitometer (Model P.D) and quantitation of the bands was carried out by area integration.

5.2.4. Immunocytochemistry

The four polyclonal antisera used were (1) anti-histone H2B (from *Gallus*) (Muller et al., 1984), (2) anti-peptide (1-20) H2A (calf thymus), (3) anti-peptide (85-102) H4 (calf thymus), and (4) anti-histone H4 from mussel sperm (*Mytilus*), all raised in rabbits. The peptide sequences of both H2A and H4 are surface accessible regions on the nucleosome (Meziere et al., 1994; Monestier et al., 1993).

5.2.4.1. Immunofluorescence microscopy

Spermatozoa from three *Sminthopsis* were extruded from the cauda epididymidis into PBS, pH 7.5, washed three times with the buffer and fixed in 3% paraformaldehyde for 5 min. The sperm were washed twice for 5 min each time using 10 mM Tris, pH 7.7, containing 0.15 M NaCl, 0.1% Triton X-100, and 0.1% bovine serum albumin (BSA) (fraction V, Sigma, St Louis, MO).

The sperm were then incubated in 1:20 dilution each of the four antisera, for 1.5 h at room temperature, washed twice with buffer for 10 min, and incubated with FITC labelled goat anti-rabbit secondary antibody, for 30 min at 37°C. Following this, the sperm were washed twice and resuspended in 20μl of mounting medium. A drop of the suspension was placed on a slide for observation by confocal microscopy (MRC-1000, BioRad) using two filter combinations of wavelengths 488/522 nm and 568/605 nm. In control samples the primary antibody was omitted.

5.2.4.2. Immunoelectron microscopy

Epididymal and testicular tissues from three *Sminthopsis* were cut into approximately 1 mm^3 pieces and fixed with 0.25% glutaraldehyde and 0.4% paraformaldehyde (Appendix 1) for 4 h. The tissues were washed in 0.1 M phosphate buffer, dehydrated in ethanol, and embedded in LRW resin and polymerised at 50°C (Appendix 3). Thin sections were placed on nickel grids prior to immunolabelling with histone antibodies. Sections were washed twice for 5 min in PBS, pH 7.4 and then for 30 min in PBS containing 0.1% BSA and 0.05% Tween 20 (Sigma). They were incubated in a 1:100 dilution in PBS of normal goat serum for 10 min and washed in BSA and Tween 20.

The sections were incubated in 1:10 dilution of the antisera for 30 min at room temperature, and then for 16 h at 4°C, followed by two washes in 0.05% Tween 20 and PBS. They were incubated in a 1:20 dilution of the secondary antibody, goat anti-rabbit IgGs conjugated to 15 nm gold (Sigma), for 30 min at room temperature. Finally, the sections were washed in PBS, followed by distilled water, stained with 2% aqueous uranyl acetate and visualised in the transmission electron microscope (Phillips CM 100) at 60 kV. Control sections were treated as above with the omission of the primary antisera.

5.2.5. Production of antibodies to *Sminthopsis* protamine 1

5.2.5.1. Preparation of antigen

For the production of antibodies to protamine 1 of *Sminthopsis,* 7 animals were sacrificed and the spermatozoa, obtained from the cauda epididymidis. The protamines were extracted and purified as described in Section 5.2.1. The HPLC purified factions, dried in a speedvac, were pooled into three tubes, each containing approximately, 30 μg of protamines. This amount was estimated by area integration of HPLC peaks using salmon protamines of known concentrations as standards.

Saline (170 μl) was added to 30 μg of protamines in an Eppendorf tube and the mixture was vortexed until the proteins have dissolved. Heparin (30 μl at a concentration of 1000u/ml) was added to the protamine solution and kept on ice for 30 min to allow the molecules to conjugate. Freund's Complete Adjuvant (200 μl) was added and the solution was vortexed vigorously and passed through a syringe attached to a 20 G needle several times to create a thick emulsion.

Two 10-12 week old male Balb/C mice were each inoculated with approximately 200 μl of the emulsion, given a booster injection after 3 weeks, and another injection after 6 weeks. Retro-orbital bleeds from the immunised mice were taken 10 days after the third injection and the final bleed took place a week later. The blood was left for 1h to clot at room temperature, placed at 4°C for 6h, and centrifuged at 10 000 rpm for 10 min. The serum was removed using a pipette and stored at -20°C until further use.

5.2.5.2. Fluorescence tests for protamine antibodies

Immunocytochemistry

The method for this test has been described in Section 5.2.4.1. The antisera were diluted 1:20, 1:40, and 1:80 with PBS, pH 7.5, prior to use.

Polystyrene latex beads assay

Polystyrene latex beads (10μl) (Boehringer, Germany) were added to 100 μl of a solution of protamine 1 from *Sminthopsis* (10 μg/ml). The mixture was incubated at room temperature for 2h in an Eppendorf tube to allow the protamines to attach to the latex beads. The bead/protamine complexes were

collected by centrifugation at 10 000 rpm for 5 min and washed twice with PBS, pH 7.5. The complexes were blocked with a solution of bovine serum albumin (BSA) (1 mg/ml) for 2h, washed twice with PBS and stored at 4°C in 10 mM sodium azide. As a positive control, mouse IgG (Sigma) was incubated with latex beads in place of protamines.

The following fluorescent study was used to determine whether the immune mouse serum contained antibodies to protamines from *Sminthopsis*. The antisera were diluted 1:10, 1:20, 1:40 and 1:80 with PBS, incubated with the bead/protamine complex for 1h, and washed twice with PBS. This was followed by incubation for 30 min with a secondary antibody, sheep anti-mouse IgG conjugated to FITC (Silenus, Hawthorn, Australia) diluted 1:20 with PBS. After two washes with PBS, an aliquot (20 μl) of the mixture was placed on a slide, mounted with Slow Fade medium (Molecular Probes) and visualised using a fluorescence microscope (Olympus). For the positive control, the latex bead/mouse IgG complexes were incubated with non-immune mouse serum followed by the secondary antibody. For the negative control, untreated latex beads were similarly incubated with non-immune mouse serum and the secondary antibody.

5.3. RESULTS

5.3.1. Sperm protamine purification and partial sequencing

Reverse-phase HPLC revealed the presence of a single protamine class in *Sminthopsis* spermatozoa that was eluted at 19% acetonitrile following a 32 min retention time (Fig. 5.1). Guanidine hydrochloride, Urea, NaCl and PMSF were eluted early during the flow. The purified protamine was partially sequenced and the N-terminus was found to begin with the ARYR tetrapeptide, a feature characteristic of type 1 protamine or P1 (Oliva and Dixon, 1991). The partial sequence was aligned and compared with the DNA derived amino acid sequence of protamine 1 from *Sminthopsis crassicaudata* (Retief et al., 1995a) (Fig. 5.2). Acid-urea gel electrophoresis indicated the *Sminthopsis* protamine to be a low molecular weight protein that differed in electrophoretic mobility from boar and salmon protamines (Fig. 5.3A).

5.3.2. Extraction of spermatozoa histones

Approximately $5x10^6$ cauda epididymidal spermatozoa containing about 20 μg of DNA were used for the extraction of SNBPs. Phase contrast observations showed no contamination with somatic cells.

In order to visualise the SNBP histone fraction, spermatozoa nuclei from *Sminthopsis* were first extracted with 35% acetic acid. In contrast to 0.4 N HCl which tends to extract both protamines and histones with similar efficiency, this concentration of acetic acid preferentialy solubilizes histones (Subirana et al., 1973). Extraction of SNBPs from cauda epididymidal spermatozoa using this method showed that all five histones, H1, H2B, H2A, H3 and H4 were present as illustrated by acid-urea gel electrophoretic analysis (Fig. 5.3B, Lane 1). Hydrochloric acid extraction following that of 35% acetic acid, produced mainly protamines (Fig. 5.3B, Lane 2). Analysis of 0.4 N HCl extraction of caput epididymidal spermatozoa nuclei showed that both histones and protamines are present (Fig. 5.3B, Lane 3).

Densitometric analyses of the electrophoretic patterns shown in Figure 5.3B measured the approximate amount of histones present in the cauda epididymal and in caput epididymal spermatozoa fractions to be 25% and 45%

respectively. The major SNBP component is the low molecular weight protamine 1.

5.3.3. Immunolabelling of histone antibodies

Immuocytochemistry showed that antiserum to histone H4, labelled the apical, lateral and posterior regions of the mature spermatozoon nucleus. The localisation of histone H4 is illustrated in Figure 5.4A which is a composite of z-series optical sections obtained by confocal microscopy. The labelling, shown in green fluorescence, corresponded regionally to the location of C2 chromatin (Fig. 5.4A). Similar results were obtained for the other histone antisera, H2B and antisera for the peptides of histones H2A and H4 (not shown). In the control experiment, where the primary antibody was omitted, there was no positive immunofluorescence of the nuclei (Fig. 5.4B).

EM sections of cauda epididymal spermatozoa following immunogold labelling using histone H2B antibody, revealed 18-40 gold particles/μm^2 (from 30 spermatozoa; n=3 animals) in the C2 region (Figs. 5.5A and B). There was neither any significant labelling of structures in the C1 region nor in the control sections.

In testicular spermatozoa, an enlarged nuclear envelope (ENE) that resulted following nuclear condensation (Chapter 3; Soon and Breed, 1996), contained material which labelled positively with the histone antibodies (Fig. 5.5C). During spermatozoa transport along the epididymis, the ENE gradually disappeared as the spermatozoon head rotated from a T-configuration in relation to the sperm tail, to a streamlined position (Chapter 3; Soon and Breed, 1996). Concurrent with the disappearance of the ENE, a reduction in antibody labelling of the ENE material occurred in corpus epididymidal spermatozoa (Fig. 5.5D). In contrast, the C2 chromatin retained a positive labelling for the histone antibodies in the mature spermatozoon (Figs. 5.5A, B and D).

5.3.4. Immunolabelling tests for antibodies to protamines

5.3.4.1. Immunocytochemistry

The spermatozoa nuclei of *Sminthopsis* incubated with immune sera from the two mice did not display any fluorescence (not shown).

5.3.4.2. Polystyrene latex beads assay

The positive control showed that the polystyrene latex bead/mouse IgG complexes were fluorescent whereas the negative control did not display any fluorescence as expected (not shown). However, there was no fluorescence observed for the polystyrene latex bead/protamine complexes incubated with the immune mouse serum indicating an absence of a primary antibody (to protamine 1) (not shown).

5.4. DISCUSSION

This study shows that the mature spermatozoa of *Sminthopsis crassicaudata* contain protamine as the major protein component. The N-terminal region of the protamine molecule, as determined by sequential Edman degradation, contains the tetrapeptide, ARYR that is characteristic of mammalian (Oliva and Dixon, 1990), and avian (Chiva et al., 1987; 1988), P1 or Type 1 protamine. This partial amino acid sequence is also identical to the N-terminus of the complete protamine sequence deduced from the nucleotide sequence of the gene (Retief et al., 1995a, b).

The electrophoretic mobility of the protamine of *Sminthopsis* indicates that it has a higher molecular weight than both boar and salmon protamines. Indeed *Sminthopsis* P1 consists of 65 amino acids (Retief et al., 1995a) whereas the lengths of bull P1 and salmine are 45 and 30 amino acids, respectively (Balhorn, 1989).

The attempt to raise monoclonal antisera to *Sminthopsis* P1 has been unsuccessful. Due in part to their small size, protamines are generally poor immunogens (Le Lannic et al., 1993). However, polyclonal antisera to protamines from ram (Courtens et al., 1983), mouse (Rodman et al., 1984), and boar (Courtens et al., 1988) have been successfully elicited in rabbits. In addition, Le Lannic et al., (1993) have raised monoclonal antibodies to both P1 and P2 protamines of humans.

In an attempt to increase immunogenicity, human protamines have been conjugated to significantly larger molecules such as methylated bovine serum albumin (Roux et al., 1987) and ram protamines have been complexed with RNA (Courtens et al., 1983). In this study, *Sminthopsis* protamine 1 was associated with heparin for the same reason. Others have found that it is possible to raise antibodies to unconjugated protamines (Stanker et al., 1987, Le Lannic et al., 1993) using protein concentrations of 80-100 μg/injection in mouse. Why this present study has been unsuccessful can perhaps be partially explained by the low amount of antigen used (15 μg/injection) regardless that the protamines have been coupled to heparin.

Electrophoresis of total proteins from the mature spermatozoa showed that in addition to the protamine, also present is a subset of histones comprising approximately 25% of nuclear proteins. All five histones (H1, H2A, H2B, H3,

H4) are present in nearly stochiometric ratios. Approximately equal amounts of H2A, H2B, H3 and H4 molecules are detected whereas histone H1 amounts to half the concentration of the other histones. This ratio is similar to the proportion of histones that occur in eukaryotic cells, regardless of the physiological state of the cell (Kornberg and Klug, 1981).

The amino acid sequence of histone molecules are remarkably well conserved, for example, histone H4 from pea seedlings differs in only two out of 102 amino acids from histone H4 isolated from calf thymus (Kleinsmith and Kish, 1995).

Table 5.1 shows the different classes of histones and their approximate molecular weights. These proteins are larger than protamines which have molecular weights that range from 5000 daltons (Balhorn, 1989) to 8000 daltons as in *Sminthopsis* P1. In addition, there are fewer arginine molecules in histones compared to protamines which may contain up to 65% arginines.

TABLE 5.1: THE HISTONE CLASSES (Kleinsmith and Kish, 1995)

Type of histone	Number of amino acids	Size (daltons)	Arginine
H1	215	23 000	1%
H2A	129	14 000	9%
H2B	125	13 800	6%
H3	135	15 300	13%
H4	102	11 200	14%

Although the amino acid sequence of the core histones is highly conserved, the chromatin structure may be altered by differences in the sequence of histone H1. In the inactive chromatin of chicken erythrocytes and the spermatozoa of the sea urchin, variable forms of histone H1 are known to exist (Poccia and Green, 1992). Histones are also subject to reversible chemical modifications such as acetylation (Ausio and van Holde, 1986), methylation (Selker, 1990),

phosphorylation (Hunter and Karin, 1992), and ADP ribosylation (Latchman, 1990).

It is unknown at this stage whether the spermatozoa histones of *Sminthopsis* are different with respect to the amino acid sequence compared to somatic cell histones and whether they are post-translationally modified as in the acetylated variety found in the mature spermatozoa of humans.

Caput epididymal spermatozoa retain an enlarged nuclear envelope (ENE) which contains nuclear pores (Chapter 3; Soon and Breed, 1996). In eutherian testicular spermatids, there is a similar presence of an electron-lucent region surrounded by a nuclear envelope (Courtens and Loir, 1981b), however, the occurrence of this structure in caput epididymal spermatozoa appears to be unique to the dasyurids.

The ENE does not contain DNA, but stains positively for lysine-rich proteins (Chapter 3; Soon and Breed, 1996), and the present immunocytochemical study demonstrates that histones are present but become removed along with the ENE as spermatozoa travel along the epididymis. In addtion, extraction of SNBPs and densitometric measurements indicate that spermatozoa from the caput epididymidis contain a larger percentage of histones, approximately 45%, compared to those from the cauda epididymidis (25%). Histones within the ENE may be residual from sperm nuclear condensation in the testis and become removed from the nucleus via nuclear pores during epididymal transit.

The mature spermatozoon, however, retains a subset of histones within the C2 chromatin region. Unlike the spermatozoa histones of other species of mammals so far described (Gatewood et al., 1987), those of *Sminthopsis* have a defined location within the nucleus.

It is not clear whether the histones of C2 chromatin are acetylated or not. This could have implications in both transcriptional activity (Grunstein, 1991; Turner, 1991; Ausio, 1992b; Felsenfeld, 1992, Woodcock et al., 1993) and histone removal during spermiogenesis (Christensen and Dixon, 1982). As shown in Chapter 3, DNAase-gold conjugates have been localised to the C2 region and it appears that the DNA binds to histones. Therefore the spermatozoa histones are unlikely to be residual from spermatogenesis, but like the protamines, they may have a role in the structural organisation of the chromatin. Although the significance of this is unknown, the impact on the physiology of spermatozoa

transportation and survival must be profound since DNA of nucleohistones is more vulnerable to attack by nucleases and damage by free radicals compared to DNA packed within the almost crystalline structure of nucleoprotamines. This raises the question of how this marsupial species protects its spermatozoa chromatin, and a possible mechanism may be the secretion of high levels of DNA stabilising factors such as polyamines within the reproductive tracts.

5.5. CONCLUSION

In this study, sperm nuclear basic proteins were fractionated by reverse-phase HPLC and characterised using acetic acid-urea PAGE. The main protein component was partially sequenced and identified as protamine 1. A subset of histones consisting of H1, H2A, H2B, H3 and H4 was detected in nearly stochiometric amounts and constituted approximately 25% of total protein. Immunocytochemistry demonstrates that histones occur within the peripheral C2 region but not in the C1 chromatin. The contents of the ENE also localised to histone H2B antibodies. The ENE may serve to remove testicular histones that are displaced from the chromatin during nuclear condensation. In eutherians, similar allusions to the basal knobs at the posterior of spermatids as being residual histone and/or centromeric proteins that are eventually removed from the nucleus, have been made (Courtens et al., 1992). The attempt to raise antibodies to protamine 1 has not been successful.

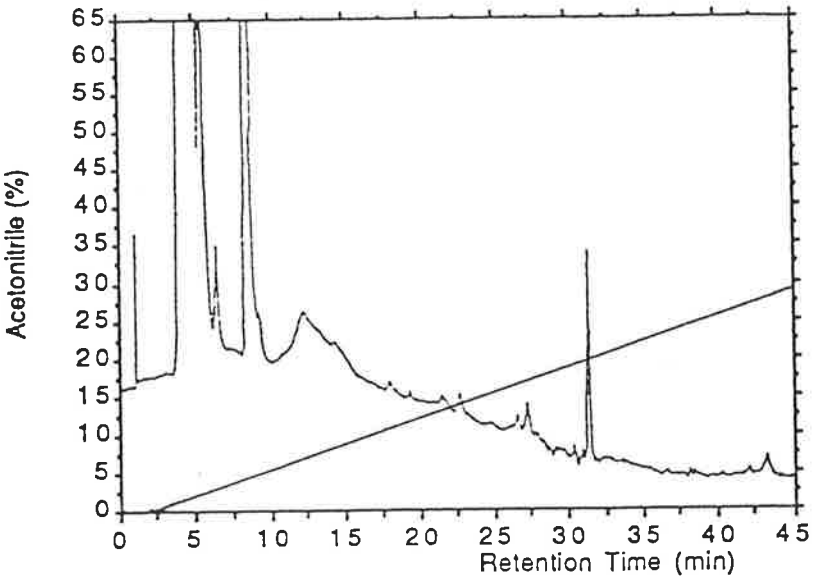

Figure 5.1. Reverse-phase HPLC of total protein from *Sminthopsis* spermatozoa. Proteins were eluted in a 10 to 30% acetonitrile gradient with 0.1% trifluoroacetic acid, within a run-time period of 45 min. Initial peaks represent runoffs of urea, salt and PMSF. The bound protamine was detected as a major peak eluted at 19% acetonitrile following a retention time of 32 min.

```
                          10                  20                  30
(A)   - A R Y R R H S R S R S R S R Y R R R R R R S R H H N R R R T Y
(B)   M A R Y R R H S R S R S R S R Y R R R R R R S R H H N R R R T Y
                  40                  50                  60
(A)   - - - - - - - - - - - - - - - - - - - - - - - - - - - - - - -
(B)   R R S R R H R R H S R R R R G R R R G Y S R R R Y S R R G R R R Y
```

Figure 5.2. Protamine 1 partial sequence of *Sminthopsis crassicaudata* obtained by automated sequencing of HPLC purified protein (A), aligned with the full protein sequence deduced from DNA (B) (Retief et al., 1995a).

Figure 5.3A. Gel electrophoretic analysis of *Sminthopsis* protamine (Lane 1), in comparison to the spermatozoa nuclear basic proteins (SNBPs) from boar (Lane 2). (CE = chicken erythrocyte histones; Sl = salmon protamine (salmine); Scr = *Sminthopsis* protamine; Br = boar protamine).

Figure 5.3B. Proteins extracted with 35% acetic acid from cauda epididymides of *Sminthopsis* (Lane 1), proteins recovered using 0.4 N HCl following the 35% acetic acid extraction (Lane 2), and, total proteins extracted with 0.4 N HCl from caput epididymal sperm of *Sminthopsis* (Lane 3). (CE = chicken erythrocyte histones).

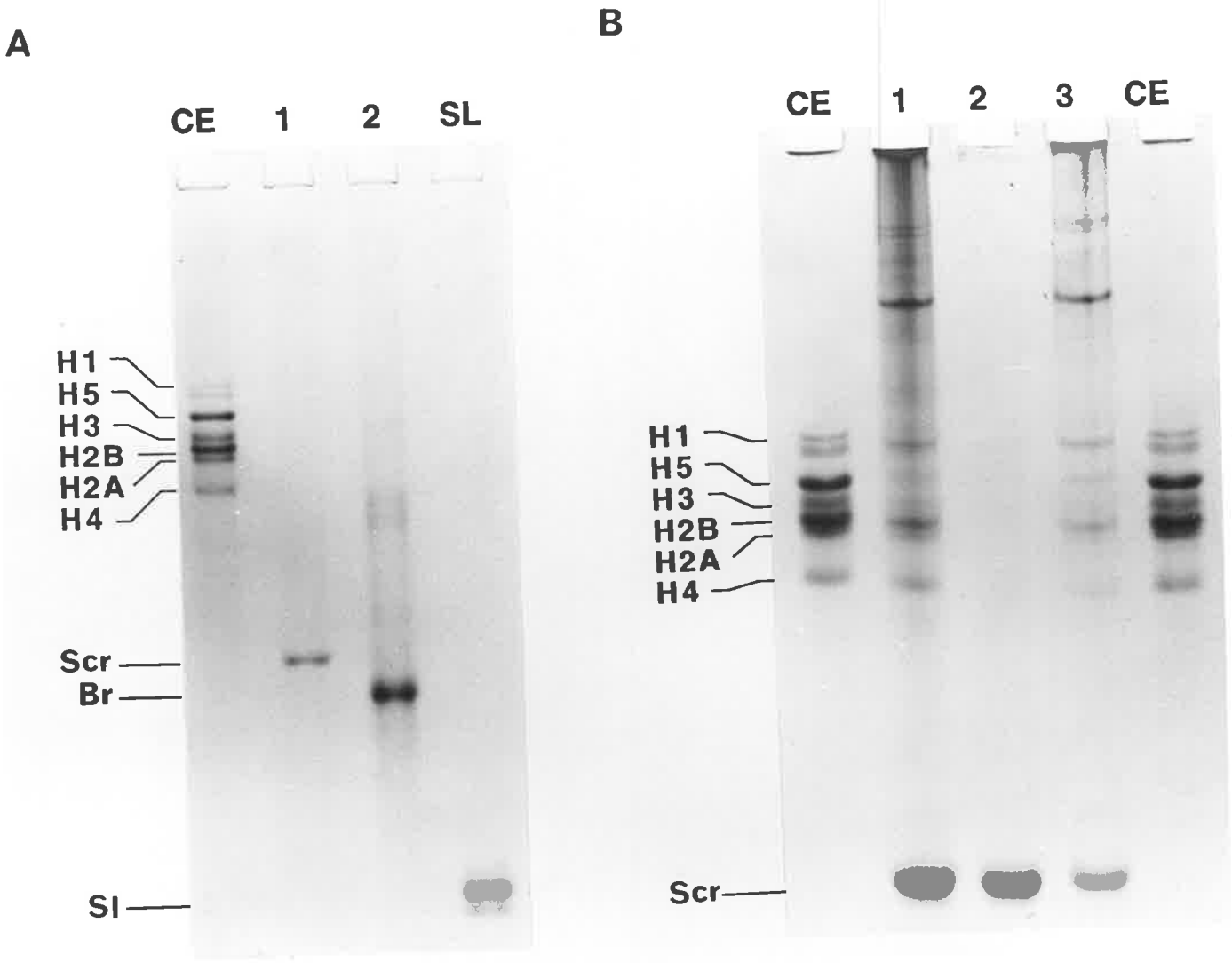
A
CE
1
2
SL
H1
H5
H3
H2B
H2A
H4
Scr
Br
Sl
B
CE
1
2
3
CE
H1
H5
H3
H2B
H2A
H4
Scr

Fig 5.4. Merged confocal optical sections of *Sminthopsis* sperm nucleus showing localisation of histone H4 antibodies to peripheral chromatin (green fluorescence), and propidium iodide counterstaining of chromatin is in red fluorescence (A). Control sperm showed staining with propidium iodide but not with FITC (B). Bar = 5 μm.

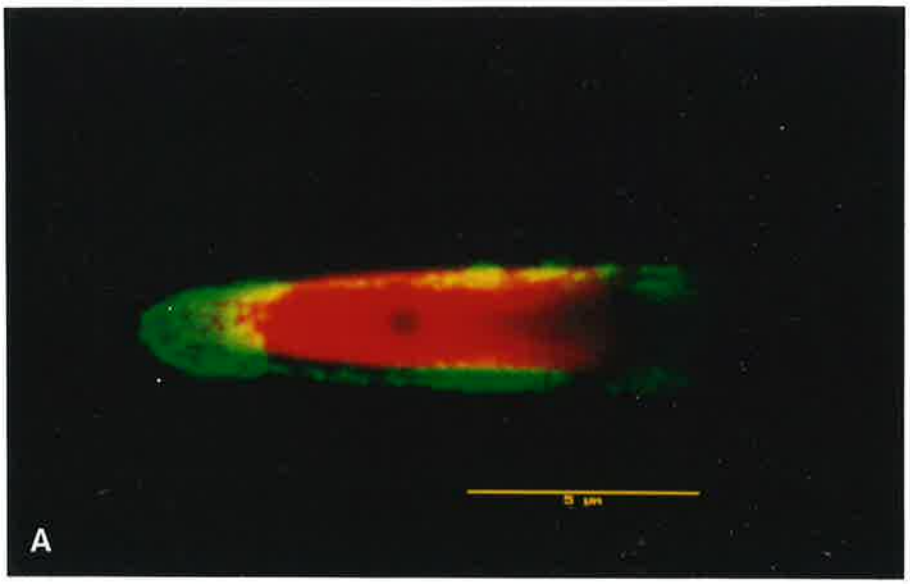
5 µm
A

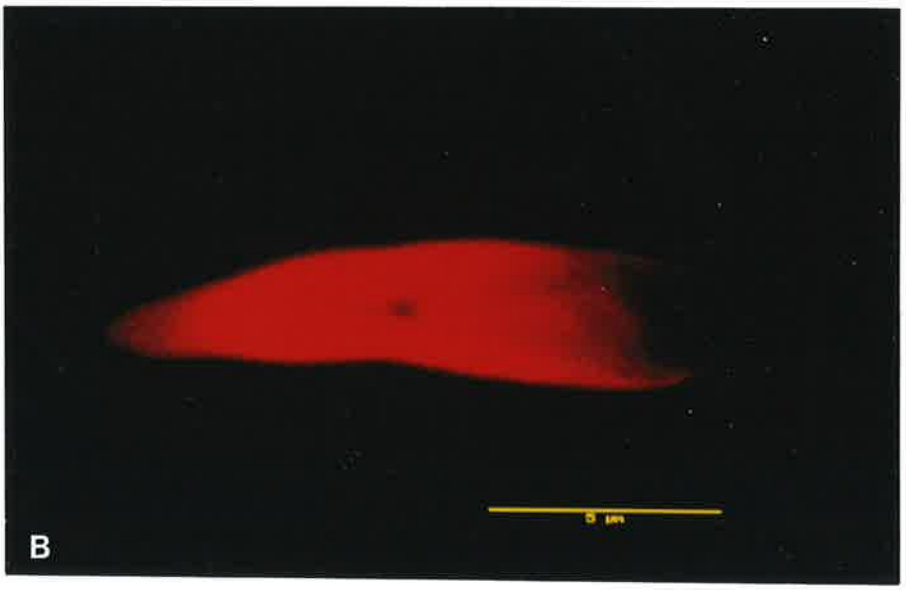
5 µm
B

Fig 5.5. Immunogold labelling with histone H2B antibodies. Anterior region of the sperm head from cauda epididymides showing localisation of antibodies to C2 chromatin (A and B). Longitudinal section of the posterior region of a testicular sperm, showing localisation of antibodies to material within the ENE (C). Transverse section of the posterior head region of a spermatozoon from corpus epididymidis, showing the last vestiges of the ENE and labelling of the C2 chromatin (D). (Cyt, cytoplasm; ENE, enlarged nuclear envelope; N, nucleus). Bar = 210 nm.

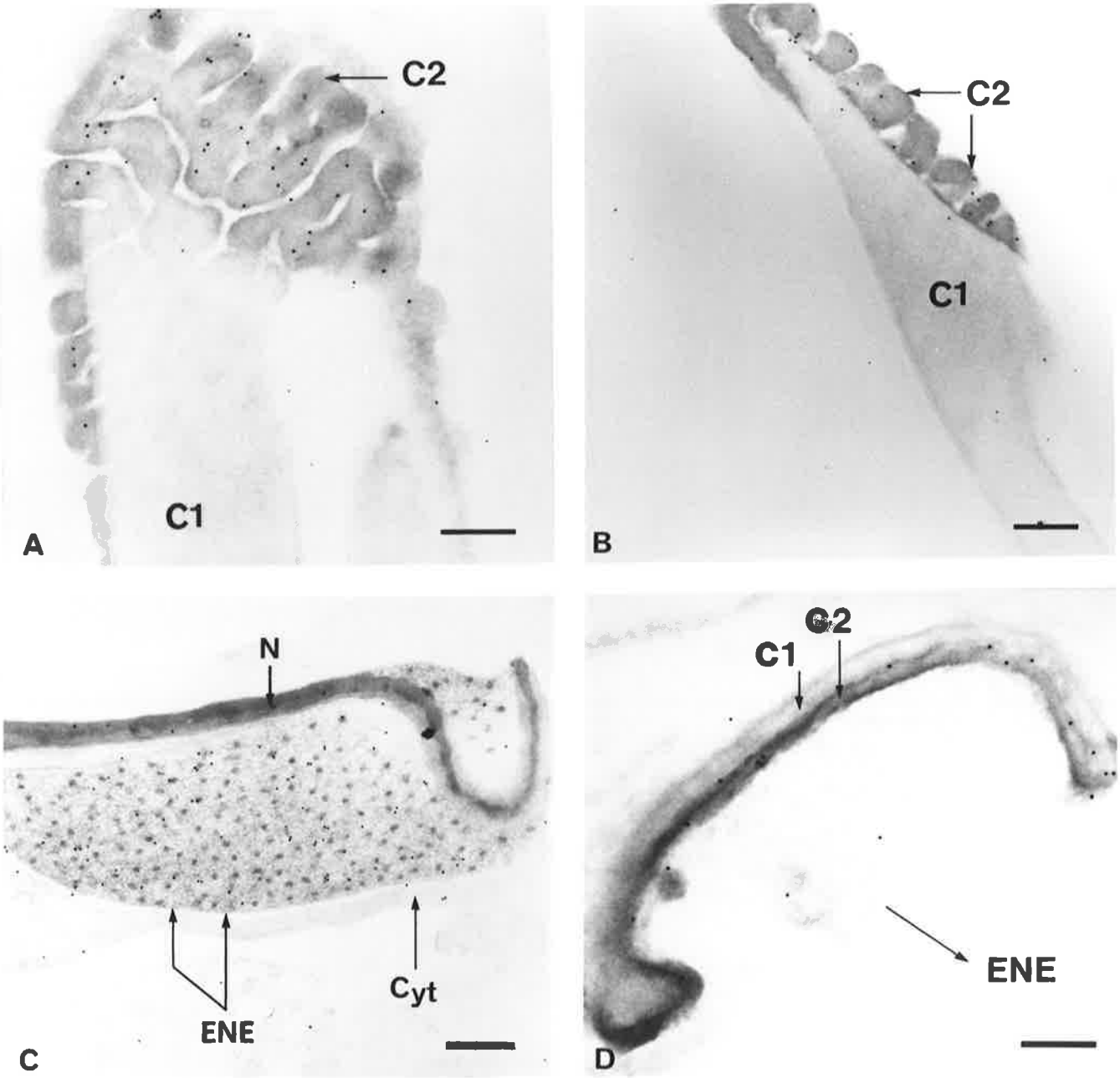
C2
C1
A
C2
C1
B
N
ENE
Cyt
C
C2
C1
ENE
D

Chapter 6. VISUALISATION OF SPERMATOZOA HIGHER ORDER CHROMATIN STRUCTURES: ATOMIC FORCE MICROSCOPE AND TRANSMISSION ELECTRON MICROSCOPE STUDIES

6.1. INTRODUCTION

The packaging of DNA into a small nuclear volume is facilitated by tertiary level organisations of DNA-protein fibres of nucleohistones and nucleoprotamines. The higher order organisation of chromatin has been investigated using various microscopical methods such as transmission electron microscopy, (Thoma et al., 1979; Rattner and Hamkalo, 1978) and more recently the native three-dimensional chromatin structure has been studied using cryo-electron microscopy (Woodcock and Horowitz, 1995) and scanning force microscopy (Allen et al., 1993; 1995; Leuba et al., 1994). The lower level organisation of the chromatin could be studied by unravelling the native structure using enzymatic and/or diffusion techniques.

One of the objectives of the present study was to examine the peculiar morphology of the spermatozoon nucleus of *Sminthopsis crassicaudata,* using the atomic force microscope (AFM). The AFM is a relatively new application in the study of biological materials and has some advantages over other high resolution imaging techniques especially in the relatively mild sample preparation required for the scanning of organic surfaces. AFM allows visualisation of the unfixed, uncoated, and partially hydrated samples at nanometer resolutions (Hoh and Hansma, 1992). The extensive dehydration and harsh processing conditions required for transmission electron microscopy (TEM) is thus avoided. AFM applications also include scanning in liquids, whereby cells are monitored and studied under physiological conditions avoiding the effects of degenerative changes.

AFM instrumentation (Topometrix) consists of the force sensor unit, peizoelectric ceramics, a feedback electronic circuit (EPU unit), and a computer (CPU unit) containing softwares for the control of the instrument, conversion of the electronic signals into a visual representation, and image processing and analysis.

A small video camera is focused onto the cantilever and is used to monitor the distance between the probe tip and sample surface and to visually estimate the position of the sample and probe.

The force sensor is an essential component of the AFM and offers very high spatial resolution, routinely measuring distances with an accuracy of 1Å. The sensor consists of a cantilever which secures the sensing probe, a laser source, a pair of mirrors which reflect the laser beam and a photodetector that transmits the imaging signals through the feedback circuit (Fig. 6.1).

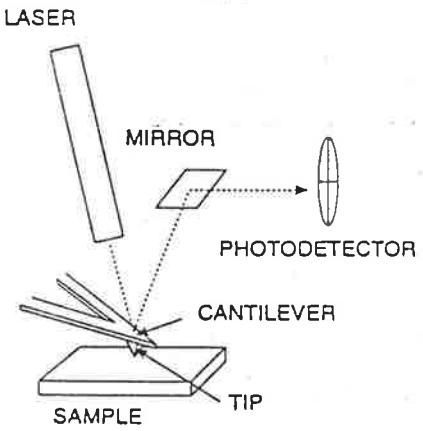

Fig. 6.1. Force Sensor (Topometrix Instrument Manual). During topographic image acquisition, the distance between the probe tip and specimen surface is determined by the peizoceramics and is kept constant by a feedback mechanism (not shown).

To begin imaging, the laser beam is focused onto the edge of the cantilever and the probe is brought into contact with the specimen. The cantilever is activated to raster across the surface. Deflections of the cantilever during scanning are detected by the laser beam and reflected by the mirrors to the photodetector. The difference in light intensity reflecting movement of the cantilever is translated into height data, and a feedback mechanism adjusts the height of the stage (specimen holder) relative to the probe tip to maintain constant force (/distance). The feedback circuit therefore causes dimensional changes in the peizo to keep applied vertical forces within a user-defined limit.

The relationship between the cantilever's motion, x, and the force required to generate the motion, F, is given by Hooke's Law:

F = -kx, where k is the force constant measured in newton/meter.

As the scanning continues, the x, y, and z data which depict the topography of the specimen within a designated area, are collected and translated into a three-dimensional image.

In this study, the AFM has been used to study the nuclear topology of *Sminthopsis* spermatozoa and as a comparison, spermatozoa nuclei of another species of marsupial from a different family, the brush-tail possum, *Trichosurus vulpecula*, have also been similarly imaged. Unlike the spermatozoa chromatin of *Sminthopsis* which is packaged by both histones and protamines, that of *Trichosurus*, is packaged by two types of protamines. Both the possum protamines are arginine-rich and are likely to have similar biochemical properties (R Balhorn, personal communication).

For AFM imaging, spermatozoa from both species were demembranated, adhered to glass coverslips and scanned in both the fixed and unfixed states with the AFM. Using an image analysis software, the size of the higher order chromatin structures of the nucleohistone and nucleoprotamine regions were measured.

Another objective of this study was to investigate the effects of micrococcal nuclease on the spermatozoa chromatin of *Sminthopsis*. This enzyme has been extensively used in the study of chromatin due to its ability to discriminately cleave the linker region of nucleosomal DNA (Zabal et al., 1993). The spermatozoa nuclei from *Sminthopsis* were incubated with micrococcal nuclease, and the digestion products, as well as the undigested sperm chromatin, were observed using the TEM.

6.2. MATERIALS AND METHODS

6.2.1. Atomic force microscopy

Removal of sperm membranes

The cauda epididymides from three adult male *Sminthopsis* and two brush-tailed possums were removed from the scrotum, cut into smaller pieces and spermatozoa were expressed into 10 mM Tris-HCl, pH 7.5. The sperm were demembranated by incubating for 20 min in 5 mM DTT together with either 1% MTAB or 0.05% Triton-X 100. Following three centrifugations and resuspensions of spermatozoa nuclei into 10 mM Tris-HCl, pH 7.5 to remove the reagents, a sample of the nuclei was fixed with 3% paraformaldehyde for 5 min and another was left unfixed. The samples were washed with buffer and resuspended in 5 mM Tris-HCl, pH 7.5.

Scanning with AFM

Droplets of the spermatozoa nuclei were placed onto coverslips, air-dried, and washed twice with distilled water. Samples were mounted on the Explorer stage of the atomic force microscope designed for the imaging of biological specimens (Topometrix, California). The nuclei were scanned in contact mode which operated in the repulsive force region. The cantilever curved away from the sample due to the forces generated between the surface of the specimen and the tip of the probe. The displacement of the probe was signalled through the feedback loop to adjust the z-piezoelectric ceramic so that a constant force was maintained throughout the scan. The probe used, Supertips #10 (Topometrix), was fabricated as a thin extension of a pyrimidal base (Appendix 5; cantilever/tip specifications). The sharp probe was susceptable to breakage and could cause damage to the specimen due to the high forces generated during scanning. However, with careful optimisation of scanning parameters such as the scan speed and feedback settings, high resolution data within tens of nanometer or less could be obtained.

All samples were scanned less than 12 h following sample preparation unless otherwise indicated. Some *Sminthopsis* spermatozoa were desiccated in a chamber containing sodium hydroxide pellets for more than 36 h and similarly imaged with the AFM. Chromatin structures were measured using the

microscope's image analysis package (Topometrix). Computer images in TIFF format were converted to PICT files using Adobe Photoshop v3.0. Images were grouped, labelled and printed as illustrated in the Figures, using Powerpoint v4.0.

6.2.2. Micrococcal nuclease digestion

This study follows the method of Zabal et al., (1993) with some modifications. All buffers and solutions used contain 1 mM PMSF and incubations were conducted at 4°C unless otherwise indicated. Epididymal spermatozoa were washed three times in 15 mM Tris-HCl, pH 7.5 containing 22% sucrose, 60 mM KCl, 15 mM NaCl, followed by a 30 min incubation with 0.05% Triton X-100 and 5 mM dithiothreitol (DTT) (Sigma) made up in the above buffer. For cell lysis, spermatozoa were washed three times with 5 mM Tris-HCl, pH 7.8.

The resulting sperm nuclei were digested in a solution containing 1 mM $CaCl_2$ and 300 units/ml micrococcal nuclease (Worthington) made up in 5 mM Tris-HCl for 3 h, at 37°C. The reaction was halted by adding ethylenediaminetetraacetic acid (EDTA) in 50 mM stock solution to a concentration of 2 mM and incubated for 20 min. The sample was centrifuged at 12 000 g for 10 min and the supernatant containing digested chromatin was collected. H1-containing material was precipitated by adding an equal volume of 15 mM Tris-HCl, pH 7.4, containing 200 mM NaCl, to the supernatant and incubated for 45 min (Zabal et al., 1993).

Chromatin was collected on coated grids for electron microscopy (Section 6.2.3), and pellets containing residual chromatin were fixed in 3% glutaraldehyde, washed twice with 0.2 M phosphate buffer pH 7.5, post-fixed with 1% osmium tetroxide and dehydrated in a series of alcohol. The sperm were then embedded in TAAB resin which was polymerised at 60°C for 48 h (Appendix 3). Thin sections were cut and stained with 2% uranyl acetate before visualisation under the transmission electron microscope (Phillips CM100).

6.2.3. Transmission electron microscopy of nucleosomes

Micrococcal digested sperm chromatin was either placed immediately onto carbon-coated grids or was spread using tri-L-(dimethylaminomethyl)phenol (DMP 30) (Tousimis Research Corporation, Rockville, MD). DMP 30 was freshly diluted in double-distilled water to 2 %, and 5 μl was added to a 200 μl solution

containing approximately 0.2 μg of DNA (Bratosin-Guttman, 1992). A 30 μl droplet of the mixture was placed on a parafilm sheet, covered for protection, and left for 10 min at room temperature to allow a monolayer of DMP 30 to form at the air-water interface. Celloidin- and carbon-coated grids were placed on top of the droplets and the monolayers containing diffused nucleosomes, were lifted onto the grids and left at room temperature for 3 min. The specimens were washed by placing the grids on droplets of PBS. They were then fixed with 3% paraformaldehyde, washed again with distilled water, and stained with 2% aqueous uranyl acetate for 1 min. After a final wash in distilled water, they were air-dried and viewed with the transmission electron microscope (Phillips CM100).

6.3. RESULTS

6.3.1. Atomic force microscopy

Atomic force microscopy and image analysis of *Sminthopsis* spermatozoa chromatin showed that the C1 and C2 chromatin can be distinguished by differences in (1) the arrangement of the higher order chromatin structures and (2) the size of these structures. High resolution AFM images showed that the higher order chromatin units from both regions were composed of nodules. Those of C1 chromatin appeared tightly packed against one another (Fig. 6.2A), whereas nodules from the C2 chromatin have a loose arrangement (Figs. 6.2A, B and C). The diameter of the higher order structures of C1 chromatin range from 45 to 60 nm. Larger nodules of 120-160 nm in diameter were measured for the C2 chromatin (Fig. 6.2C, D; Fig. 6.5).

Spermatozoa chromatin that was stored in a desiccator consisted of nodules that appeared somewhat flattened or depressed compared to those that were not desiccated and imaged less than 12 h following sample preparation (Figs. 6.3A and B). In addition, nodules of the C1 chromatin in the desiccated specimen have adopted a linear arrangement (Fig. 6.3B). The chromatin nodules of the C1 regions are smaller than those from the C2 region (Fig. 6.3A). In the possum, nucleoprotein particle sizes were of the similar magnitude as those observed for the C1 chromatin in the dunnart (Fig. 6.4A and B). These nodules were also tightly packed together similar to those of the C1 chromatin (Fig. 6.5).

There was no difference in the topology of the nuclear surfaces nor in the size of structures measured for the fixed and unfixed specimens. However, the chromatin was more readily disrupted when unfixed which caused the probe to adhere to the chromatin resulting in distortions of the images and costly replacements of probes. Unless scanning is conducted under physiological conditions, the specimen is best fixed briefly in 3% paraformaldehyde prior to scanning in air.

6.3.2. Micrococcal nuclease digestion

Following incubation with micrococcal nuclease for 3h, the C2 chromatin was enzymatically cleaved from the C1 region (Figs. 6.6A and B; 6.7A and B). TEM of the separated C2 chromatin showed the presence of 30-38 nm

agglomerates (Figs. 6.6A and B) which appeared to disperse into smaller 11-14 nm structures (Figs. 6.7A and B) upon spreading of the chromatin using DMP 30 (Bratosin-Guttman, 1992). The remaining chromatin retained the shape of the spermatozoon head as observed by UV fluorescence following treatment with the nuclear fluorochrome, DAPI (not shown). When visualised with the TEM, the residual spermatozoa were devoid of C2 chromatin and appeared to consist only of C1 chromatin (Figs. 6.8A and B).

6.4. DISCUSSION

Atomic force microscopy of the spermatozoa nuclei of *Sminthopsis* shows that the higher order chromatin structures of the two nuclear regions are very different. The C1 region appears to consist of 45-60 nm chromatin nodules, whereas the C2 chromatin contains bundles of 120-160 nm sized particles. In the spermatozoa nuclei of the brush-tailed possum, only one nuclear region occurs, and AFM scanning indicates that chromatin particle sizes are similar to those found within the C1 chromatin of *Sminthopsis* spermatozoa nuclei. In addition, AFM studies on eutherian spermatozoa (mouse and bull), showed that the chromatin consisted of closely packed 50-100 nm sized nodules (Allen et al., 1993; 1995). Therefore, it appears that the higher order structures of spermatozoa nucleohistones (120-160 nm in diameter) in *Sminthopsis*, are considerably larger than those of nucleoprotamines from *Trichosurus* (45-80 nm) and the eutherian species (50-100 nm). Interestingly, the micrococcal nuclease-resistant C1 chromatin contain nucleoprotein structures (45-60 nm) that fall within the range of sizes of nucleoprotamine higher order structures from the other species.

The organisation of chromatin particles appears to differ in those packaged by histones from those packaged by protamines. AFM images show that the nucleoprotamine particles of *Trichosurus* and the particles within the C1 chromatin occur as a tight assemblage, whereas those of nucleohistones pack in loose bundles. The clustered three-dimensional organisation of the latter may account for the numerous fissures observed in EM sections of the C2 chromatin in *Sminthopsis* spermatozoa. Imaging at later stages following desiccation of the samples, shows chromatin nodules that appear flattened and which adopt a linear arrangement. Whether these are artifacts as a result of drying or whether they give an insight into the arrangement of the particles is unknown. However, these observations caution against interpreting linearity in chromatin organisation in samples that have been extensively dehydrated.

There are some technical limitations associated with AFM imaging of biological structures that could lead to anomalies in the images. The tip geometry is sometimes convoluted into the image and the shape of the tip becomes integrated into the topographic data of the specimen (Butt et al., 1992). Such tip effects observed as 'edge broadening' (Fig. 6.3A) are, to a certain extent, an inherent part of AFM imaging.

The resolution of the AFM is limited by the dimension of the tip of the probe that is in closest contact with the specimen surface. Small contact areas using sharp probes, although theoretically improves resolution, can bring additional stress onto the specimen (Peachey and Eckhardt, 1994). Tip compression tends to occur during scanning at high resolution when force loads are at the highest as the tip approaches very close to the specimen (Worcester et al., 1988). Most biological specimens are soft and have elastic properties. The surfaces tend to flatten during scanning but regain the original dimensions once the tip has moved on. This effect is also seen during the scanning of spermatozoa nuclei at high resolutions. As an example, the nodules in the C2 region appear clustered in the 4 μm scan but are more diffused in the 2 μm scan (Figs. 2C and D). Inelastic deformation causes more permanent damage to the specimen and this has happened in the unfixed spermatozoa.

The C2 chromatin is readily cleaved by micrococcal nuclease from the C1 chromatin which remains intact even after a three hour period of digestion. This suggests that the C1 region consists of nucleoprotamines that form highly condensed, and nuclease-resistant, chromatin (Tanphaichitr et al., 1982), in contrast to nucleohistones in the C2 region. The product of micrococcal nuclease digestion of C2 chromatin, as visualised on coated-grids, is fibres or agglomerates of 32-38 nm structures that are of similar dimensions to the higher order chromatin structures of isolated somatic cell chromatin (Thoma et al., 1979; Rattner and Hamkalo, 1978). In *Sminthopsis,* these structures unravel into 11-14 nm nucleosomal structures upon dispersion of the chromatin with a spreading agent. These observations are consistent with the view of a somewhat irregular folding of the 11 nm nucleosomal fibre into a 30 nm fibre in the presence of histone H1 (Horowitz et al., 1994; Woodcock et al., 1993). In human spermatozoa, which lack histone H1 in the histone complement (Gatewood et al., 1990), higher order chromatin structures probably do not occur.

6.5. CONCLUSION

The chromatin of spermatozoa from *Trichosurus* consists of nodules that are between 45 to 80 nm in diameter and the C1 chromatin of the spermatozoa from *Sminthopsis*, contain closely packed nodules of 45-60 nm in diameter. The C2 chromatin which consists of nucleohistones, has larger, higher order, structures that range from 120 to 160 nm in diameter. Enzymatic studies and *in situ* observations show that 11 nm nucleosomal filaments are arranged as larger 30 nm fibres. These are in turn folded into the 120-160 nm fibres of the C2 region, as observed by AFM imaging.

AFM of the posterior end of spermatozoa nucleus of Sminthopsis imaged within 12 hours following sample preparation.

Fig. 6.2A. On the dorsal surface, imprints of the acrosome (a) and periacrosomal ring (p) are evident. The C2 chromatin occurs along both lateral sides (black arrows) of the nucleus and within an area, approximately 1.5 μm from the caudal extremity of the nucleus. Two long furrows (black arrows) along both sides of the nuclei may demarcate the border between the two chromatin regions; C2 lies on the outer edge and C1 occurs interior to the groove. Note the clustering of particles in the C2 region that result in a loose arrangement, and the presence of indentations or grooves (blue arrows). By contrast, nodules within the C1 region are closely packed against one another (unfilled arrows). Boxed region represents the approximate area of magnification of Figure 6.2B.

Fig. 6.2B. High resolution image of the dorsal nuclear surface posterior to the acrosome. Green arrows show the edge of the periacrosomal ring. Nodules of the C1 chromatin appear closely packed together (unfilled arrows), whereas those of the C2 chromatin are less closely opposed to one another (blue arrows).

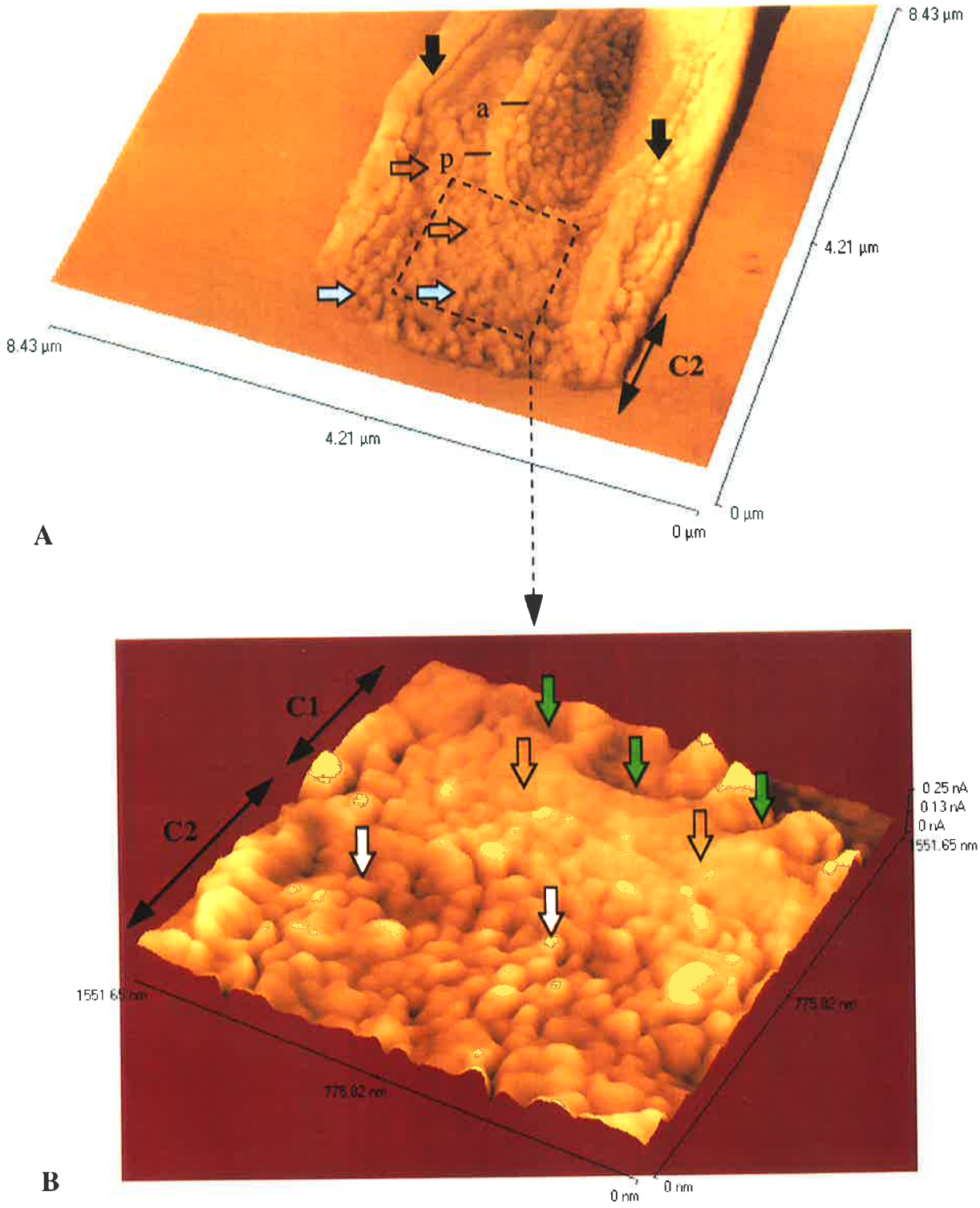
8.43 µm
a
p
4.21 µm
C2
8.43 µm
4.21 µm
0 µm
0 µm
A
C1
C2
0.25 nA
0.13 nA
0 nA
551.65 nm
775.82 nm
775.82 nm
0 nm
0 nm
B

Fig. 6.2C. Ventral surface of spermatozoa nuclei at the posterior, showing nodules of 120-140 nm in diameter, occurring as bundles within the C2 nucleohistone region (blue arrows).

Fig. 6.2D. High resolution of ventral surface of the nuclei. Red arrows indicate an arbitrary division line between the C1 region (blank arrow) and the C2 region (blue arrow). The C2 nodules appear less clustered due perhaps to surface deformation caused by high sample-probe interactive forces.

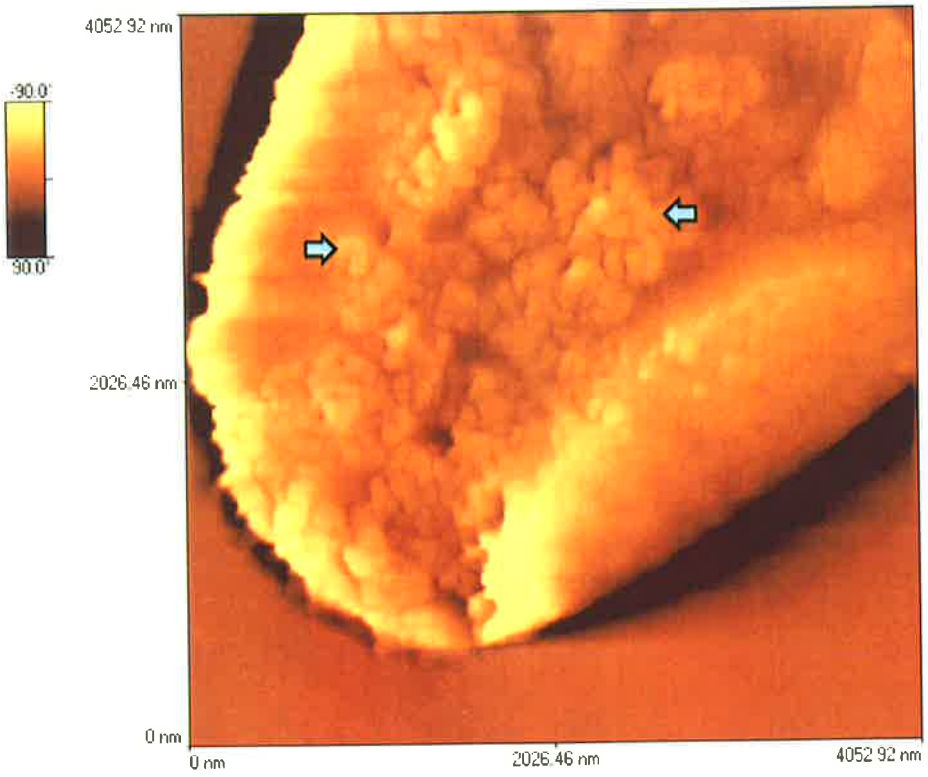
4052.92 nm
-90.0°
90.0°
2026.46 nm
0 nm
0 nm
2026.46 nm
4052.92 nm

C

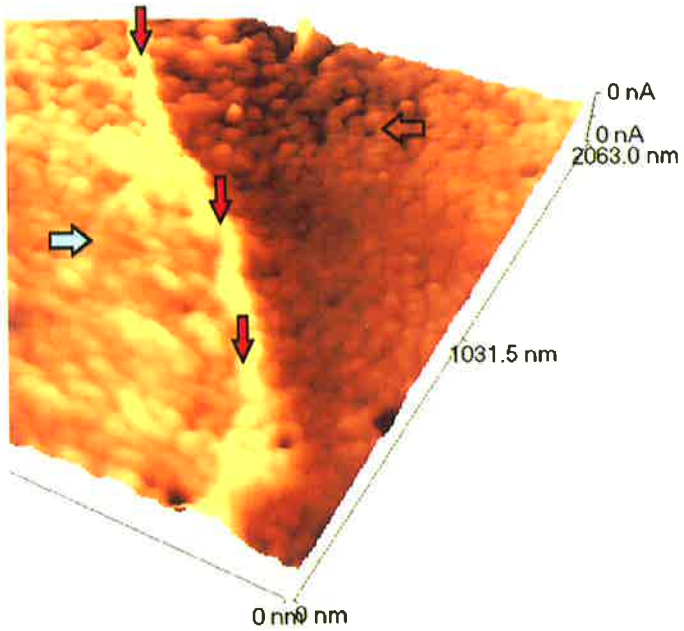
0 nA
0 nA
2063.0 nm
1031.5 nm
0 nm
0 nm

D

Cauda region of the nucleus of Sminthopsis spermatozoa (stored in a disiccator for more than 36h).

Fig. 6.3A. Ventral surface showing larger nodular structures in the C2 chromatin (grey arrows) compared to those within the C1 chromatin (blank arrows). These nodules have a more flattened appearance unlike those of Fig. 6.1. Black arrows indicate artifactual imaging of the sides of the tip where there is a sudden increase in height along the lateral edges of the nuclei. Boxed region indicates the magnified area of the nucleus of Figure 6.3B.

Fig. 6.3B. High resolution of the C1 chromatin showing a linear alignment of the nodules, parallel to the long axis of the spermatozoa nuclei. Note the flattened appearance of the nodules.

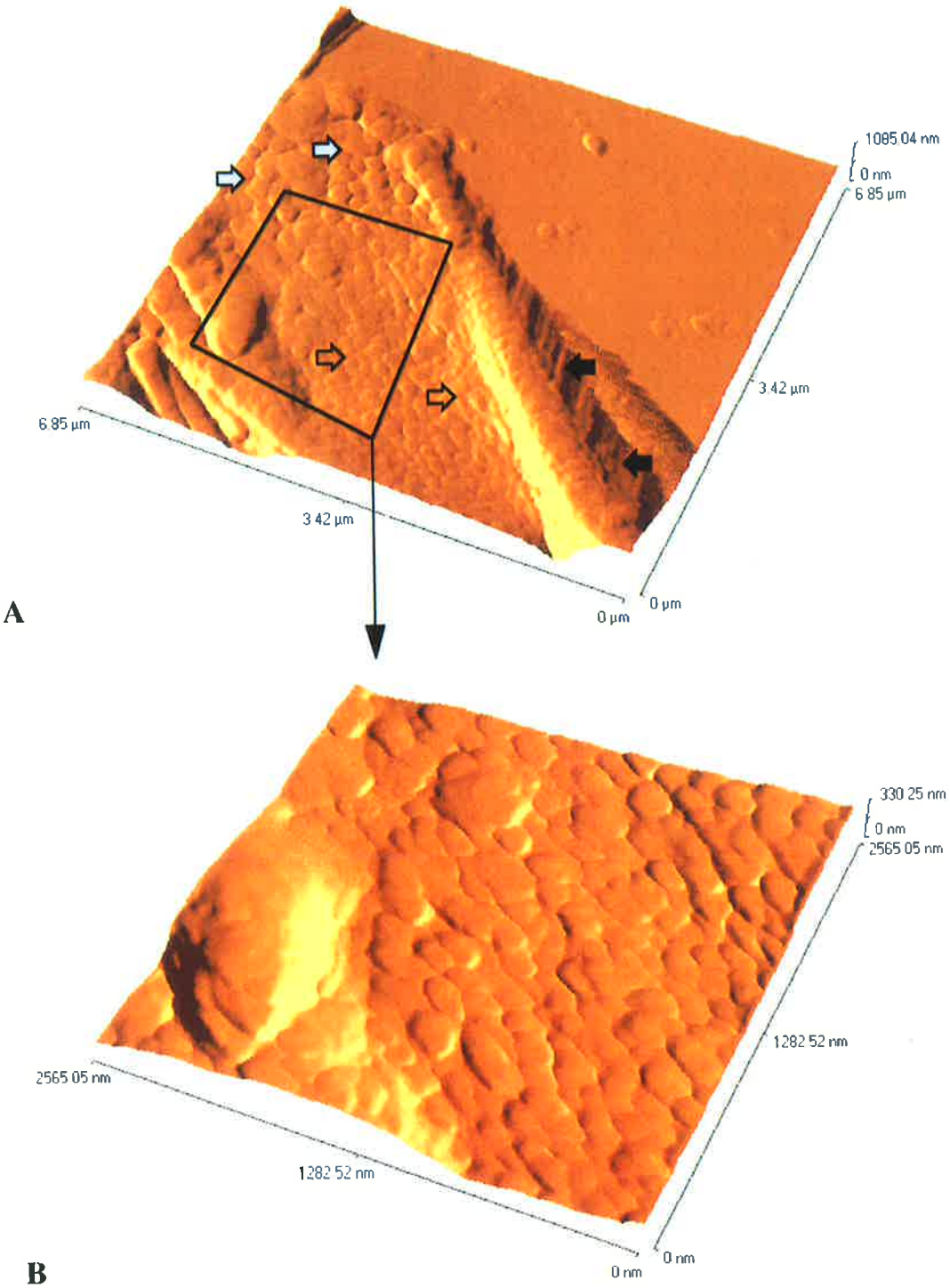
1085.04 nm
0 nm
6.85 µm
3.42 µm
6.85 µm
3.42 µm
0 µm
0 µm
A
330.25 nm
0 nm
2565.05 nm
1282.52 nm
2565.05 nm
1282.52 nm
0 nm
0 nm
B

Fig. 6.4A. Low resolution image of the ventral surface of *Trichosurus* spermatozoon nucleus. Red arrow shows the implantation site of the flagellum.

Fig. 6.4B. High resolution scanning of the ventral surface of *Trichosurus* spermatozoon nucleus. Particles within the size range of 50-80 nm are present on the nuclear surface (blank arrows). Red arrow indicates region of flagellum implantation.

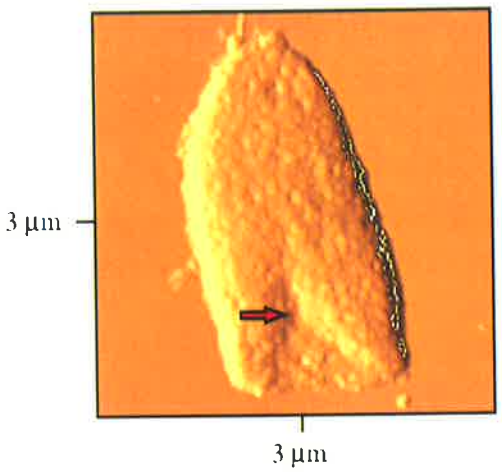
3 µm
3 µm

A

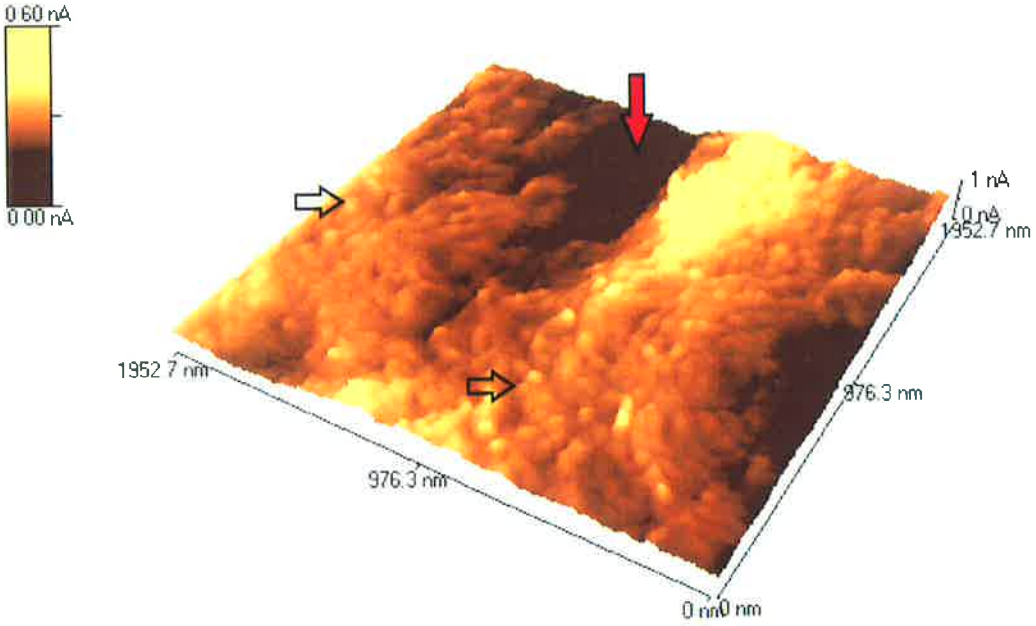
0 60 nA
0 00 nA
1 nA
0 nA
1952 7 nm
1952 7 nm
976.3 nm
976.3 nm
0 nm
0 nm

B

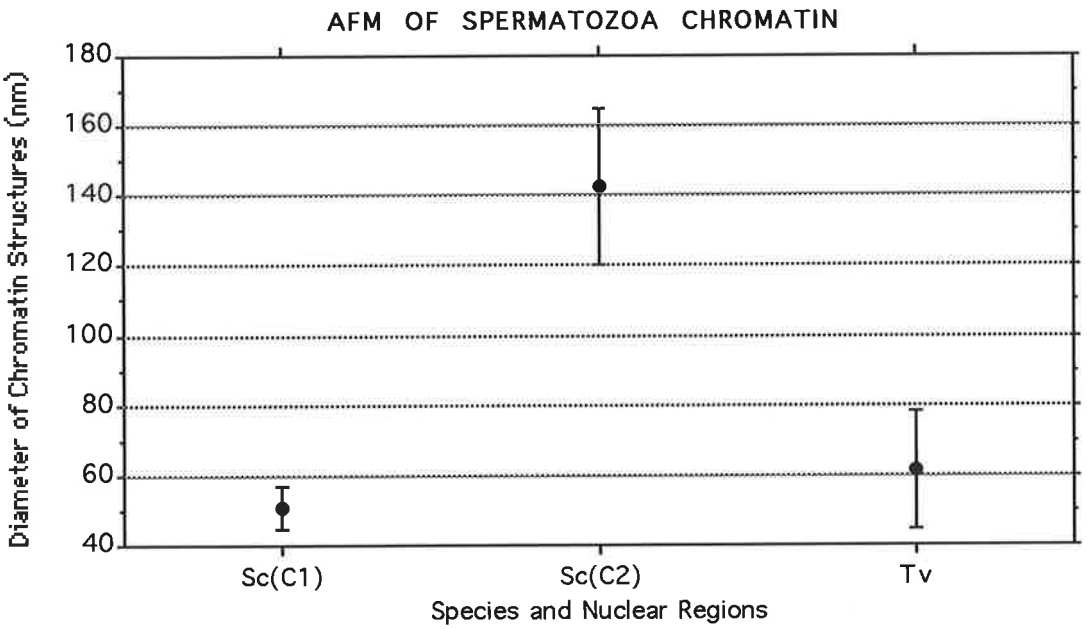

Fig. 6.5. Means and standard deviations of the diameter of chromatin nodules measured for the respective nuclear regions of *Sminthopsis* spermatozoa (Sc) and for the nucleus of the spermatozoa of possum (Tv). The nodule sizes of the C1 region (Sc(C1)) falls within the range of those for possum. These nodules are much smaller than those from the C2 region (Sc(C2)). The mean of nodule diameter of Sc(C2) is approximately 140 nm and is more than twice the means for that of Sc(C1) (~50) and Tv (~60nm).

Fig. 6.6. C2 chromatin cleaved with micrococcal nuclease showing agglomerates of 30-38 nm in diameter (A and B). Bar = 144 nm.

Fig. 6.7. Smaller (11-14 nm) structures (arrows) unravelled at the edges of 30-38 nm agglomerates, following spreading of chromatin using DMP-30 (A and B). Bar = 102 nm.

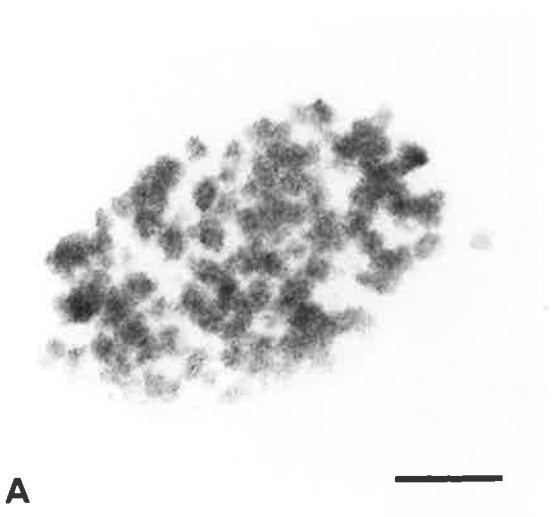

A

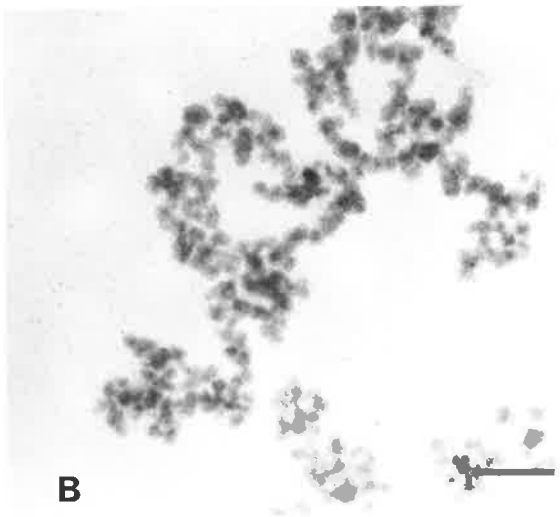

B

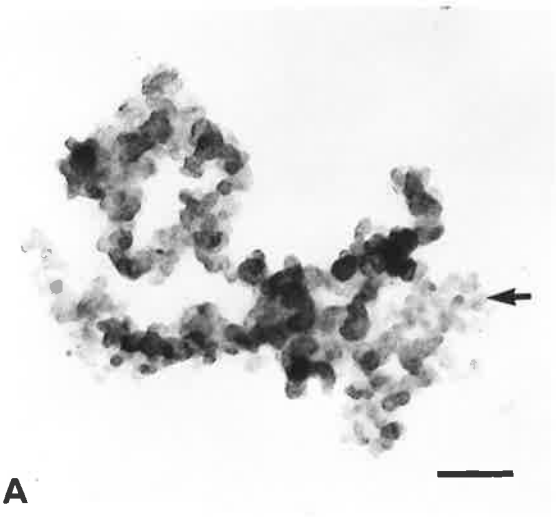

A

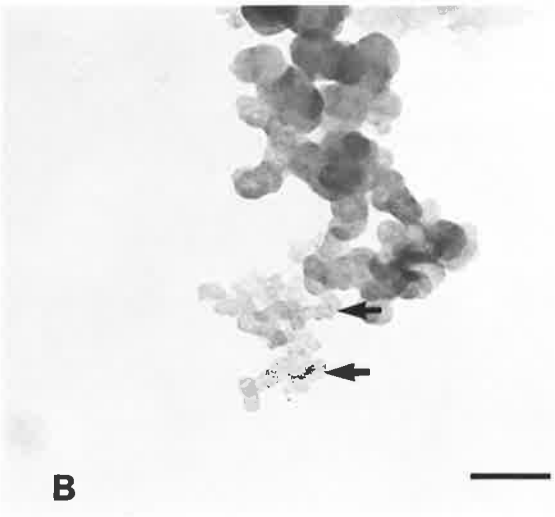

B

Fig. 6.8. Transmission electron microscopy of sperm nucleus incubated with micrococcal nuclease, showing the absence of C2 chromatin. C1 chromatin however, remained condensed. Transverse section at the mid-region of *Sminthopsis* sperm nucleus (A) and (B) illustrates an oblique section. Bar = 389 nm.

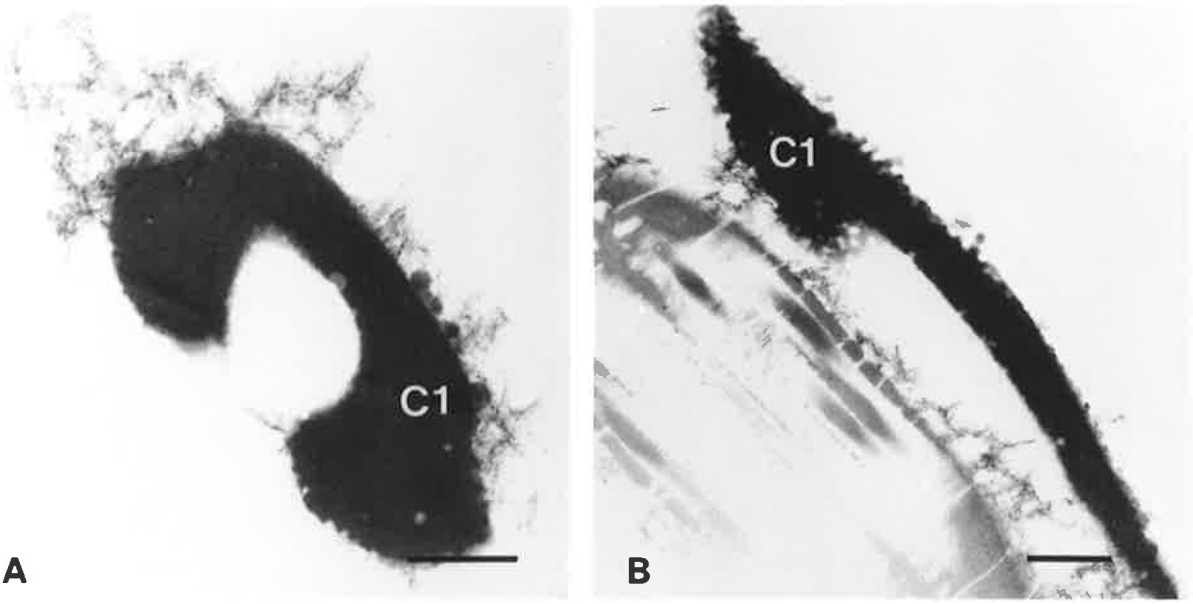
C1
A
C1
B

Chapter 7. CHARACTERISATION OF DNA FROM THE NUCLEOSOMAL REGION OF SPERMATOZOA NUCLEI

7.1. INTRODUCTION

This study aimed to (1) determine whether or not DNA from the two nuclear regions, C1 and C2, contains sequences that are specific to each region, (2) characterise region-specific DNA sequences, and (3) localise these sequences and other structural DNA such as telomeres to the spermatozoa nuclei.

In Chapter 6, it was shown that C2 chromatin (nucleohistone region) can be separated from the C1 region using micrococcal nuclease. Ultrastructural observations indicated that C1 chromatin remained intact following incubation with the enzyme, whereas C2 chromatin was preferentially digested. In the present study, micrococcal nuclease was used separate the two chromatin regions and DNA from the C2 chromatin was purified for molecular cloning. Plasmids containing the cloned DNA fragments from the C2 region were radiolabelled for use as probes in Southern blot analyses to determine whether the probes localised to specific genomic factions of spermatozoa DNA. The cloned sequences were also biotinylated for fluorescence *in situ* hybridisation studies to determine the localisation of the sequences within the spermatozoa nuclei and within fibroblast chromosomes. In addition, the cloned inserts were characterised by sequencing. Purified DNA from the C1 chromatin region was used in similar Southern analyses and *in situ* hybridisation studies to ascertain whether or not the DNA occurred in regions of the spermatozoa and fibroblast genome that are different from DNA derived from the C2 region.

Human telomeric sequences were made into probes to determine the localisation of telomeres in the spermatozoa of *Sminthopsis*. Telomeric DNA caps the ends of linear eukaryotic chromosomes and protect the chromosome ends against recombination. These sequences consist of simple tandem repeats that are G-rich on one strand, and are highly conserved between species. The same human telomeric repeat, (TTAGGG)n is found in *Neurospora crassa*, a filementous fungus (Schechtman, 1990). The localisation of telomeric DNA in spermatozoa nuclei may help to further elucidate the organisation of the chromatin, given their distinctive position at the tips of chromosomes.

7.2. MATERIAL AND METHODS

7.2.1. Micrococcal nuclease digestion

Spermatozoa chromatin from four animals was digested with micrococcal nuclease as described in Section 6.2.1. The reaction was halted with 2 mM EDTA and the sample was centrifuged at 14 000 g for 10 min. Proteinase K was added to the supernatant containing the digested C2 chromatin and incubated for two hours at 37°C. The DNA (Fraction I) was extracted using phenol-chloroform, and precipitated in 90% ethanol. Salts were removed by washing the precipitate with 70% ethanol. The DNA was collected by centrifugation at 14 000 g for 10 min and the ethanol removed with a micropipette. The purified DNA was air-dried, resuspended in distilled water and stored at -20°C until further use in molecular cloning. DNA from spermatozoa C1 chromatin which remained intact after micrococcal nuclease digestion (Fraction II) was similarly purified for Southern hybridisation studies.

7.2.2. DNA cloning

Micrococcal nuclease digested DNA was end-filled using T4 kinase (Boehringer, Mannheim, Germany), co-precipitated with tRNA and resuspended in distilled water. The blunt-ended DNA fragments were incubated with a cloning vector, PCR-Script (Stratagene, Melbourne, Australia), a restriction enzyme *Srf* I, which recognises the octanucleotide sequence 5'-GCCC/GGGC-3', and T4 DNA ligase (Boehringer, Mannheim). Following a two hour incubation at room temperature and a 10 min incubation at 65°C, the ligation sample was ethanol precipitated, resuspended in distilled water, and transformed into competent DH5α *E coli* bacteria by electroporation (BioRad, Richmond, CA, USA) (Appendix 6). The cells were spread onto agar plates containing ampicillin and incubated for 10 h at 37 °C. White colonies were selected, streaked onto agar plates and grown overnight at 37°C. Positive transformants were selected to grow overnight in LB broth (Appendix 6). A plasmid preparation was made from the bacterial harvest and used for hybridisation studies and sequencing as described in the following sections.

7.2.3. DNA sequencing

The inserts were characterised by automated DNA sequencing (Model 373A, Applied Biosystems).

7.2.4. Southern hybridisation

7.2.4.1. Genomic and spermatozoa DNA preparation

Liver tissue (~1 g) from two *Sminthopsis* was homogenised in 2 ml of 5 M guanidine thiocynate (Promega) and left to cool on ice for 5 min. Sodium acetate (3M, pH 5.2) (200μl) was added and the solution was chilled on ice until the reaction has stopped. An equal volume of phenol:chloroform (1:1) in 0.1M Tris buffer containing 10mM EDTA, pH 8, was added to the homogenate, and incubated for 15 min on ice followed by centrifugation at 13 000 g for 15 min.

The supernatant containing liver DNA was removed and the DNA was precipitated with an equal volume of isopropanol. The isopropanol was removed following centrifugation at 13 000 for 5 min and 70% ethanol was added to remove excess salts. The ethanol was removed following centrifugation of the sample and the pellet of DNA was left to dry at 37° for 15 min. The dry pellet was resuspended in TE buffer pH 8, containing 0.5 M NaCl. RNAse (10 μg/ml) (20 μl) was added and the solution was left at room temperature for 3h. The DNA was purified using 1:1 phenol-chloroform, precipitated as before, and dissolved in TE buffer, pH 8.0 until further use.

Spermatozoa DNA was purified as described in Section 7.2.1.

7.2.4.2. DNA transfer and hybridisation

Approximately equal amounts of DNA (10 μg) from Fraction II (Section 7.2.1) and total *Sminthopsis* genomic DNA were digested with *Eco*RI (Promega, Madison, WI, USA), electrophoresed in a 1.5% agarose gel, transferred onto a nylon membrane (Hybond, Amersham) and UV cross-linked for 1 min (365 nm). The membrane was incubated in a solution containing a blocking reagent (Boehringer, Mannheim) (Appendix 1) for four hours. The clones were labelled with ^{32}dCTP by nick translation according to instructions from the Bionick kit (Promega). The probe was hybridised to the membrane overnight at 42°C. The radioactive solution was removed the following day and three washes with a

solution containing 6xSSC (Appendix 1) and 0.1%SDS were carried out at 42°C. The membrane was exposed to X-ray film at -80°C for 24 h and autoradiographed.

7.2.5. Fluorescence *in situ* hybridisation

7.2.5.1. Metaphase chromosome preparation

Sminthopsis fibroblasts were grown overnight until confluent in RPM1 1640 medium (CSL Biosciences, VIC, Australia) containing 10% fetal bovine serum (CSL Biosciences). On the following day the culture medium was discarded and the cells were rinsed three times with PBS. Trypsin (0.05%) (CSL Biosciences) was added to the cells and incubated at 37°C for a few minutes. The cells were dislodged by tapping the flask, added to 10 ml of medium and collected by centrifugation at 15 000 rpm for 5 min. Following two more washes in culture medium, the cells were grown in a new flask containing 1 μl/ml of 5-bromo-deoxyuridine (BrDU) (CSL Biosciences) for 7 h at 37°C. Two drops of colchicine (100μg/ml) were added to the cells which were incubated for another hour. The cells were harvested (Appendix 7) and rinsed with 75 mM KCl. Fixative (3:1 methanol:acetic acid) was added and a drop of cell suspension was placed onto clean slides and air-dried.

7.2.5.2. Spermatozoa DNA preparation

Cauda epididymal spermatozoa from two male *Sminthopsis* were treated with 0.05% Triton X-100 and 5 mM DTT for 20 min at 4°C. The spermatozoa were washed three times with PBS to remove the reagents and resuspended in distilled water. The cells were fixed with (3:1) methanol and acetic acid and drops of the sperm suspension were placed onto clean slides and air-dried.

7.2.5.3. In situ hybridisation

DNA from spermatozoa and chromosomes was denatured by placing slides in a coplin jar containing 70% deionised formamide heated to 70°C, for 2 min. The DNA was cooled in 70% ethanol at 4°C for 2 min, dehydrated in 80%, 95% and 100% ethanol at room temperature and air dried. The three probes, (1) Fraction I DNA (L1Sc probes), (2) Fraction II DNA and (3) human telomeric probes consisting of the 6 bp repeat, TTAGGG (Oncor, Bethesda, MD, USA) were labelled with biotin-7-deoxyadenosine triphosphate by nick translation

according to kit instructions (GIBCO BRL, Gaithersburg, MD, USA). The probes were heated to 70°C, snap-cooled in ice water, and hybridised to the samples at 37°C for 16 h. The slides were washed in 50% formamide at 42°C and rinsed three times under low stringency conditions.

Avidin-FITC (Boehringer, Mannheim) diluted 1:200 in 1.0% BSA was incubated with the slides for 30 min at room temperature. Following two washes with 0.05% Tween 20, the samples were incubated with biotinylated goat anti-avidin for 30 min at room temperature. The avidin-FITC step was repeated and the slides were stained with 4 μg/ml propidium iodide. Following two twenty second rinses with PBS, the slides were mounted with a high pH (pH 11) anti-fade solution, PPD11 (Lemieux et al., 1992). PPD11 contained 100 mg of *p*-phenylenediamine free base (Sigma) diluted in 100 ml of nine parts glycerol to one part PBS. A coverslip was placed over each slide and the specimens were viewed with both the fluorescent (Olympus) and confocal laser scanning microscope (Bio-Rad MRC 1000).

7.3. RESULTS

7.3.1. DNA cloning using PCR-Script and DNA sequencing

DNA from the C2 region digested with micrococcal nuclease (Fraction I) was cloned into PCRScript. Positive transformants were checked for inserts using vector primers flanking the cloning site in a PCR reaction. The PCR products were electrophoresed on an agarose gel (not shown). The sizes of the cloned fragments were confirmed by removing the inserts using two restriction enzymes, *Pst* I and *Not* I, and separating the fragments by gel electrophoresis (Fig. 7.1). *Pst* I and *Not* I are located 16 bp and 8 bp, respectively, on either side the *Srf* I site in the vector. Therefore, a short 24 bp vector sequence is expected to remain with the inserts. Of the eight plasmid clones cut with the enzymes, only four had inserts; two were ~720 bp long whereas two others were ~550 bp in size (Fig. 7.1).

Automated sequencing of the plasmid inserts and database comparisons (Genbank and EMBL) of the sequences showed that both 720 bp fragments shared homology with a family of long interspersed repeat elements called LINEs (Fig. 7.2A). The 550 bp inserts however, contained some homology to mitochondrial DNA (Fig. 7.2B).

7.3.2. Southern hybridisation

A probe made from one of the Fraction I LINE clones, L1Sc, was used for Southern blot analysis of (1) genomic DNA and (2) sperm DNA that remained intact following micrococcal nuclease treatment (Fraction II). Hybridisation showed that a range of DNA fragments (100-720 bp) of the genomic DNA was not detected by Fraction I probes in Fraction II of spermatozoa DNA (Fig. 7.3). This indicates that micrococcal nuclease had effectively removed a fraction of DNA from the sperm nuclei that was present in untreated nuclei. However, the probe also detected a faint 1.8 kb band in Fraction II DNA (Fig. 7.3) which showed that micrococcal nuclease may not have completely removed LINE sequences from the nuclei.

7.3.3. Fluorescence *in situ* hybridisation

Labelling of Nuclei with Fraction I probes (DNA from the C2 region)

Fluorescence *in situ* hybridisation using L1Sc probes showed localisation to the periphery of the spermatozoa nuclei (Fig. 7.4A). This region corresponds to the site of the nucleohistone or C2 chromatin where the probe had originated. The same probe labelled the dark R-bands that correspond to Geimsa/Quinicrine bands on metaphase chromosomes from *Sminthopsis* fibroblast cells (Figs. 7.4B, C and D). Figures 7.5A, B and C are the result of superimposition of confocal scanning data obtained using both 488/522 nm and 568/605 nm filter combinations. Figure 7.5D was obtained by confocal scanning at excitation-emission wavelengths of 488/522 nm which limited data collection to fluorescence induced by propidium iodide staining. The banding pattern in Fig. 7.4D was induced by the raised pH of the anti-fade solution that was used (Lemieux et al., 1992). Figures 7.4C and D, which both show the same chromosome set, clearly illustrate that labelling of L1Sc probes occurred in the dark R-banded regions of the *Sminthopsis* fibroblast chromosomes.

Labelling of Nuclei with Fraction II probes (DNA from the C1 region)

Probes made from Fraction II DNA labelled to the spermatozoa nuclei homogeneously (Fig. 7.5A). A banding pattern was also produced on metaphase chromosomes in a reverse manner to the pattern observed for Fraction I probes (Fig. 7.5B). Fraction II probes labelled the centromeres and the bright R-bands as opposed to the dark R-bands labelled by Fraction I probe (Fig. 7.5B).

Labelling of Nuclei with Human telomeric probes

Human telomeric probes were localised to the nuclei of *Sminthopsis* spermatozoa as fluorescent spots around the periphery of the nucleus (Fig.7.6).

7.4. DISCUSSION

Histones occur in a defined region within the spermatozoa nuclei of *Sminthopsis*, that has been shown, by immunocytochemistry, to be restricted to the peripheral C2 chromatin. Protamines, on the other hand, presumably occur in the nuclease-resistant C1 region of the spermatozoon nucleus (Chapter 6). In this study, cloning of DNA from the C2 region resulted in two positive inserts that have sequences in common with mitochondrial DNA and may have been cloned from mitochondrial DNA from the mid-piece of spermatozoa.

Among the cloned fragments are also sequences that bear resemblance to a family of interspersed repeats found in mammalian genomes, known as long interspersed elements or LINEs. The human L1 family, 'L1H', consists of about 50 000 members and full length primate L1 repeats are 6.4 kb in length. In some L1 members, two long open-reading frames (ORF) are present (Fanning and Singer, 1987). L1H contains a 1-kb 5' ORF-1 which is linked by a 33-nt segment to a 4-kb ORF-2. The 33-nt segment is flanked by stop codons, which are conserved in most of the member sequences (Martin et al., 1991). The product of ORF-1 is unknown but has been postulated to be a structural protein (Holmes et al., 1992). ORF-2, however, appears to code for a reverse transcriptase based on enzymatic activity studies as well as sequence similarity (Mathias et al., 1991). It is assumed that apart from the master sequences that retain their ability for transposition, the rest of the LINE sequences are inactivated due to either random mutations in the ORFs or from errors that occurred during reverse transcription (Loeb et al., 1986; Prescott et al., 1992). The 5' end of many L1 family members contains internal deletions and rearrangements, but most have very similar 3'ends.

Another family of repeats, known as short interspersed elements (SINEs) have been well studied in recent years and have been implicated to perform structural roles such as nucleosomal positioning (Englander and Howard, 1995). The human Alu sequence is found to be intrinsically flexible and bends at critical regions to facilitate the wrapping of DNA around the histone octamer (Englander and Howard, 1995). It is also recognized that SINEs have an important effect in the transcription of gene by bridging control elements that are far apart in the sequence (Burton et al., 1986; Norris et al., 1995). By contrast, LINE repeats have, so far, not been determined to have any specific function in the genome even though they may amount to 5-15% of total DNA content. Much of this

represents relics of transposition events that have occurred in the evolutionary history of LINEs that may pre-date the divergence of marsupials from eutherians (Dorner and Paabo, 1995). The few functional master genes code for a reverse transcriptase, an enzyme that is required for its own amplification in the genome. SINE sequences proliferate in the same manner as the LINEs but do not synthesis their own reverse transcriptase and may therefore be dependent on LINE master genes as the major if not only, source of this enzyme in the mammalian 'host' genome. Therefore the evolution of both types of interspersed repeats may well be co-dependent on one another.

Southern hybridisation studies indicate that probes made from a 720 bp segment (L1Sc) of a *Sminthopsis* LINE repeat isolated from the C2 region, detected a large array of DNA fragments in total genomic DNA. These probes, however, did not generally hybridise to spermatozoa DNA that was left intact after treatment with micrococcal nuclease (Fraction II). Since the same amount of DNA (10 μg) for both genomic and Fraction II DNA has been loaded onto the gels, the differences in the labelling are likely to be real and not due to a discrepancy in the concentration of DNA. It appears that the majority of LINE sequences occur within the C2 region and most of it has been removed following digestion with micrococcal nuclease since the L1Sc probe did not generally label to Fraction II DNA. However a faint band detected by L1Sc probes may indicate that not all LINE repeats have been removed from the C2 chromatin. Alternatively, some LINE sequences may be present in DNA from the C1 region.

Bernardi et al., (1985) has shown using density gradient centrifugation that specific genomic regions called isochores are characterised by either (1) high GC content, comprising short interspersed repeats (SINE) sequences and expressed genes, or (2) high AT content, consisting mainly of LINE sequences. Other evidence that suggests genomic clustering of SINE and LINE sequences comes from fluorescence *in situ* hybridisation studies using probes made from a human SINE sequence (Alu) and a human LINE sequence (L1) (Korenberg and Rykowski, 1988). In metaphase chromosomes, Alu and L1 repeats representing the two major families of SINEs and LINEs in humans are localised mainly to the R- and G-bands, respectively (Korenberg and Rykowski, 1988). This observation has prompted the suggestion that LINEs and SINEs may have a role in determining chromosome structure. The specific conformity between GC-rich isochores and R-bands, however, is still unclear, as GC-rich isochores are compositionally heterogeneous. Further compositional mapping studies of eukaryotic chromosomes are required to resolve this issue (Gardiner et al., 1990).

Fluorescence *in situ* hybridisation using the *Sminthopsis* LINE sequence, L1Sc, as a probe showed that it is localised to the periphery of the spermatozoa chromatin corresponding to the site of the nucleohistone region. Therefore, it appears that LINE sequences may occur mainly at the peripheral C2 region and may be bound to histones. In fibroblast metaphase chromosomes LINE repeats labelled to the dark R-bands (equivalent to Giemsa/Quinacrine bands) which represent the AT-rich isochores of the genome. These results fit the concept of defined genomic clustering of LINE repeats in chromosomes and, in the case of *Sminthopsis,* within spermatozoa chromatin as well. By contrast, labelling of probes made from the C1 chromatin region (Fraction II) localised to the light R-bands of the chromosomes (GC- and SINE- rich bands) and also to the centromeres. In spermatozoa, the C1 probes labelled to the nuclei homogeneously. These results indicate that the gene-rich isochore of the genome and centromeric DNA may occur in the more interior regions of the spermatozoa nucleus (C1 chromatin). Therefore, in spermatozoa of *Sminthopsis*, not only is the DNA segregated or clustered, but that there may be a preference of each isochore for different packaging proteins.

In the somatic cell, LINEs generally occur in the condensed heterochromatin regions which are inactive, as opposed to euchromatin which contains active chromatin in various degrees of decondensation. During meiosis, LINEs are known to replicate late in the cell cycle and this is reflected in the banding patterns of metaphase chromosomes (Korenberg and Engels, 1978; Kuhn and Therman, 1986). In *Sminthopsis* spermatids, condensation of the peripheral nucleosomal region which consists of LINEs, occurs late in spermiogenesis following condensation of the inner chromatin region (Soon and Breed, 1996). It may be that the structural constraints which cause the time lag in DNA replication could also impose a delay in DNA condensation of the nucleosomal-LINE region of the spermatozoa nuclei. The effect is a profoundly looped chromosomal structure where 1) LINE repeats and the telomeres are situated at the periphery, 2) SINEs and gene-rich regions are looped inwards, and by inference from the investigations by Zalensky et al., (1995), 3) centromeres may form a central 'chromocentre' in the spermatozoa nuclei. However, to ascertain whether this is also true for *Sminthopsis,* further studies on the localisation of centromeric DNA in the spermatozoa of this species needs to be conducted. Similar hybridisation studies to determine the location of SINE and single copy genes in the spermatozoa of this species will also be an interesting exercise.

Fig. 7.1. Agarose (1.5%) gel electrophoresis of PGEM marker DNA (Lane 1) and nucleohistone DNA from *Sminthopsis* spermatozoa cloned in PCR-Script and cut with *Pst*I and *Not*I (Lanes 2 - 8). Four clones contain positive inserts, two of which are ~720 bp in size (Lanes 2 and 7) and two others are ~550 bp (Lanes 5 and 6). Three clones have no inserts (Lanes 3,4 and 8). The large band (< 2.65 kb) for all the clones (Lanes 2 - 8) is the plasmid DNA and small bands (> 300 bp) are residual bacterial RNAs.

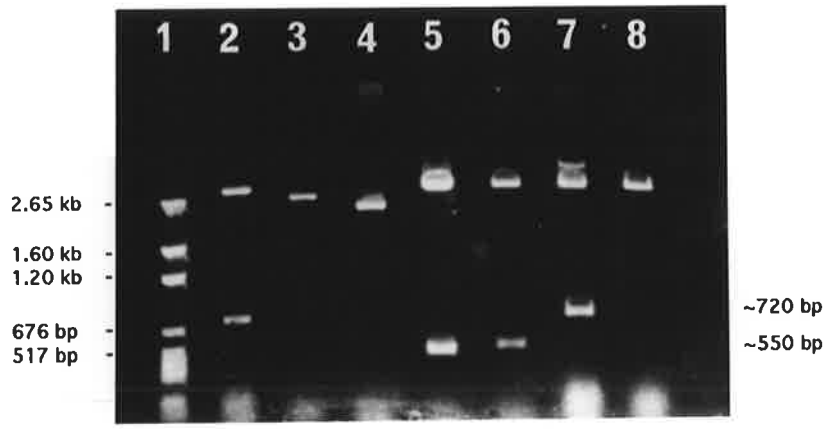
1
2
3
4
5
6
7
8
2.65 kb
1.60 kb
1.20 kb
676 bp
517 bp
~720 bp
~550 bp

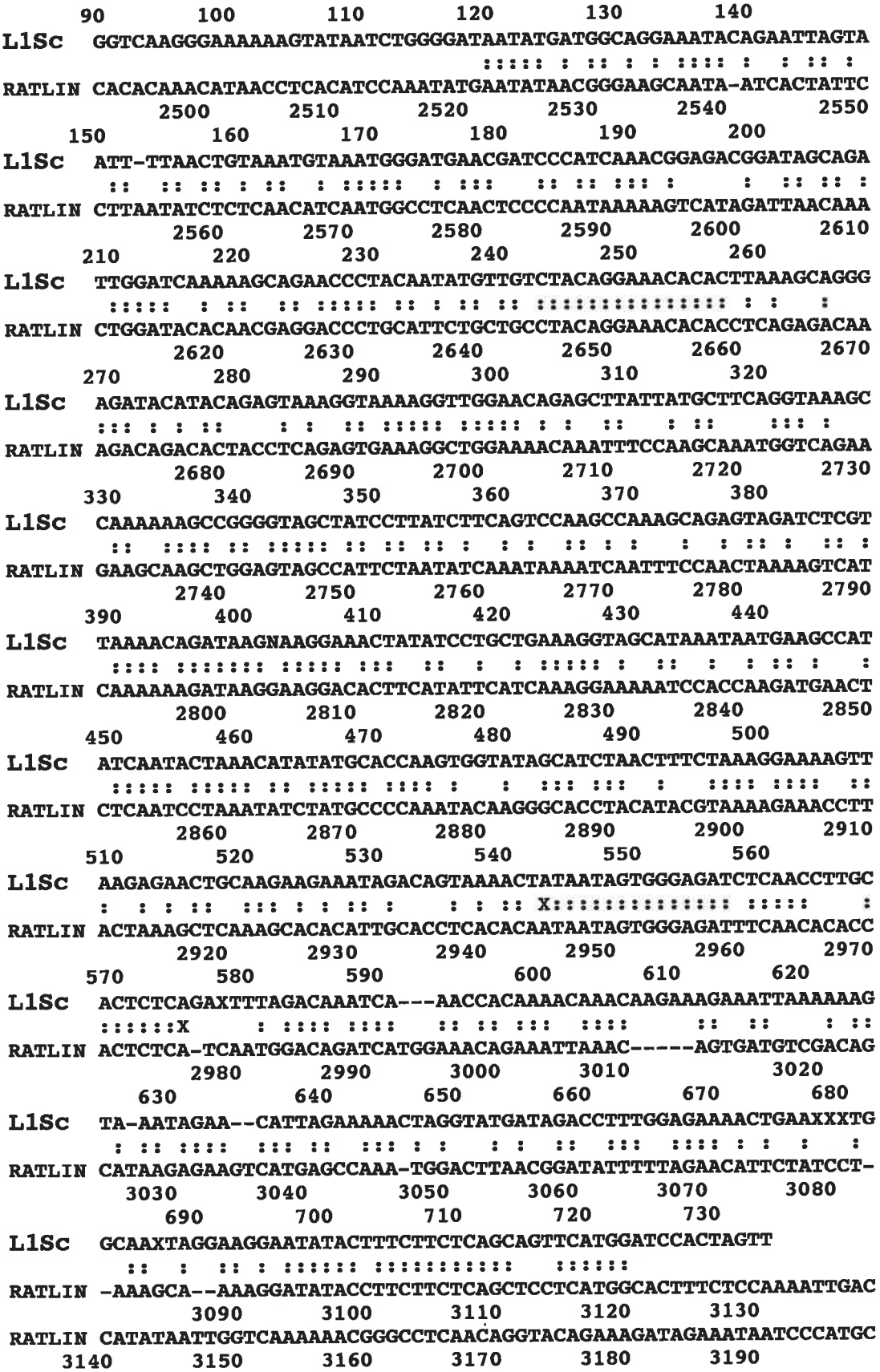

Fig. 7.2A. The plasmid insert, L1Sc (720 bp) shares 60.2% identity in 611 bp overlap with a long interspersed repeats from the rat, RATLIN (8048 bp).

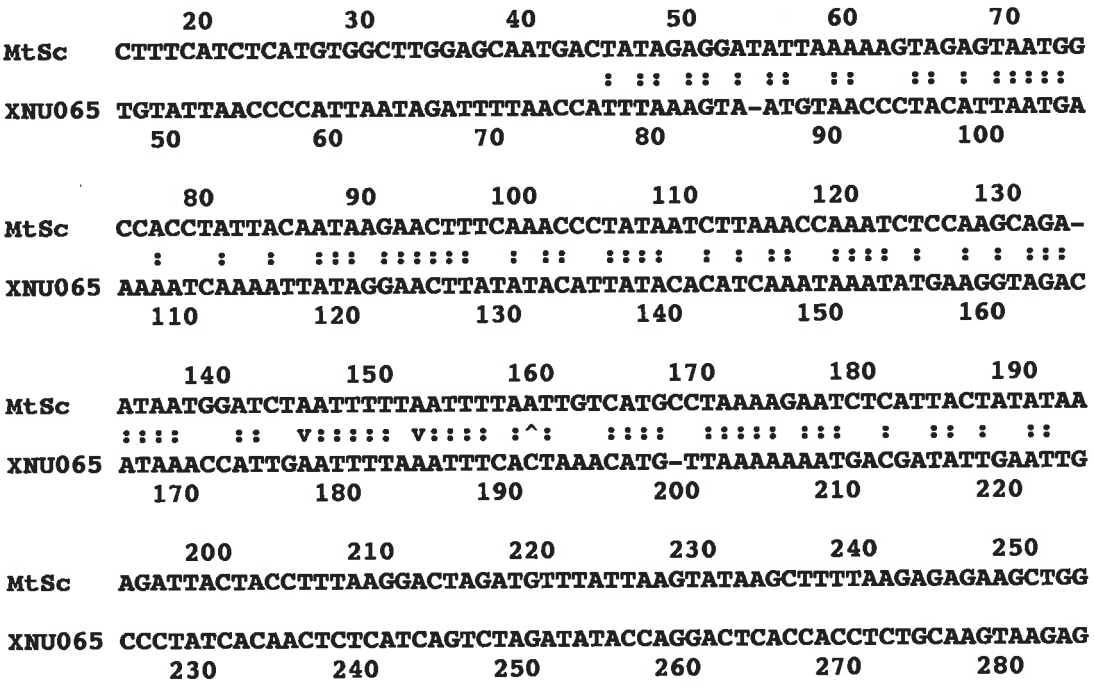

Fig. 7.2B. The plasmid insert, MtSc (550 bp) shares 59.5% identity in 148 bp overlap with mitochondria DNA from *Xiphophorus nigrensis* (370 bp).

Fig. 7.3. Southern hybridization using probes made from L1Sc of micrococcal nuclease-treated sperm DNA (Lane 1), genomic DNA (Lane 2), and L1Sc fragment cut from plasmid using *Pst*I and *Not*I (Lane 3). A range of fragments from between 100 to 720 bp in length, are detected in the genomic DNA (Lane 2) but are not present in the sperm DNA (Lane 1). However, Lanes 1 and 2 have a 1.8 kb band in common that appears faint in Lane 1.

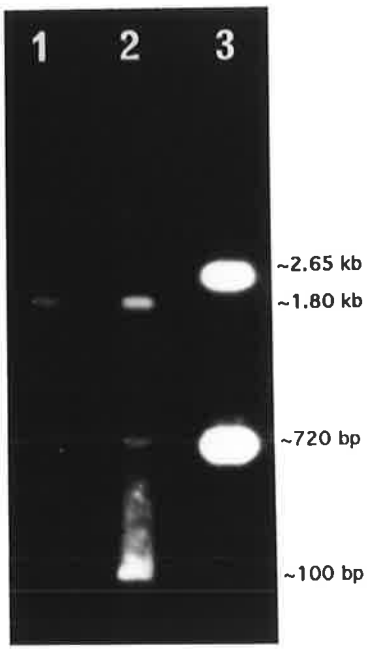
1
2
3
~2.65 kb
~1.80 kb
~720 bp
~100 bp

Fig. 7.4A. Fluorescence *in situ* hybridisation of L1Sc repeat showing localisation to the periphery of the spermatozoon nucleus (green). Propidium iodide (red) stains the rest of the nucleus which is relatively free of L1Sc binding. Bar = 24 μm.

Fig. 7.4B, C and D. Fluorescence *in situ* hybridisation of L1Sc repeat in fibroblast chromosomes. The probes appear to bind to the dark R-bands shown by green fluorescence in (B and C) and dark regions of chromosomes (D). Bar = 10 μm.

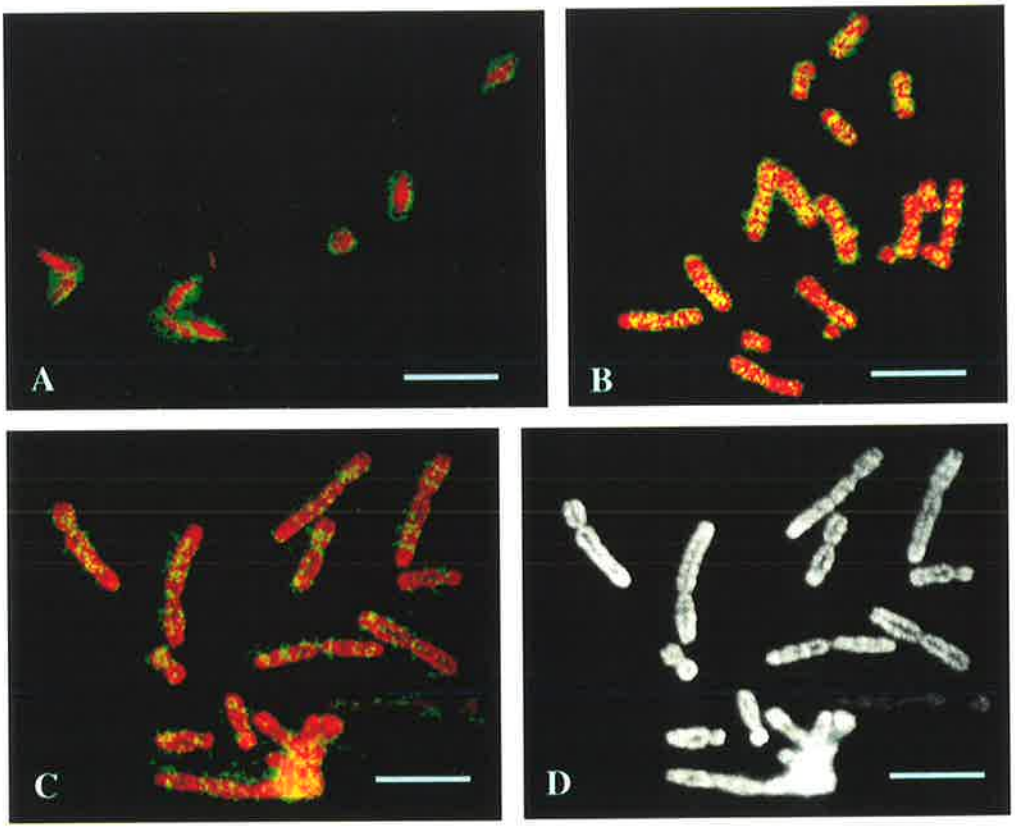
A
B
C
D

Fig. 7.5A. Labelling of the spermatozoa nuclei by probes made from Fraction II DNA. Bar = 20 μm.

Fig. 7.5B. On fibroblast chromosomes, Fraction II probes bind to the light R-bands and to the centromeres (green fluorescence). The chromosomes have not been counterstained with propidium iodide. Bar = 10 μm.

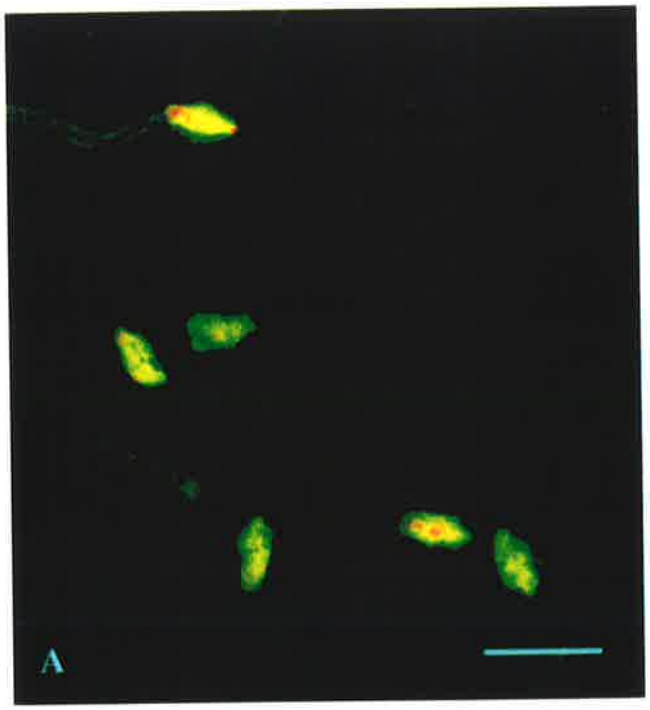
A

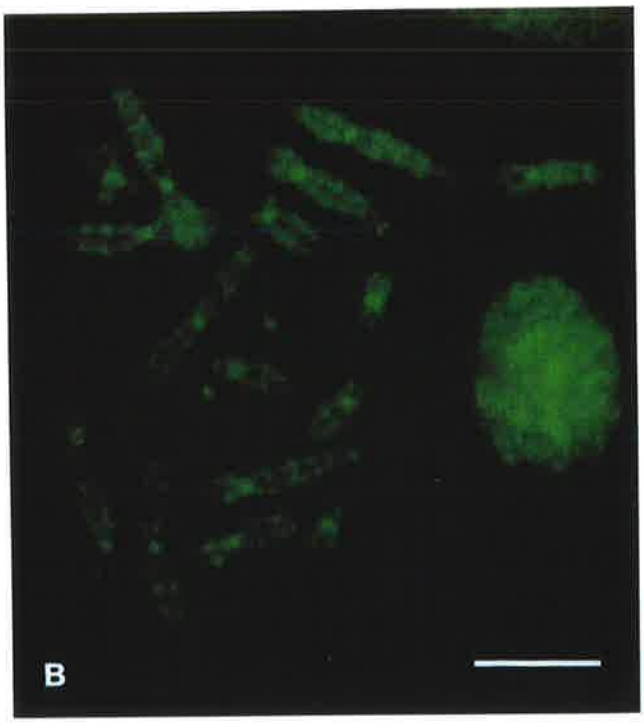
B

Fig. 7.6. Localisation of telomeres (green fluorescence) in the spermatozoa nuclei of *Sminthopsis* using human telomeric probes. Bar = 3.2 μm.

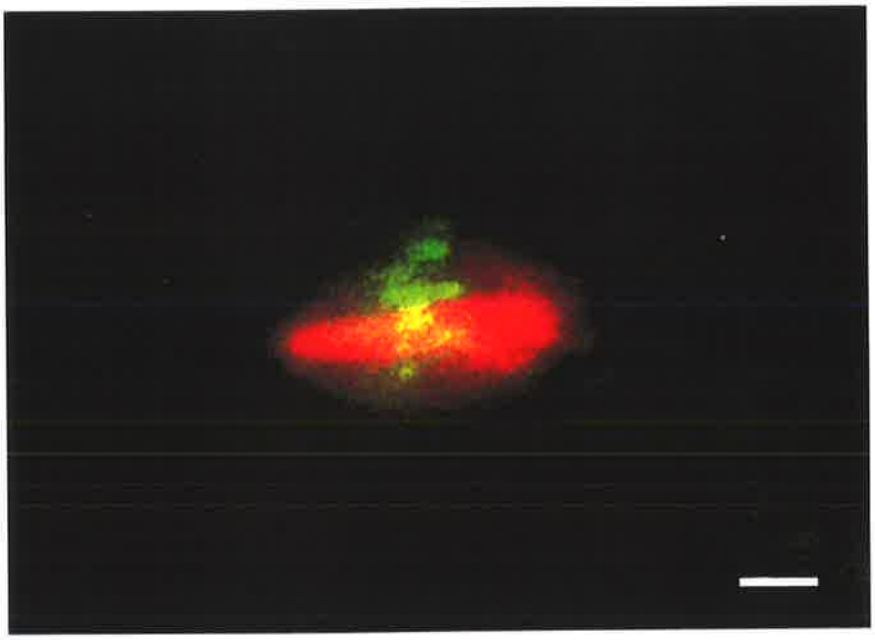

Chapter 8. CONCLUDING DISCUSSION

In an attempt to determine the substructure of the spermatozoa nuclei of *Sminthopsis,* we have previously carried out a series of incubation studies to investigate the effects of SDS, NaCl, and guanidine hydrochloride on the chromatin structure (Breed et al., 1994). TEM observations showed that the nuclei displayed a range of states of decondensation.

In this present study, however, a few technical changes have been made to eliminate variability in the TEM results. These include (1) using a phosphate-based buffer instead of Tris buffer in the incubation solutions, since Tris is reactive to glutaraldehyde (Hayat, 1981), and (2) collecting spermatozoa by centrifugation at 14 000 g for 1.5 min, instead of using the filter-sedimentation method (Breed et al., 1994) which is prolonged and may thus promote the degeneration of spermatozoa. Implementation of these changes has resulted in 90-95% uniformity in the spermatozoa chromatin structure following various treatments such as demembranation using Triton-X and DTT, *in situ* incubation with protamines (Chapter 4) and micrococcal nuclease digestion (Chapter 6).

In our paper, Breed et al., (1994) we suggested that the two chromatin regions may have different chemical properties. The homogenous, inner region has been defined as the C1 chromatin and the fissured, outer region of the nucleus, the C2 chromatin. These terms have been adopted for use in this thesis. Some of the issues previously raised such as (1) the constituent(s) of the C2 region; whether its composition is purely of proteins or whether DNA is present as well (Harding et al., 1982; Breed et al., 1994), (2) the differential intensities in the fluorescence of the two nuclear regions stained with DNA fluorochromes, and (3) the greater electron-density of the C2 region compared to the C1 region (Breed et al., 1994), have been addressed in this thesis.

In the following discussion, I will give a summary of the results for this project and then attempt to bring into context the findings of this thesis with current knowledge on the structure and function of nucleohistones and nucleoprotamines.

8.1. SUMMARY OF RESULTS

8.1.1. Nuclear condensation

Ultrastructural and cytochemical studies have been used to investigate the morphogenesis of the sperm nucleus. Spermiogenesis in *Sminthopsis* can be divided into 15 steps and by Step 10 condensation of the C1 region appears complete. At the caudal extremity of the spermatid nucleus at this stage, the nuclear envelope encloses an electron-lucent space. This space, and the surrounding nuclear envelope, becomes very enlarged by Step 11. At this stage, a plate of approximately 70 nm in thickness becomes evident along the caudal segment of the C1 region; this 'nuclear mantle' does not bind DNAase-gold conjugates but stains for lysine-rich proteins using alcoholic phosphotungstic acid (Courtens and Loir 1981b).

Chromatin condensation resumes at Step 12 with the appearance of spherical chromatin structures peripheral to the C1 chromatin. These structures then partially coalesce and indentations of the C2 region appear. The spherical chromatin units are reminiscent of the globular units observed during the condensation of the spermatid nuclei in eutherians (Loir et al., 1985). Unlike the partial condensation observed in the C2 region, sperm nuclear condensation in most eutherians results in a uniform, and amorphous mass as the globular chromatin units completely coalesce. Immunocytochemical studies in the ram (Courtens et al., 1983) and mouse (Biggiogera et al., 1992), show that the incorporation of protamines corresponds to the formation of a homogenous chromatin from course fibres, the latter being likely to consist of transition protein-DNA complexes.

The lack of large fibres during condensation of the C1 region may be due to the absence of histones or transition proteins. In round spermatids, the chromatin has the appearance of fine granules as shown in those of the bandicoot (Sapsford et al., 1969). Thereafter, the granules appear to condense in the caudo-ventral direction into an electron-dense mass. The fine granules may represent naked DNA following the removal of somatic histones and the aggregation of the granules may be a consequence of the binding of protamine molecules.

There appears to be fundamental morphological and possibly biochemical differences in the condensation of chromatin between the marsupials studied so far and the eutherians. It remains to be seen whether transition proteins are

required in the marsupial system to guide the condensation of the sperm chromatin.

The expanded nuclear envelope at the caudal extremity persists in caput epididymal spermatozoa. Spherical inclusions within it do not bind to DNAase-gold conjugates but stain for lysine-rich proteins and anti-histone H2B antibodies. Further along the epididymis, these inclusions amass near the nuclear pores and become removed from the nucleus. In addition, the nuclear mantle has disappeared by the time the spermatozoa reach the corpus epididymidis (Chapter 3). The prolonged existence of the nuclear pore complex as well as the ENE in the spermatozoa of *Sminthopsis* suggests that metabolic activity remains high and transport of molecules still occurs whilst spermatozoa pass along the epididymidis. The labelling of anti-histone H2B antibodies to material contained within the ENE suggests that the nuclear pore complexes may have a role in the removal of histones from the nucleus (Chapter 5).

By contrast, in eutherian spermatids, the nuclear pore complexes become localised to the redundant folds of the nuclear envelope during the maturation phase (Bellvé and O'Brien, 1983). In the mature spermatids of ram, the posterior region of the nucleus contains an electron-lucent region that is surrounded by 'redundant' nuclear envelope and maybe similar to the ENE of *Sminthopsis*. Unlike the ENE however, the redundant nuclear folds of the ram spermatozoa, become removed following spermiation (Courtens and Loir, 1981b).

8.1.2. Spermatozoa nuclear structure of *Sminthopsis*

8.1.2.1. Content of the nucleus

In this thesis, one of the early experiments conducted was to determine whether or not DNA is present within the C2 region and the ENE of caput spermatozoa. DNAase-gold conjugates (Bendayan, 1981), labelled to both C1 and C2 nuclear regions, indicating that DNA occurs in both regions (Chapter 3). However, contents of the ENE were not labelled by the conjugates.

To determine whether the unusual morphology of *Sminthopsis* spermatozoa nuclei is due to the incorporation of different packaging proteins, spermatozoa nuclear proteins were characterised using acetic acid-urea PAGE and fractionated by reverse-phase HPLC. Purification and partial sequencing of the main protein component showed it to be protamine 1. About 25% of the total

spermatozoa nuclear basic proteins, however, consists of the five histones, H1, H2A, H2B, H3 and H4.

Immunofluorescence labelling using anti-H4, anti-H2B and anti-H2A antibodies, showed localisation of the antibodies to the periphery of demembranated spermatozoa nuclei, a region that corresponds to the C2 chromatin, and high resolution immunoelectron microscopy using anti-histone H2B localised the histone to the electron-dense globular regions of C2 chromatin. Unlike in any other mammals described so far, the spermatozoa histones of *Sminthopsis crassicaudata* have a precise and definite location within the nuclei. These histones are likely to be associated with DNA within the C2 chromatin.

Whilst histones appear to localise within the C2 region, the nuclease-resistant C1 region presumably contains protamine 1 (Chapter 6). The C1 chromatin remains intact when treated with micrococcal nuclease (MN) whereas the C2 region is preferentially digested. This suggests that the C1 region may consist of highly condensed nucleoprotamines that are steriochemically inaccessibile to micrococcal nuclease (MN), in contrast to the C2 nucleohistone region. The products of MN digestion of the C2 chromatin are aggregates of almost spherical structures of approximately 35 nm in diameter. When these agglomerates are dispersed using a spreading agent, smaller 11 nm nucleosomal structures can be observed.

Atomic force microscopy (AFM) of the spermatozoa nuclear topology of *Sminthopsis* showed that at high resolution, bundles of 120-140 sized nodular structures are present within the C2 chromatin region (Chapter 6). This result, and the MN digestion studies, suggest that DNA within the C2 chromatin is packaged by histones into 11 nm nucleosomes which form larger 35 nm fibres (*in vitro*) that are in turn aggregated into clusters of 120-140 nm structures.

High resolution AFM imaging of the C1 chromatin revealed the presence of 45-60 nm chromatin structures. The chromatin from spermatozoa nuclei of *Trichosurus* consists of similar sized nodules (45-80 nm) (Chapter 6). A separate AFM study by Allen et al., (1993), demonstrated the presence of 50-100 nm nodules in the spermatozoa chromatin of mouse and bull. Since the eutherians and *Trichosurus* spermatozoa are known to be packaged mainly by protamines, these nodules may be the higher order structures of nucleoprotamines in spermatozoa of mammals, including perhaps the C1 region of *Sminthopsis*.

The nucleohistone C2 chromatin appears to contain the AT-rich isochore of the genome including the majority of the long interspersed repeats or LINE sequences, whereas the C1 region appears to contain the gene-rich or GC-rich isochore (Chapter 7).

8.1.2.2. Why are grooves present in C2 but not C1 chromatin?

To test the hypothesis that the C2 chromatin is only partially condensed relative to nucleoprotamines, spermatozoa nuclei were treated with herring and salmon protamines *in situ*. The resulting C2 chromatin was almost devoid of the fissures so that it appeared homogeneously amorphous like the C1 chromatin. In the control spermatozoa, the fissures were invariably present. The fish protamines may have bound to negative charges of the DNA by simple electrostatic interaction to cause further condensation of the C2 chromatin. The naturally condensed C1 chromatin, however, showed no changes in its ultrastructure.

These results are consistent with the presence of histones in the C2 chromatin which only neutralise 40-60% of the phosphodiester charges of DNA molecules, leaving a large proportion of the phosphate groups available for binding (Sen and Crothers, 1986; Subirana 1990). On the other hand, the nuclease-resistant C1 region presumably contains protamines that completely neutralise the DNA negative charges and in essence prevent any further binding of DNA to basic proteins.

Following incubation with fish protamines, the previously faint fluorescence at the peripheral C2 region of DAPI-stained spermatozoa, fluoresces as brightly as the rest of the chromatin. The uniform fluorescence of the nuclei may be due to more evenly distributed DNA as a result of increased compaction of C2 chromatin by the fish protamines. Hence, in the untreated spermatozoa nuclei, distribution of DNA may be more sparse within the C2 region compared to the C1 and this may explain why the former region fluoresces less brightly.

The physico-chemical nature of both the C1 and C2 regions, in terms of chromatin density and affinity for cationic stains, has been studied by observing the effects of cationic stains on the electron-density of the chromatin. The results show that, in the unstained specimens, the C2 region appears more electron-lucent compared to the C1 region. Without the aid of cationic stains, the amount of electron scattering becomes dependent on inherent density of the structures. Therefore, it appears that the mass-density of the C1 chromatin is greater than that of the C2 chromatin since there is greater contrast in this region in the unstained specimens.

The enhanced electron-density of the C2 compared to the C1 region in the stained specimens however, indicates that this region has a greater affinity for heavy metals and this could reflect the presence of negatively charged residues such as the phosphate groups of DNA. It seems likely that within the C2 chromatin more of the phosphodiester negative charges in DNA remain free to interact with the cationic stains.

These results indicate that the C2 region is less dense than the C1 region, and contains more sites or net negative charges which attract the large cations present in stains. In support of the latter conclusion, studies on the TEM visualisation of chromatin by Richardson and Davies (1980) have prompted these authors to suggest that rapid diffusion of uranyl acetate solutions is facilitated by the hydrophilic DNA-histone passages that form between the two surfaces of the section.

8.2. NUCLEOHISTONES

8.2.1. Somatic cell nucleohistones

8.2.1.1. Nucleosomes

Hewish and Burgoyne (1973) elucidated the structure of the nucleosome by showing that somatic cell chromatin can be digested by cellular enzymes into fragments that are multiples of approximately 200 bp. They correctly perceived that the basic nucleohistone unit consists of a combination of protein and DNA that occurs once every 200 bp in what is known as a nucleosome. The following year (1974), Olins and Olins visualised nucleosomes under the electron microscope as a series of chromatin "beads" along an extended DNA "string". Finch et al., in 1977, used X-ray crystallography to investigate the three-dimensional structure of the histone octamer and the associated DNA structure. By also using electron microscopy and enzyme-digestion methods, Finch et al. (1977) demonstrated that 150 bp of DNA wrap in 1.75 turns around the histone octamer into a shallow, left-handed supercoil containing about 80 bp per turn. Subsequent crystallographic studies at higher resolutions (Richmond et al., 1984) reveal that the octamer has a diameter of about 60 Å, and the outer thickness of the DNA is approximately 20 Å, resulting in a total diameter of about 100Å for the nucleosome particle. The histones H2A and H2B lie near the ends of the DNA supercoil, while H3 and H4 occur near its centre (Richmond et al., 1984).

In recent years, the structure of nucleosomes in eukaryotic somatic cells has been shown to have implicit roles in gene activity (Wolffe, 1994). Histones have been found to be positioned along the DNA molecule so that regulatory sequences are exposed or are found in linker DNA (Lewin, 1994). In some cases, regulatory sequences are in contact with specific histones that become slightly dissociated with the DNA following post-translational modifications to allow greater access of the sequences to regulatory elements (Grunstein, 1991). In addition, nucleosomes have been found to facilitate transcription by bringing into contact regulatory elements that are separated by DNA segments the length of a single turn or double turns of DNA within the nucleosomes (van Holde, 1993).

The nucleosomal structure is dynamic and this flexibility is important for gene function. Using various physicochemical and immunochemical methods, the structure of the nucleosome is shown to vary its conformation with ionic strength and pH (Libertini and Small, 1982) histone acetylation (Ausio and van Holde,

1986; Oliva et al., 1990), transcriptional activity (Sterner et al., 1987), and cellular transformation (Leonardson and Levy, 1989).

8.2.1.2. Higher order organisation of nucleosomes

Nucleosomes confer a 5:1 compaction ratio to the DNA, however, total genomic DNA in eukaryotic somatic cells is compacted a thousand fold. Therefore, additional higher order folding of the nucleosomal fibre must somehow exist. Finch and Klug, (1976) demonstrated that at low ionic conditions of Mg^{2+} (0.2 mM), 11 nm nucleosomal filaments condense into a fibre of about 30 nm in diameter. They suggested a model that describes the winding of nucleosomal fibres into a helical solenoid with a pitch of about 11 nm. This model became established in textbooks as the accepted higher order structure of nucleohistones.

Subsequently, specific models for the higher level organisation of nucleosomes have been proposed including one that is a refinement of the solenoidal model (McGhee et al., 1980) and another that describes the twisting of nucleosomes and linker DNA into a zig zag configuration (Woodcock et al., 1984; Williams et al., 1986). Another school of thought completely refutes the existence of a regular order in the folding of nucleosomes (van Holde and Zlatanova, 1995). It has been argued that chromatin structures seen in early electron microscopical observations may be artifacts due to chemical fixation and dehydration of the samples. Also it was suggested that selection of favourable images for the explanation of a preconceived model may have occurred (see review by van Holde and Zlatanova, 1995).

In their review, van Holde and Zlatanova, (1995) discuss the implications of experimental results from diverse studies such as X-ray and neutron scattering, and linear and flow dichroism. They concluded that, at most, there may be some evidence for limited regions of regularity within a very irregular helix. The idea of an irregular conformation in the folding of nucleosomes has been supported by recent studies using scanning force microscopy (Leuba et al., 1994) and cryoelectron microscopy (Woodcock, 1994).

Direct attempts to observe the structure of the condensed fibre have not been very successful due to the tight packing of the nucleosomes. An alternate approach has been to study the orientation of the unravelled fibre at low ionic concentrations and then make predictions on how the fibre may fold as the ionic

strength increased. Thoma et al., (1979) described from TEM studies a flattened zigzag conformation of nucleosomes that interdigitate into a closed conformation at high ionic concentrations. Cryoelectron microscopy of frozen-hydrated chromatin suspensions by Dubochet et al., (1988), showed that at salt concentrations from 5-40 mM NaCl, oligonucleosomes appear to have a zigzag conformation, with the linker DNA extended between randomly oriented nucleosomes. On the basis of these observations, and the reconstruction of the chromatin structure by computer modelling, Woodcock and Horowitz (1995) presented a model, where nucleosomes produce an irregular 3D zigzag structure that interdigitates with adjacent zigzags.

The 30 nm fibres of nucleohistones, however, are not observed *in vivo* in most cells except for the transcriptionally inactive spermatozoa nuclei of echinoderms and in avian erythrocyte nuclei (Section 8.2.2). The denomination of the 30 nm fibre as a real and consistent structure and the existence of a zigzag configuration are considered tenuous by some researchers (McDowall et al., 1986; van Holde and Zlantanova, 1995). Instead a more fluid type of organisation of chromatin is the preferred model (McDowall et al., (1986). In this model, extensive interdigitation of preliminary fibres results in a fibreless organisation observed for the chromatin in typical nuclei and chromosomes (McDowall et al., 1986).

A similar model proposed by van Holde and Zlantanova, (1995) suggests that compaction of the nucleosomes results in an open, irregular quasi-helical structure that interdigitates to lose its fibrous state.

There is, however, a consensus in recent literature that the nucleosomal filament conforms to an irregular fold that is a consequence of the variability of the length of linker DNA. Extensive interdigitation of the irregular fibres results in a fibreless morphology. As a consequence, "the accessibility of a specific DNA sequence to proteins is no longer reliant on the fibre, but on the compaction state of the chromatin mass" (Woodcock and Horowitz, 1995).

8.2.1.3. Loop domains

The organisation of DNA into loops of 60-100 kb, further compacts and restrains the DNA within topological domains. The loops are anchored to a proteinaceous nuclear matrix where the sites of attachment contain replication origins and are associated with gene function (Vaughn et al., 1990; Pardoll et al.,

1980). Specific DNA sequences known as long interspersed repeats (LINEs) have been found to be attached to the nuclear matrix. LINEs occur at the boundaries of gene domains which, together with their association with the nuclear matrix, suggests that they may participate in the regulation of particular genes (Chimera et al., 1985).

Within chromosomes, LINE sequences have been localised by *in situ* hybridisation to the Giemsa (G) or Quinacrine (Q) bands which are regions that have largely an adenine and thymidine (AT) component and are poor in gene sequences (Korenberg and Rykowski, 1988). In Chapter 7 of this thesis, similar localisation to the dark R bands (equivalent to G bands) for a LINE sequence isolated from *Sminthopsis* is also observed.

Apart from the G bands, the karyotype of metaphase banding patterns contains two other structural sets of regions, Reverse (R), and the Centromeric (C) bands. Fluorescent dyes, proteolytic digestion, or differential denaturing conditions can be used to produce these bands (Comings, 1978). DNA within the G/Q bands replicates late during the DNA synthetic period and condenses early during mitosis (Korenberg and Engels, 1978; Therman 1986). In contrast to the G/Q bands, the R bands are relatively rich in guanine and cytosine (GC), their DNA replicates early in the DNA synthetic period, and condenses late in mitotic prophase. In addition, R bands are the chromosomal regions in which active genes are concentrated (Korenberg et al, 1978; Kuhn and Therman, 1986).

Similar to those of interphase chromatin, nucleosomes of metaphase chromosomes are organised into loops of about 50 kb at intervals along the length of a chromosome. Each loop compacts the DNA longitudinally, and is anchored at its base in two places to proteins that provide a firm support or "scaffold" for the flexible loop (Lewis and Laemmli, 1982). Chromatin-loops within the R bands are generally longer or less compacted compared to the loops from within the G bands (Poljak and Käs, 1995).

8.2.2. Spermatozoa nucleohistones

As described in the previous section, eukaryotic chromatin from actively transcribing cells and the metaphase chromosomes from dividing cells, do not exhibit discrete fibres in thin EM sections, nor in frozen hydrated sections (Dubochet et al., 1988; McDowall et al., 1986). The 30 nm fibres are observed only in isolated chromatin from these cells. There are, however, some exceptions

where discrete 30 nm fibres are present in chromatin from thin sections, such as within the nuclei of avian erythrocytes and the mature spermatozoa nuclei of a starfish.

Woodcock, (1994) using cryoelectron microscopy has shown that the unfixed and vitrified nuclei of both the spermatozoa of the starfish, *P miniata* and the erythrocytes of *gallus,* demonstrate the presence of 30 nm fibres. By using observations from the unfixed and frozen-hydrated specimens as a benchmark for comparison, he has also shown that fixation with glutaraldehyde and low temperature embedding in Lowicryl preserved both fibre morphology and diameter. Some common features shared by *P miniata* and chicken erythrocyte chromatin that have been suggested as explaining the presence of fibres include (1) the formation of relatively large nucleosomal repeats, and (2) the presence of low amounts of non-histone chromosomal proteins compared to chromatin of active nuclei.

Not all spermatozoa that contain histones display 30 nm fibres. For example, the C2 nucleohistone region of *Sminthopsis* spermatozoa contains 120-180 nm size fibres or globules in TEM sections (Breed et al., 1994; Chapter 4 and 5). These fibres are likely to be real structures and not the result of dehydration, fixation or embedding as Woodcock (1994) has shown that fibre morphology is not effected by these conditions. Why such large fibres are formed is unknown, however, further characterisation of the histones and other non-basic proteins from the spermatozoa nuclei, may provide some clues as to its occurrence (Section 8.5). Although the size of the 120-180 nm structures measured from EM sections is similar to the nodules observed by AFM, measurements of the fibre diameter from EM sections need to be treated with caution since embedding of the nuclei using conventional epoxy resins can cause approximately 25% shrinkage of chromatin (Langmore and Paulson, 1983; Woodcock, 1994). Conversely, measurements from the AFM may be overestimated due to limitations in the design of a probe tip.

Another example where 30 nm fibres are not present in spermatozoa nuclei that is packaged by histones, comes from the echinoderm, *Strongylocentrotus purpuratus*. Not only does the chromatin from mature spermatozoa of this species lack a fibrous morphology, but it also has a uniformly electron-dense appearance similar to protamine packaged chromatin even though protamines are not incorporated by the DNA. In this case, the lack of formation

of fibres is attributed to the spermatozoa-specific and very lysine-rich histones that are effective in condensing the chromatin (Poccia and Green, 1992).

By contrast, the lack of higher order nucleohistone fibres in the spermatozoa of humans may be due to the absence of histone H1. This histone binds to linker DNA to further condense the chromatin and consequently has a role in the folding of nucleosomal filaments. The four core histones isolated from the spermatozoa of humans are, TH2B which is the major histone component (Tanphaichitr et al., 1978; 1982), H3, H4 (Gusse et al., 1986) and H2A (Gatewood et al., 1990), and these histones constitute approximately 15% of total spermatozoa basic proteins. Histone H1 is conspicuously missing.

8.3. NUCLEOPROTAMINES

A variety of conformations have been postulated for the secondary structure of protamines, among them are, α-helices (Warrant and Kim, 1978; Verdaguer et al., 1993), β-sheets (Cid and Arellano, 1982), extended configurations (Feughelman et al., 1955; Balhorn, 1982) and, more recently, γ-turns which contain 1-3 hydrogen bonds (Hud et al., 1994).

The interactions between protamines and DNA have received equally conflicting hypotheses. There are at least four models that have been put forward for the structure of nucleoprotamines: (1) protamine adopts an α-helical structure and binds to the DNA in the major groove (Warrant and Kim, 1978), (2) the central arginine-rich region of eutherian protamines lies in an extended conformation within the minor groove of the DNA helix and forms intra and intermolecular disulphide bonds (Balhorn, 1982), (3) protamine consists of α-helices that bind to three double-stranded DNA molecules in a parallel arrangement (Subirana, 1990), (4) the arginine-rich region of protamines binds to the major groove of DNA and adopts a conformation that facilitates a 1-3 intramolecular hydrogen bonding (Hud et al., 1994).

8.3.1. Secondary structure of protamine

Toniolo (1979) used circular dichroism to study the secondary structure composition of the herring protamine, clupeine, and discovered that it had 51% α-helical content. However, using a secondary structure prediction program, (Chou and Fasman, 1978), no helix was predicted to be present in clupeine. Toniolo (1980) rationalised that the algorithm of the program is based on the statistical analysis of globular proteins and may therefore not be entirely appropriate for the analysis of highly basic proteins. Upon modification of the Chou and Fasman method such that arginine would be predicted to be more helicogenic, Toniolo (1980), estimated that two stretches of α-helices occur along the protamine molecule. This was supported by circular dichroism studies and prediction methods using synthetic arginine-rich decapeptides, which demonstrated that arginine appears to be more helicogenic than is predicted by standard procedures (Verdaguer et al., 1993).

X-ray crystallographic studies of DNA-protamine complexes for molluscs and fish showed that the diffraction patterns for the complexes are very similar

for both species (Suau and Subirana, 1977; Ausio and Suau, 1983). However, there appeared to be insufficient order in the diffraction patterns which could suggest the presence of helical structures within the protein. A single crystal of a protamine-tRNA complex studied by Warrant and Kim (1978) resulted in electron density maps that suggest the binding of protamines to DNA is in an α-helix conformation. By contrast, deuterium-exchange studies of the DNA-protamine complex do not indicate the presence of α-helix or β-sheet secondary structure (Herskovits and Brahms, 1976). From studies using Raman spectroscopy of salmine-DNA complexes, Hud et al. (1994), determined that the DNA-bound salmine exhibits a configuration that is neither an α–helix nor β-sheet, but one that consists of γ-turns.

Even though the literature contains many studies on the secondary structure of protamines, it appears that the structure has not been unequivocally resolved. This may be due to the problem of growing quality crystals of protamine-DNA complexes compounded by limitations in the interpretation of data from fibre diffraction patterns.

8.3.2. Protamine-DNA interactions

The early physical investigations of the protamine-DNA complex by Feughelman et al., (1955) using X-ray diffraction showed an increase in the first-layer line of the X-ray fibre diffraction patterns. This was interpreted to be an indication that protamines bind within the minor groove. On the other hand, the data may also have resulted from the extension of the side-chains of neutral amino acids into the minor grooves of adjacent DNA molecules. Later investigations using polyarginine-DNA complexes by Fita et al., (1983) showed an absence of the increase in the first layer line in diffraction patterns. The model resulting from this study suggests that these complexes and possibly the main regions of protamines including the arginine-rich regions, bind within the major grooves of DNA.

Hud et al., (1994) produced an alternate model that showed a 20 amino acid sequence of salmine that fitted snugly within the major groove of B-DNA. In the model, the six arginine residues span four base pairs along the DNA helix covering a distance of approximately 104 Å. The amino acid side chains are outstreched in alternate directions to interact with phosphate groups of the DNA. The protamines of eutherians and marsupials are twice as long as those of salmine (~60 amino acids) and in marsupials there are usually two stretches of

arginine-rich regions along the proteins. Therefore, if the protamine of *Sminthopsis* is to adopt the configuration suggested by Hud et al., (1994), the length of the protein spans 340 Å which is much larger than can be accommodated in the major groove.

The fluorochrome, Hoechst 33258 which becomes fluorescent when bound to the minor groove of DNA, was used by Bianchi et al., (1994) to determine whether protamines bind to the minor groove of the DNA double helix. The addition of protamine P1 and/or P2 from human to Hoechst-DNA complexes, resulted in an increase in the intensity of the fluorescence. This effect is opposite to that induced by the addition of basic peptides from histone H1 which resulted in the quenching of the fluorescence (Suzuki, 1989). The results suggest that protamines do not displace Hoechst from the minor groove of DNA (Bianchi et al., 1994).

In the same paper by Bianchi et al., (1994) DNA footprinting studies were claimed to show that protamines do not bind to either the major or minor grooves but may instead bind to the surface of the DNA molecule. The footprinting pattern produced following DNAase 1 digestion of the nucleoprotamine complex, does not suggest the binding of protamines to either groove of the DNA. The results, however, could also be interpreted as the inability of the enzyme to access the base pairs for cutting due to the large steric hindrance encountered by the relatively large DNAase I molecule when approaching the dense nucleoprotamine structure. The DNA footprinting studies can be improved to single-nucleotide resolution by using hydroxyl radical ions (Tullius et al., 1987) which are able to access narrow passages between DNA-bound protamines to cut unbound regions of the DNA (Section 8.5).

Although the Hoechst 33258 fluorescence study may indicate that human P1 and P2 protamines do not bind to the minor groove of DNA, the DNA footprinting results do not show conclusively that they are not bound to the grooves of the DNA. This leaves the possibility that protamines may bind to the major groove, however, more studies are needed to resolve this issue (Section 8.5).

8.3.3. Higher order nucleoprotamine structures

The basic packaging unit of nucleoprotamines was unknown until the recent atomic force microscopical investigations of Allen et al., (1993) were

carried out. The workers observed the presence of 50-100 nm nodules on the nuclear surface of mouse and bull spermatozoa which may represent the next level of packaging above that of the protamine-DNA complex. In partially decondensed spermatozoa nuclei, the 50-100 nm nodules appear to be packaged in a meshwork of loops that radiate from the edge of the nucleus. Atomic force imaging studies described in this thesis (Chapter 7) indicate that similar packaging units (45-80 nm in diameter) are found in the nuclei of the spermatozoa of the Australian marsupials, *Sminthopsis crassicaudata* and *Trichosurus vulpecula.* In *Sminthopsis*, these units are present in the C1 nuclease-resistant region, that is likely to consist of nucleoprotamines.

In vitro studies on the condensation of DNA using herring protamines demonstrated the formation of rods and toroidal particles, the size of which is dependent on the ionic strength of the solution (Garcia-Ramírez and Subirana, 1994). Under physiological ionic conditions (100mM Na^+), the thickness of the toroidal complexes is found to be between 20-30 nm. Similar sized fibres have been measured for nucleoprotamines in spermatids of bivalve molluscs, suggesting that toroids may indeed occur *in vivo.* The discrepancy between the size of these nucleoprotamine fibres in the mollusc spermatozoa and the nodules observed in the spermatozoa of mammals by AFM may be due to inherent biochemical differences of the protamines or differences in the technology and sample preparation employed (Section 8.2.2).

The winding of the DNA-protamine complex into higher order structures is expected to either tighten or relax the double helix, in other words, induce a positive or negative supercoil depending on the direction of twist. Risley et al., (1986), using ethidium bromide to study the topology of DNA from the sperm of *Xenopus laevis* and *Bufo fowleri*, observed that the sperm nucleoids (nuclei deprived of proteins) were relaxed at low concentrations of the dye (0.5-6 μg/ml) but became condensed as the concentrations increased (6-100 μg/ml). Since ethidium bromide generates positive supercoiling in the DNA double helix, these results show that the sperm DNA exists in a relaxed state. Similar results that point to negligible degrees of supercoiling in nucleoprotamines have been observed for the spermatozoa of humans (Barone et al., 1994).

The general lack of supercoiling in spermatozoa DNA does not correspond to the existence of higher order, 45-80 nm fibres that result from the folding of the protamine-DNA complex. However, any increase or decrease in the tension of the DNA in nucleoprotamines as a result of folding can be offset by (1) an

interspersed array of left-handed and right-handed twists/rotation of the primary protamine-DNA fibre, or (2) conversion of the state of supercoiling by enzymes such as topoisomerases.

Interestingly, van Holde and Zlantanova (1995) have suggested that an equal mix of both senses of the 30 nm quasi-helix in nucleosomal structures may exist, a condition that could relieve the superhelical stress of condensed DNA. In addition, Bartolomé et al., (1994) reported the presence of such secondary arrangements at the ends of chromatin fragments from EM preparations. An interesting twist to this paradigm is the interspersion of nucleosomal structures between nucleoprotamines in the spermatozoa of *Sminthopsis* (Chapter 8). It is conceivable that the nucleosomes may to some degree counterbalance the supercoiling effect induced by protamines.

Topoisomerase II has been localised to spermatids of rats and may aid in the transition of nucleohistones to nucleoprotamines (McPherson and Longo, 1993). Topoisomerases function by adhering to a supercoiled DNA double helix and producing a transient break, or nick, in the strands. The two strands then rotate relative to each other, followed by resealing of the nick, relaxing superhelical stress (Liu, 1983; Poljak and Käs, 1995).

The putative model for the transition from nucleosomal structures to nucleoprotamine "toroidal" particles is given in a review by Ward and Coffey, (1991). In brief, DNA from six nucleosomes consisting of one turn of the 30 nm solenoid, becomes unravelled whilst the solenoid configuration is maintained by transition proteins. These proteins are replaced by protamines resulting in a chromatin unit that is shaped like a torus with a diameter similar to the solenoidal fibre, but greatly reduced in height. Although the concept that nucleoprotamine higher order structures are mapped from preceding nucleohistone fibres is feasible, this model is in need of a revision for a few reasons. Firstly, it is now widely believed the nucleosomal filament does not coil into a regular 30 nm solenoid due to the variability in the length of the linker DNA. An alternate view describes an irregular fibre with a mass/length ratio of about 1-2 nucleosomes/11 nm for the folding of nucleosomes (Woodcock and Horowitz, 1995; van Holde and Zlantanova, 1995). In addition, toroids[3] have never been visualised *in vivo* within the nuclei of spermatozoa, and the term fibre

[3]The nodules observed from AFM imaging of sperm nuclear topology are not toroidal (doughnut-shape), but are basically units of chromatin of unknown conformation.

may be preferable for the higher order folding of nucleoprotamines as it is inclusive of other possible configurations.

The nucleoprotamine fibre consisting of nodules is anchored to the nuclear matrix and constrained in loop domains (Ward and Coffey, 1991). The large scale arrangement of the 50-100 nm units of the fibre, however, remains unknown. The viewpoint of an apparent linear arrangement or lamellar arrays derived from topological (Allen et al., 1993) or sectional (Koehler et al., 1983) information, disregards the three-dimensional organisation of the nodules. To illustrate this point, in all three types of sphere-packing cubic, face-centred cubic and hexagonal, (Bishop, 1972), a two-dimensional assessment of the surface of a given section, can falsely convey the impression of a linear mode of packaging. In addition, the linear structures that are parallel to the nuclear membrane observed in freeze-fracture studies have recently been interpreted as consisting of non-chromatin structures that are part of the constituents of the nuclear matrix (Santi et al., 1994).

The nucleoprotamine nodules are more or less neutral or uncharged and may tend to aggregate into a stable arrangement similar to the behaviour of bubbles on the surface of a schooner of beer. Their packaging may be compared to the crystallisation process where atoms aggregate (under optimal pressure-temperature conditions) until the attractive forces are counteracted by short-range repulsive forces. The organisation of nucleoprotamine nodules in a form similar to crystal lattices satisfies the criteria of low volume, low energy and close-packing of spermatozoa chromatin. However, the density of packaging and the type of lattice formed (Bishop, 1972) depend on the variability in the size of the nodules. Further information on the three-dimensional packaging of spermatozoa chromatin may be obtained from Fourier microscopy or electron crystallography (Section 8.5).

8.3.4. An alternate hypothesis

All previous hypotheses regarding the structure of the protamine-DNA complex have focused on models that suggest a regular repeating secondary structure based upon the periodic nature of DNA and the corresponding periodic orientation of arginine residues in protamines. A substitute model may be considered, where there may exist intrinsic disorder in the structure of nucleoprotamines, both in the binding and positioning of protamines and secondarily in the folding of the complex into larger fibres.

I suggest two lines of argument for this model; (1) the long and flexible side chains of arginines have a tendency to offset their favourable electrostatic interactions with the DNA phosphodiester groups, a trait that has been recognised in the interactions of lysines and arginines of transcription factor proteins with DNA (Pabo and Sauer, 1992). In the case of protamines, the side chains of arginines may reduce the long-range stereospecificity of protamine binding to DNA. As a consequence, there may exist regional differences in the positioning of the protamine molecule with respect to the DNA double helix, and (2) the variation in the size of nucleoprotamine nodules may be a legacy of its predecessor, the irregular quasi-helical nucleosomal fibre (Woodcock and Horowitz, 1995; van Holde and Zlantanova, 1995). Therefore, irrespective of whether the protamines bind in an irregular and non periodic manner to the DNA or not, an irregular secondary structure may still result because of restrictions imposed by an earlier (nucleosomal) conformation.

8.4. A MODEL FOR THE SPERMATOZOA CHROMATIN OF *SMINTHOPSIS CRASSICAUDATA*

The spermatozoa nuclei of *Sminthopsis* are characterised by the packaging of the DNA by two types of proteins; protamine 1 and, to a lesser extent, histones (Chapters 5 and 6). This occurrence is not commonly reported in mammals, however within the spermatozoa nuclei of many mollusc and fish species, histones and an additional protamine-like protein are known to be incorporated (Ausio, 1986). To date, the significance of the presence of histones in spermatozoa nuclei that are mainly organised by protamines or its equivalent, remains unknown.

Gatewood et al., (1987) demonstrated by using Southern hybridisation methods, that the nucleohistone DNA isolated from the spermatozoa of humans is sequence-specific and has suggested that spermatozoa histones may be involved in the expression of genes during early embryogenesis. Perhaps some evidence for this can be derived from the determination that the nucleohistone region of *Sminthopsis* spermatozoa consists mainly of LINEs (Chapter 8), a family of repeats some of which have also been localised to the nuclear matrix of somatic cells (Chimera et al., 1985). It remains to be seen whether LINEs are indeed associated with the nuclear matrix in *Sminthopsis* spermatozoa and whether they have a role in the expression of particular genes.

The spermatozoa chromatin of *Sminthopsis crassicaudata* may have the following organisation:

(1) *Sminthopsis* LINE repeats are bound to histones and form 11-14 nm nucleosomal structures that are folded into higher order 120-140 nm fibres (Chapters 5, 6 and 7). The larger fibres consist of nodules that are loosely arranged and may account for the grooves observed within the C2 region in TEM sections. Each cluster of the 120-140 nm nodules may represent a loop domain similar to that observed for metaphase chromosomes. (The 30-40 nm fibres observed following the extraction of C2 chromatin using micrococcal nuclease may not exist *in vivo*, but they correspond to previous TEM observations on the structure of extracted chromatin).

(2) The nuclease-resistant C1 region is likely to incorporate protamine 1 molecules (Chapters 5 and 6). DNA within this region appears to contain the gene-rich or GC-rich isochore of the genome (Chapter 7). The primary structure of protamine-DNA binding remains a mystery. However, there is evidence for

the existence of higher order folding of these structures into closely packed, 45-60 nm fibres (Chapter 6).

(3) Finally, the nucleosomal regions are interspersed between the nucleoprotamine regions within the structural context of the continuous DNA sequence of chromosomes. This conclusion is derived from the localisation of *Sminthopsis* LINE repeats to (i) the dark R-bands of mitotic chromosomes and (ii) the peripheral, nucleohistone C2 region in spermatozoa nuclei. A similar model has been proposed by Olivares et al., (1993) for the sperm of the bivalve mollusc *Protothaca thaca,* where the nucleosomal chromatin is suggested as being arranged in short oligonucleosomal stretches that are interspersed within protamine-containing DNA regions.

8.5. FUTURE INVESTIGATIONS

8.5.1. Protein Chemistry

8.5.1.1. Characterisation of spermatozoa histones

Research from this thesis has shown that the unusual morphology of the nuclei from the spermatozoa of *Sminthopsis crassicaudata* is largely due to the organisation of the chromatin by two different sets of proteins; histones and protamines. There is however, still more work that can be done to further elucidate the structure of these nuclei such as investigations on why the nucleosomal fibres are exceptionally large (Section 8.2.2) and how the chromatin is organised with respect to the nuclear matrix.

The large nucleosomal fibres (120-160) measured from images of the demembranated nuclear surface obtained by AFM scanning, may be the result of extensive folding of the nucleosomal filament aided by sperm-specific histones or other non-basic proteins. Histones that are isolated from mature spermatozoa need to be further characterised by determining the amino acid content or its sequence.

8.5.1.2. Non-basic proteins of spermatozoa nuclei

To investigate the presence of non-basic proteins that are associated with the C2 region, micrococcal nuclease digestion can initially be carried out to separate the two nuclear regions. Following this, non-basic proteins can be extracted from the C2 region and visualised by conventional SDS-PAGE gel electrophoresis. Their presence may not have been detected by methods designed for basic proteins such as histones and protamines where acid-urea based gels were used and the gels electrophoresed in the positive to negative direction from the top to the bottom of the gel tank. The high positive charges of basic proteins cause their precipitation in SDS and removal from gel columns if they are electrophoresed in the conventional manner. This method would however, be suitable for the characterisation of non-basic proteins from the C2 region of the spermatozoa nucleus. This study may have important structural implications in nucleosomal folding in sperm.

8.5.1.3. Nuclear matrix proteins of spermatozoa

To study the nuclear matrix, spermatozoa nuclear basic proteins (SNBPs) are removed using high ionic strength salt concentrations (2M NaCl) and the residual nuclei containing the matrix and DNA are used for the extraction of matrix-associated proteins and DNA. The preparation of the nuclear matrix have been previously described by Santi et al., (1994) and Ferrington et al., (1991).

Proteins of the nuclear matrix can be characterised by firstly homogenising the matrix and collecting the proteins by acetone precipitation. The matrix extracts are then electrophoresed to determine the size and numbers of proteins. Some of the proteins can be purified for the raising of antibodies that can later be used to localise proteins within the nuclear matrix. Investigations on spermatozoa nuclear matrix proteins and associated DNA may help to elucidate how the spermatozoon nucleus is organised and the functional significance of this organisation.

8.5.1.4. Antibodies to protamine I

Further studies on the location of protamines within the spermatozoa nuclei include more attempts at the raising of antibodies to these proteins. All the above investigations are technically feasible but may be plagued by problems such as low spermatozoa numbers, and availability and cost of the animals.

8.5.2. Molecular and Structural Studies

8.5.2.1. Spermatozoa nuclear matrix DNA

The nuclear matrix of *Sminthopsis* spermatozoa is prepared as in Section 8.5.1.3. The DNA is then digested using DNAase 1 so that only short matrix-associated fragments remain. Following this, the nuclear matrix is digested with proteinase K and the matrix-associated DNA fragments is isolated by phenol-chloroform extraction and cloned into plasmid vectors. Cloned sequences are then subjected to DNA sequencing and the results compared with sequences located in databases such as EMBL and GENBANK.

8.5.2.2. Localisation of centromeric DNA and SINE sequences

Centromeric DNA is highly species-specific and can be isolated from *Sminthopsis* by using various restriction enzymes (RE) to digest purified genomic DNA followed by fractionation of the digests by agarose gel electrophoresis. Centromeric DNA exists as long tandem arrays of a sequence element that may contain recognition sites for various REs (Willard and Wayne, 1987). Hence, RE digestion is expected to produce centromeric DNA-enriched fractions that appear as one or more bands when resolved on an agarose gel. The band(s) is excised and the DNA is purified, cloned and sequenced. SINE sequences are interspersed throughout the mammalian genome (Miklos, 1985) and digestion of *Sminthopsis* genomic DNA with REs may produce SINE fragments of unique lengths that can be collected from agarose gels and cloned. The cloned sequences are compared with databank sequences and those that resemble centromeric DNA or SINEs can be used for *in situ* hybridisation studies to localise centromeric DNA and SINE sequences within spermatozoa nuclei and fibroblast chromosomes.

8.5.2.3. Refinement of experiments

8.5.2.3.1. Compositional Mapping Studies

An extension of the studies in Chapter 7 involves using *Sminthopsis* LINEs as a probe for the *in situ* hybridisation of *Sminthopsis* spermatozoa that no longer contain the C2 region (pers comm, Dr. A Swan). The C2 chromatin is removed from the spermatozoa by micrococcal nuclease digestion prior to hybridisation with LINE probes. This study is used as a negative control to confirm that LINEs occur mainly in the C2 region.

LINE sequences can also be used as probes to determine whether they localise to DNA that has been isolated from the C2 region in Southern hybridisation studies. This study is used as a positive control to show that the probes (LINEs) originate from the C2 region.

8.5.2.3.2. Protamine-DNA binding

Although it is now recognised that protamines probably do not reside within the minor groove of the DNA helix (Bianchi et al., 1994; Hud et al., 1994; Subirana, 1990), there is still controversy on whether the proteins bind to the major groove (Hud et al., 1994) or outside the grooves (Subirana, 1990). To help

the "footprint" can be achieved by using hydroxyl radicals which cuts DNA by abstracting a hydrogen atom from the deoxyribose sugar along the DNA backbone. Since hydroxyl radicals are short lived, reactive and attack sites on the surface of the DNA molecule, there is almost no sequence or base dependence in the cleavage reaction (Hayes, 1995). One important practical problem that this method overcomes is accessibility of the cleaving agent to tightly packaged chromatin since hydroxyl ions are very small.

The bound protein prevents cutting of the DNA backbone and hence footprints of the proteins on DNA sites are produced. The footprints of two opposing DNA strands will reveal the site of protein binding by inference of the geometry of B-DNA. For example, if the minima (indicating a binding site) from the densitometer scan of these two footprints are offset from each other by 3 bp, the protein-DNA contacts must be across a minor groove from each other because the closest backbone positions across a minor groove are 3 bp apart. The corresponding offset for closest approach across a major groove is 7 bp (Tullius et al., 1987). If however, protamines do not reside in any one of the grooves but instead, bind on the surface of the DNA, negligible cutting of the DNA may be expected.

8.5.2.4. Organisation of nucleoprotamine fibres and units of packaging

Fourier microscopy or electron crystallography is a technology where results from electron diffraction and electron microscopy are combined in image processing. This type of microscopy can be used for the detection and elucidation of the order in the packaging of the higher order nucleoprotamine structures. Although this method does not give as a high a resolution as X-ray crystallography, there are some preparative advantages over the latter method. For example, crystals are not required but thin sections of spermatozoa nuclei as prepared for conventional TEM can be used (Slayter and Slayter, 1992). The sections are imaged by transmission electron microscopy and the electron diffraction patterns are retrieved - by recording an image and computing its inverse transform. Fourier microscopy of spermatozoa nuclei may help determine whether or not there is order in the packaging of the 45-80 nm nucleoprotamine units.

CONCLUDING REMARKS

This research shows that a heterogeneous SNBP composition results in a non-homogenous chromatin structure that is responsible for the unusual morphology of the spermatozoa nuclei of *Sminthopsis*. There is also evidence which suggests sequence-specific organisation of the nucleoprotein compartments. Why this occurs and the mechanisms involved, remain unknown. It is envisaged that future investigations involving *in vivo*, high-resolution footprinting studies of chromatin structures, and computer modelling and prediction studies of DNA structure and flexibility, may help answer these questions.

REFERENCES

Allen MJ, Lee C, Lee JD, Pogany GC, Balooch M, Siekhaus WJ, Balhorn R (1993): Atomic force microscopy of mammalian sperm chromatin. Chromosoma 102:623-630.

Allen MJ, Bradbury EM, Balhorn R (1995): The natural subcellular surface structure of the bovine sperm cell. J Struct Biol 114:197-208.

Amman AP (1981): A critical review of methods for evaluation of spermatogenesis from seminal characteristics. J Androl 2:37-58.

Ammer H, Henschen A (1988): Primary structure of rabbit sperm protamine, the first protamine of its type with an aberrant N-terminal. FEBS Lett 242:111-116.

Ausio J, Suau P (1983): Structural heterogeneity of reconstituted complexes of DNA with typical and intermediate protamines. Biophys Chem 18:257-267.

Ausio J (1986): Structural variability and compositional homology of the protamine-like components of the sperm from the bivalve molluscs. Comp Biochem Physiol 85:439-449.

Ausio J, van Holde KE (1986): Histone hyperacetylation: its effect on nucleosome conformation and stability. Biochemistry 22:1421-1428.

Ausio J (1992a): Presence of a highly specific histone H1-like protein in the chromatin of the sperm of the bivalve molluscs. Mol Cell Biochem 115:163-172.

Ausio J (1992b): Structure and dynamics of transcriptionally active chromatin. J Cell Sci 102:1-5.

Austin CR, Braden AWH (1955): Observation on nuclear size and form in living rat and mouse eggs. Exp Cell Res 8:163-172.

Austin CR, Walton A (1960): Fertilisation. In: Marshall's Physiology of Reproduction. Parkes AS (e.d), Longmans, Green, London Vol 1 pp310-416.

Balhorn R, Gledhill BL, Wyrobek AJ (1977): Mouse sperm chromatin proteins: quantitative isolation and partial characterisation. Biochemistry 16, 4074-4080.

Balhorn R (1982): A model for the structure of chromatin in mammalian sperm. J Cell Biol 93:298-305.

Balhorn R, Weston S, Thomas C, Wyrobek A J (1984): DNA packaging in mouse spermatids: synthesis of protamine variants and four transition proteins. Exp Cell Res 150, 298-308.

Balhorn R, Reed S, Tanphaichitr N (1988): Aberrant protamine 1/protamine 2 ratios in sperm of infertile human males. Experientia 14:52-55.

Balhorn R (1989): Mammalian protamines: structure and molecular interaction. In: Molecular biology of chromosome function. Adolf KW (ed) Springer-Verlag, New York pp386-395.

Barone JG, De Lara J, Cummings KB, Ward WS (1994): DNA organisation in human spermatozoa. J Androl 15:139-144.

Bartolomé S, Bermúdez A, Daban JR (1994): Internal structure of the 30 nm chromatin fiber. J Cell Sci 107:2983-2992.

Belaiche D, Loir M, Kruggle W, Sautiere P (1987): Isolation and characterisation of two protamines St1 and St2 from stallion spermatozoa, and amino-acid sequence of the major protamine St1. Biochem Biophys Acta 913:145-149.

Bellvé AR, O'Brien DA (1983): The mammalian spermatozoon: structure and temporal assembly. In: Mechanism and control of animal fertilisation. Hartman JF (ed) Academic Press, New York pp55-137.

Bellvé AR, McKay DJ, Renaux BS, Dixon GH (1988): Purification and characterisation of mouse protamine P1 and P2. Amino acid sequence of P2. Biochemistry 27:2890-2897.

Bellvé AR, Chandrika R, Barth AH (1990): Temporal expression, polar distribution and transition of an epitope domain in perinuclear theca during mouse spermatogenesis. J Cell Sci 96:745-756.

Bellvé AR, Chandrika R, Martinova YS, Barth AH (1992): The perinuclear matrix as a structural element of the mouse sperm nucleus. Biol Reprod 47:451-456.

Belokopytova IA, Kostyleva EI, Tomolin AN, Vorobev VI (1993): Human male infertility may be due to a decrease of the protamine P2 content in sperm chromatin. Mol Reprod Dev 24:53-57.

Bendayan M (1981): Ultrastructural localisation of nucleic acids by the use of enzyme-gold complexes. J Histochem Cytochem 29:531-541.

Bennett JH, Breed WG, Hayman DL, Hope RM (1990): Reproductive and genetical studies with a laboratory colony of the dasyurid marsupial *Sminthopsis crassicaudata* Aust J Zool 37:201-222.

Berlot-Picard F, Vodjdani G, Doly J (1986): Nucleotide sequence of a cDNA clone encoding *Scylliorhinus caniculus* protamine Z2. Eur J Biochem 160:305-310.

Bernardi G, Olofsson B, Filipski J, Zerial M, Salinas J, Cuny G, Meunierand-Rodier F (1985): The mosaic genome of warm-blooded vertebrates. Science 228:953-958.

Bianchi F, Rousseaux-Prevost R, Bailly C, Rousseaux J (1994): Interaction of human P1 and P2 protamines with DNA. Biochem Biophys Res Comm 201:1197-1204.

Biggiogera M, Muller S, Courtens JL, Fakan S, Romanini MGM (1992): Immunoelectron microscopical distribution of histones H2B and H3 and protamines in the course of mouse spermiogenesis. Micro Res Tech 20:259-267.

Bishop AC (1972): An outline of crystal morphology. Hutchinson Scientific and Technical, London.

Black JA, Dixon GH (1967): Evolution of protamine: a further example of partial gene duplication. Nature 216:152-154.

Bloch (1969): A catalog of sperm histones. Genetics (Suppl) 61:93-111.

Bower PA, Yelick PC, Hecht NB (1987): Both protamines 1 and 2 genes are expressed in the mouse, hamster, and rat. Biol Reprod 37:479-488.

Brandt WF, Strickland WN, Strickland M, Carlisle L, Woods O, von Holt C (1979): A histone programme during the life cycle of the sea urchin. Eur J Biochem 94:1-10.

Bratosin-Guttman S (1992): A new method for the routine speading of DNA in protein-free conditions. J Struct Biol 108:162-167.

Breed WG, Leigh CM, Bennett JH (1989): Sperm morphology and storage in the female reproductive tract of the fat-tailed dunnart, *Sminthopsis crassicaudata* (Marsupialia: Dasyuridae). Gam Res 23:61-75.

Breed WG, Leigh CM (1992): Marsupial fertilization: some further ultrastructural observations on the dasyurid, *Sminthopsis crassicaudata*. Mol Reprod Dev 32:277-292.

Breed WG (1983): Variation in sperm morphology in the Australian rodent genus, *Pseudomys* (Muridae). Cell Tissue Res 229:611-625.

Breed WG, Leigh CM, Washington JM, Soon LLL (1994): Unusual nuclear structure of the spermatozoon in a marsupial, *Sminthopsis crassicaudata*. Mol Reprod Dev 37:78-86.

Burgos MH, Fawcett DW (1955): Studies on the structure of the mammalian testis I. Differentiation of spermatids of the cat (*Felis domestica*). J Biophys Biochem Cytol 1:287-300.

Burton FH, Loeb DD, Voliva CF, Martin SL, Edgell MH, Hutchison CA (1986): Conservation throughout mammalia and extensive protein-encoding capacity of the highly repeated DNA long interspersed sequence one. J Mol Biol, 187:291-304.

Butt HJ, Guckenberger R, Rabe JP (1992): Quantitative scanning tunneling microscopy and scanning force microscopy of organic materials. Ultramicroscopy 46:375-393.

Calvin HI, Grosshans K, Blake EF (1986): Estimation and manipulation of glutathione levels in prepubertal mouse ovaries and ova: relevance to sperm nucleus transformation in the fertilized egg. Gam Res 14:265-275.

Chesnokov IN, Schmid CW (1995): Specific Alu binding protein from human sperm chromatin prevents DNA methylation. J Biol Chem 270:18539-18542.

Chimera JA, Musich PR (1985): The association of the interspersed repetitive *Kpn*I sequences with the nuclear matrix. J Biol Chem 260:9373-9379.

Chiva M, Kasinsky HF, Subirana JA (1987): Characterisation of protamines from four avian species. FEBS Letters 215:237-240.

Chiva M, Kasinsky HE, Mann M, Subirana JA (1988): On the diversity of sperm basic proteins in the vertebates: VI. Cytochemical and biochemical analysis in birds. J Exp Zool 245:304-317.

Chou PY, Fasman GD (1978): Empirical predictions of protein conformation. Ann Rev Biochem 47:251-276.

Christensen ME, Dixon GH (1982): Hyperacetylation of histone H4 correlates with the terminal, transcriptionally inactive stages of spermatogenesis in rainbow trout. Dev Biol 93:404-415.

Christensen ME, Rattner JB, Dixon GH (1984): Hyperacetylation of histone H4 promotes chromatin decondensation prior to histone replacement by protamines during spermatogenesis in rainbow trout. Nucl Acids Res 12:4575-4592.

Cid H, Arellano A (1982): Secondary structure prediction of protamines. Int J Biol Macromol 4:3-8.

Clemens WA (1968): Origin and early evolution of marsupials. Evolution 22:1-18.

Clemens WA, Richardson BJ, Baverstock PR (1989): Biogeography and phylogeny of the metatheria. In: Fauna of Australia. Walton DW, Richardson BJ (eds), AGPS Press, Canberra pp 527-548.

Cockerill PN, Garrard WT (1986): Chromosomal loop anchorage of the kappa immunoglobulin gene occurs next to the enhancer in a region containing topoisomerase II sites. Cell 44:273-282.

Comings DE (1978): Mechanisms of chromosome banding and implications for chromosome structure. Annu Rev Genet 12:25-35.

Cook PR, Brazell IA (1976): Conformational constraints in nuclear DNA. J Cell Sci 22:287-302.

Courtens JL, Loir M (1981a): Ultrastructural detection of basic nucleoproteins: alcoholic phosphotungstic acid does not bind to arginine residues. J Ultrastruct Res 74:322-326.

Courtens JL, Loir M (1981b): A cytochemical study of nuclear changes in boar, bull goat, mouse, rat and stallion spermatids. J Ultrastruct Res 74:327-340.

Courtens JL, Delaleu B, Dubois DB, Lanneau M, Loir M, Rozinek J (1983): Immunocytochemical localisation of protamine in the spermatids of the ram. Gam Res 8:21-28.

Courtens JL, Plöen L, Loir M (1988): Immunocytochemical localisation of protamine in the boar testis. J Reprod Fertil 82:635-643.

Courtens JL, Biggiogera M, Rothfield NF, Burnier M, Fakan S (1992): Migration of centromere proteins in rabbit spermatids. Mol Reprod Dev 32:369-377.

Dadoune JP, Alfonsi MF (1986): Ultrastructural and cytochemical changes of the head components of human spermatids and spermatozoa. Gamete Res 14:33-46.

Dadoune JP (1995): The nuclear status of human sperm cells. Micron 26:323-345.

DeYebra L, Ballesca JL, Vanrell JA, Bassas L, Oliva R (1993): Complete selective absence of protamine P2 in humans. J Biol Chem 268:10553-10557.

Dingwall C, Laskey RA (1991): Nuclear targeting sequences - a consensus? Trends Biochem Sci 16:478-481.

Dorner M, Paabo S (1995): Nucleotide sequence of a marsupial LINE-1 element and the evolution of placental mammals. Mol Biol Evol 12:944-948.

Driscoll DJ, Migeon BR (1990): Sex difference in methylation of single-copy genes in human meiotic germ cells: implications for X chromosome inactivation, parental imprinting, and origin of CpG mutations. Som Cell Mol Genet 16:267-282.

Dubochet J, Adrian M, Chang JJ, Homo JC, Lepault J, McDowall AW, Schultz P (1988): Cryo-electron microscopy of vitrified specimens. J Rev Biophys 21:129-228.

Earnshaw WC, Halligan N, Cooke C, Rothfield N (1984): The kinetochore is part of the metaphase chromosome scaffold. J Cell Biol 98:352-357.

Earnshaw WC, Rothfield N (1985): Identification of a family of human centromere proteins using autoimmune sera from patients with scleroderma. Chromosoma (Berl) 91:313-321.

Elsevier SM (1982): Messenger RNA encoding basic chromosomal proteins of mouse testis. Dev Biol 90:1-12.

Englander EW, Howard BH (1995): Nucleosome positioning by human Alu elements in chromatin. J Biol Cell 270:10091-10096.

Evenson DP, Thompson L, Jost LK (1994): Flow cytometric evaluation of boar semen by the sperm chromatin structure assay as related to cryopreservation and fertility. Theriogen 41:637-651.

Fanning TG, Singer MF (1987): Line 1:a mammalian transposable element. Biochem Biophys Acta 910:203-210.

Fawcett DW (1970): A comparative view of sperm ultrastructure. Biol Reprod 2:90-127.

Fawcett DW, Anderson WA, Philips DM (1971): Morphogenetic factors influencing the shape of the sperm head. Dev Biol 26, 220-251.

Felsenfeld G (1992): Chromatin as an essential part of the transcriptional mechanism. Nature 355:219-223.

Ferrington JE, Patel R, Ward WS (1991): DNA attachment to the hamster sperm nuclear matrix and nuclear annulus. Ann NY Acad Sci 637:164-173.

Feughelman M, Langridge R, Seeds WE, Stokes AR, Wilson HR (1955): Molecular structure of deoxyribose nucleic acid and nucleoprotein. Nature 175:834-838.

Fifis T, Cooper DW and Hill RJ (1990): Characterisation of the protamines of the tammar wallaby (*Macropus eugenii*). Comp Biochem Physiol 95571-575.

Finch JT, Klug A (1976): Solenoidal model for superstructure in chromatin. Proc Natl Acad Sci 73:1987-1991.

Finch JT, Lutter LC, Rhodes D, Brown RS, Rushton B, Levitt M, Klug A (1977): Structure of nucleosome core particles of chromatin. Nature 269:29-36.

Fita I, Campos JL, Puigjaner LC, Subirana JA (1983): X-ray diffraction study of DNA complexes with arginine peptides and their relation to nucleoprotamine structure. J Mol Biol 167:157-177.

Fouquet JP, Kann ML, Dadoune JP (1989): Immunogold distribution of actin during spermiogenesis in the rat, hamster, monkey and human Anat Rec 223:35-42.

Fouquet JP, Valentin A, Kann ML (1992): Perinuclear cytoskeleton of acrosomeless spermatids in the blind sterile mutant mouse. Tissue Cell 24:655-665.

Garcia-Ramírez M, Subirana JA (1994): Condensation of DNA by basic proteins does not depend on protein composition. Biopolymers 34:285-292.

Gardiner K, Aissani B, Bernardi G (1990): A compositional map of human chromosome 21. EMBO J 9:1853-1858.

Gatewood JM, Cook GR, Balhorn R, Bradbury EM, Schmid CW (1987): Sequence-specific packaging of DNA in human sperm chromatin. Science 236:962-964.

Gatewood JM, Cook GR, Balhorn R, Bradbury EM, Schmid CW, Bradbury EM (1990): Isolation of four core histones from human sperm chromatin representing a minor subset of somatic histones. J Biol Chem 265:20662-20666.

Grunstein M (1991): Histone function in transcription. Annu Rev Cell Biol 6:643-678.

Guldner HH, Lakomek, HJ, Bautz FA (1984): Human anti-centromere sera recognize a 19.5 kD non-histone chromosomal protein in HeLa cells. Clin Exp Immunol 58:13-20.

Gusse M, Sautiere P, Belaiche D, Martinage A, Roux C, Dadoune J-P, Chevaillier P (1986): Purification and characterisation of nuclear basic proteins of human sperm. Biochem Biophys Acta 884:124-134.

Hanover JA (1992): The nuclear pore: at the crossroads. FASEB J 6:2288-2295.

Harding HR, Carrick FN, Shorey CD (1979): Special features of sperm structure and function in marsupials. In: The spermatozoon. Fawcett DW, Bedford JM (eds) Urban & Schwarzenberg Inc, Baltimore-Munich pp289-302.

Harding HR, Woolley PA, Shorey CD, Carrick FN (1982): Sperm ultrastructure, spermiogenesis and epididymal sperm maturation in dasyurid marsupials: phylogenetic implications. In: Carnivorous marsupials. Archer M (Ed) Roy Zool Soc New South Wales, Sydney pp659-673.

Hayat MA (1981): Principles and techniques of electron microscopy. Vol 1, 2nd ed. University Park Press. Baltimore.

Hayes J (1995): Chemical probes of DNA structure in chromatin. Current Biol 2:127-135.

Hecht NB, Kleene KC, Yelick PC, Johnson PA, Pravtcheva DD, Ruddle FH (1986): Mapping of haploid expressed genes: genes for both mouse protamines are located on chromosome 16. Som Cell Mol Genet 12:203-208.

Hecht NB (1989): In: Histones and other basic nuclear proteins. Hnilica L, Stein G, Stein J (eds) CRC Press, Boca Raton, Florida.

Hecht NB (1990): Regulation of 'haploid expressed genes' in male germ cells. J Reprod Fertil 88:679-693.

Herskovits TT, Brahms J (1976): Structural investigations on DNA-protamine complexes. Biopolymers 15:687-706.

Hewish D, Burgoyne L (1973): Chromatin sub-structure: the digestion of chromatin DNA at regularly spaced sites by a nuclear deoxyribonuclease. Biochem Biophys Res Comm 52:504-510.

Hoh JH, Hansma PK (1992): Atomic force microscopy for high-resolution imaging in cell biology. Trends Biol Chem 2:208-213.

Holmes SE, Singer MF, Swergold GD (1992): Studies on p40, the leucine zipper motif-containing protein encoded by the first open reading frame of an active human LINE-1 transposable element. J Biol Chem 267:19765-19768.

Holstein AF, Roosen-Runge EC (1981): Atlas of human spermatogenesis. Grosse, Berlin.

Horowitz RA, Agard DA, Sedat JW, Woodcock CL (1994): The three-dimensional architecture of chromatin *in situ*: electron tomography reveals fibres composed of continuously-variable zigzag nucleosomal ribbon. J Cell Biol 125:1-10.

Howlett SK, Bolton VN (1985): Sequence and regulation of morphological and molecular events during the first cell cycle of mouse embryogenesis. J Embryol Exp Morphol 87:175-206.

Howlett SM (1986): A set of proteins showing cell cycle dependent modification in the early mouse embryo. Cell 45:387-396.

Hud NV, Allen MJ, Downing KH, Lee J, Balhorn R (1993): Identification of the elemental packing unit of DNA in mammalian sperm cells by atomic force microscopy. Biochem Biophys Res Commun 193:1347-1354.

Hud NV, Milanovich FP, Balhorn R (1994): Evidence of novel secondary structure in DNA-bound protamine is revealed by raman spectroscopy. Biochemistry 33:7528-7535.

Hunter T, Karin M (1992): The regulation of transcription by phosphorylation. Cell 70:375-387.

Itoh T, Ohsumi K, Katagiri C (1993): Remodeling of human sperm chromatin mediated by nucleoplasmin from amphibian eggs. Dev Growth Diff 35:59-66.

Iwai K, Ando T (1967): Methods in Enzymology. Hirs CHW (ed), Academic Press, New york vol 11, pp263.

Jager S (1990): Sperm nuclear stability and male infertility. Arch Androl 25:253-259.

Jankowski JM, States JC, Dixon GH (1986): Evidence of sequences resembling avian retrovirus long terminal repeats flanking the trout protamine gene. J Mol Evol 23:1-10.

Johnson PA, Peschon JJ, Yelick PC, Palmiter RD, Hecht NB (1988a): Sequence homologies in the mouse protamine 1 and 2 genes. Biochim Biophys Acta 950:45-53.

Johnson PA, Yelick PC, Liem H, Hecht NB (1988b): Differential distribution of the P1 and P2 protamine gene sequences in eutherian and marsupial mammals and a monotreme. Gam Res 19:169-175.

Karasiewicz J, Soltynska MS (1985): Ultrastructural evidence for the presence of actin filaments in mouse eggs at fertilisation. Roux's Arch Dev Biol 194:369-372.

Kasinsky HE, Mann M, Huang SY, Fabre L, Coyle B, Byrd Jr EW (1987): On the diversity of sperm basic proteins in the vertebrates: V. Cytochemical and amino acid analysis in Squamata, Testudines, and Crocodylia. J Exp Zool 243:137-151.

Kierszenbaum AL, Tres LL (1975): Structural and transcriptional features of the mouse spermatid genome. J Cell Biol 65:258-270.

Kleene KC, Distel RJ, Hecht NB (1983): cDNA clones encoding cytoplasmic poly(A)$^+$ RNAs which first appear at detectable levels in haploid phases of spermatogenesis in the mouse. Dev Biol 98:455-464.

Kleene KC, Distel RJ, Hecht NB (1984): Translational regulation and deadenylation of a protamine mRNA during spermiogenesis in the mouse. Dev Biol 105:71-79.

Kleene KC, Distel RJ, Hecht NB (1985): Nucleotide sequence of a cDNA clone encoding mouse protamine 1. Biochemistry 24:719-722.

Kleinsmith LJ, Kish VM (1995): The nucleus and transcription of genetic information. In: Principles of cell and molecular biology. Harper Collins Coll Publ, New York pp 400-468.

Koehler JK, Wurschmidt U, Larsen MP (1983): Nuclear and chromatin structure in rat spermatozoa. Gam Res 8:357-370.

Korenberg JR, Engels WR (1978): Base ratio, DNA content and Quinacrine-brightness of human chromosomes. Proc Natl Acad Sci USA 75:3382-3386.

Korenberg JR, Therman E, Denniston C (1978): Hotspots and functional organisation of human chromosomes. Hum Genet 43:13-22.

Korenberg JR, Rykowski MC (1988): Human genome organisation: Alu, Lines, and the molecular structure of metaphase chromosome bands. Cell 53:391-400.

Kornberg RD, Klug A (1981): The Nucleosome. Sci Amer 244:52-64.

Krawetz SA, Connor W, Dixon GH (1987): Cloning of bovine P1 protamine cDNA and the evolution of vertebrate P1 protamines. DNA 6:47-57.

Krawetz SA, Dixon GH (1988): Sequence similarities of the protamine genes: Implications for regulation and evolution. J Mol Evol 27:291-297.

Kuhn EM, Therman E (1986): Cytogenetics of Bloom's syndrome. Can Genet Cytogenet. 22:1-18.

Langmore JP, Paulson JR (1983): Low angle x-ray diffraction studies of chromatin structure *in vivo* and in isolated nuclei and metaphase chromosomes. J Cell Biol 96:1120-1131.

Latchman DS (1990): Gene regulation: a eukaryotic perspective. Unwin Hyman, London.

Le Lannic, Arkhis A, Vendrely E, Chevaillier P, Dadoune JP (1993): Production, characterisation, and immnocytochemical applications of monoclonal antibodies to human sperm protamines. Mol Reprod Dev 36:106-112.

Lebkowski JS and Laemmli UK (1982): Evidence for two levels of DNA folding in histone-depleted Hela interphase nuclei. J Mol Biol 156:309-324.

Lemieux N, Dutrillaux B, Viegas-Pequignot E (1992): A simple method for simultaneous R- or G-banding and fluorescence *in situ* hybridisation of small single-copy genes. Cytogenet Cell Genet 59:311-312.

Leno GH, Mills AD, Philpott A, Laskey RA (1996): Hyperphosphorylation of nucleoplasmin facilitates *Xenopus* sperm decondensation at fertilisation. J Biol Chem 271:7253-7256.

Leonardson KE, Levy SB (1989): Chromatin reorganisation during emergence of malignant friend tumors: early changes in H2A and H2B variants and nucleosome repeat length. Exp Cell Res 180:209-219.

Leuba SH, Yang G, Robert C, Samori B, van Holde K, Zlatanova J, Bustamante C (1994): Three-dimensional structure of extended chromatin fibres as revealed by tapping-mode scanning force microscopy. Proc Natl Acad Sci 91:11621-11625.

Lewin B (1994): Chromatin and gene expression: constant questions, but changing answers. Cell 79:397-406.

Lewis CD, Laemmli UK (1982): Higher order metaphase chromosome structure: evidence for metalloprotein interactions. Cell 29:171-181.

Ling V, Jergil B, Dixon GH (1971): The biosynthesis of protamine in trout testis. III. Characterisation of protamine components and their synthesis during testis development. J Biol Chem 246:1168-1176.

Liu L (1983): DNA topoisomerases-enzymes that catalyse the breaking and rejoining of DNA. CRC Crit Rev Biochem 15:1-24.

Loeb DD, Padgett RW, Hardies SC, Shehee WR, Comer MW, Edgell MH, Hutchison CA (1986): The sequence of a large LIM σ element reveals a tandemly repeated 5' end and several features found in retroposons. Mol Cell Biol 6:168.

Loir M, Bouvier D, Fornells M, Lanneau M, Subirana JA (1985): Interactions of nuclear proteins with DNA during sperm differentiation in ram. Chromosoma 92:304-312.

Longo FJ (1973): Fertilisation: a comparative ultrastructural review. Biol Reprod 9:149-215.

Longo FJ, Krohne G, Franke WW (1987): Basic proteins of the perinuclear theca of mammalian spermatozoa and spermatids: a novel class of cytoskeletal elements. J Cell Biol 105:1105-1120.

Longo FJ, Cook S (1991): Formation of the perinuclear theca in spermatozoa of diverse mammalian species: relationship of the manchette and multiple band polypeptides. Mol Reprod Dev 28: 280-293.

Macgregor HC, Walker H (1973): The arrangement of chromosomes in nuclei of sperm from *Plethodontid* salamanders. Chromosoma 40:243-262.

Macleod D, Charlton J, Mullins J, Bird AP (1994): Sp1 sites in the mouse aprt gene promoter are required to prevent methylation of the CpG island. Genes Dev 8424:2282-2292.

Maro B, Johnson MH, Webb M, Flach G (1986): Mechanism of polar body f formation in the mouse oocyte: an interaction between the chromosomes, the cytoskeleton and the plasma membrane. J Embryol Exp Morphol 92:11-32.

Martin SL (1991): Ribonucleoprotein particles with LINE-1 RNA in mouse embryonal carcinoma cells. Mol Cell Biol 11:4804-4807.

Marushige K, Dixon GH (1969): Developmental changes in chromosomal composition and template activity during spermatogenesis in trout testis. Dev Biol 19:397-414.

Marushige K, Ling V, Dixon GH (1969): Phosphorylation of chromosomal basic proteins in maturing trout testis. J Biol Chem 244:5953-5958.

Marushige Y, Marushige K (1978): Transformation of sperm histone during formation and maturation of rat spermatozoa. J Biol Chem 250:39-45.

Mathias SL, Scott AF, Kazazin HH, Boeke JD, Gabriel A (1991): Reverse transcriptase encoded by a human transposable element. Science 254: 1808-1810.

Mazo J, Prantera G, Torres M, Ferraro M (1994): DNA methylation changes during mouse spermatogenesis. Chromosome Res 2:147-152.

McDowall AW, Smith JM, Dubochet J (1986): Cryo-electron microscopy of vitrified chromosomes *in situ*. EMBO J 5:1395-1402.

McGhee JD, Rau DC, Charney E, Felsenfeld G (1980): Orientation of the nucleosome within the higher order structure of chromatin. Cell 22:87-96.

McKay D, Renaux BS, Dixon GH (1986): Human sperm protamines. Amino-acid sequences of two forms of protamine P2. Eur J Biochem 156:5-8.

McPherson SMG, Longo FJ (1993): Nicking of rat spermatid and spermatozoa DNA: possible involvement of DNA Topoisomerase II. Dev Biol 158:122-130.

Meziere C, Stockl F, Batsford S, Vogt A, Muller S (1994): Antibodies to DNA, chromatin core particles and histones in mice with graft-versus-host disease and their involvement in glomerular injury. Clin Exp Imm 98:287-294.

Miklos GLG (1985): Localised highly repetitive DNA sequences in vertebrate and invertebrate genomes. In: Molecular Evolutionary Genetics. MacIntyre RJ (ed), Plenum Press, New York.

Mirkovitch J, Gasser SM and Laemmli UK (1987): Relation of chromosome structure and gene expression. Phil Trans Roy Soc Lond 317:563-574.

Moens PB, Pearlman RE (1989): Satellite DNA I in chromatin loops of rat pachytene chromosomes and in spermatids. Chromosoma (Berl) 98:287-294.

Monestier M, Fasy TM, Losman MJ, Novick KE, Muller S (1993): Structure and binding properties of monoclonal antibodies to core histones from autoimmune mice. Mol Immunol 30:1069-1075.

Moss SB, Challoner PB, Groudine M (1989): Expression of a novel histone 2B during mouse spermiogenesis. Dev Biol 133:83-92.

Muller S, Mazen A, Martinage A, Regenmortel MHVV (1984): Use of histone antibodies for studying chromatin topography and the phosphorylation of chromatin subunits. EMBO J 3:2431-2436.

Muñoz-Guerra S, Azorín F, Casas MT, Marcet X, Maristany MA, Roca J, Subirana JA (1982): Structural organisation of sperm chromatin from the fish *Carassius auratus*. Exp Cell Res 137:47-53.

Nakano M, Tobita T, Ando T (1976): Studies on a protamine (galline) from fowl sperm: the total amino acid sequence of intact galline molecule. Int J Pept Prot Res 8:565-578.

Norris J, Fan D, Aleman C, Marks JR, Futreal PA, Wiseman RW, Iglehart JD, Deininger PL, McDonnell DP (1995): Identification of a new subclass of Alu DNA repeats which can function as estrogen receptor-dependent transcriptional enhancers. J Biol Chem, 270:22777-22782.

O'Brien DA, Bellvé AR (1980): Protein constituents of the mouse spermatozoa. Dev Biol 75:386-404.

Ohsumi K, Shimada A, Okumura E, Kishimoto T, Katagiri C (1995): Dependence of removal of sperm-specific proteins from *Xenopus* sperm nuclei on the phosphorylation state of nucleoplasmin. Dev Growth Diff 37:329-336.

Olins AL, Olins DE (1974): Spheroid chromatin units (*v* bodies). Science 183:330-331.

Oliva R, Goren R, Dixon GH (1989): Quail (*Coturnix japonica)* protamine, full-length cDNA sequence, and the function and evolution of vertebrate protamines. (Communication) 264:17627-17630.

Oliva R, Bazett-Jones DP, Locklear L, Dixon GH (1990): Histone hyperacetylation can induce unfolding of the nucleosome core particle. Nucl Acids Res 18:2739-2747.

Oliva R, Dixon GH (1990): Vertebrate protamine gene evolution I. Sequence alignments and gene structure. J Mol Evol 30:333-346.

Oliva R, Dixon GH (1991): Vertebrate protamine genes and the histone-to-protamine replacement reaction. Prog Nucleic Acid Res Mol Biol 40:25-94.

Olivares C, Ganz H, Inostroza D (1986): A comparative study of the basic nuclear proteins from sperm of bivalve molluscs. Comp Biochem Physiol 83:185-189.

Olivares C, Vera ML, Ruíz-Lara S (1993): Coexistence of two chromatin structures in sperm nuclei of the bivalve mollusc, *Protothaca thaca.* Mol Cell Biochem 125:87-95.

Pabo CO and Sauer RT (1992): Transcription factors: structural families and principles of DNA recognition. Annu Rev Biochem 61:1053-1095.

Palmer DK, Kathleen O, Margolis RL (1990): The centromere specific histone CENP-A is selectively retained in discrete foci in mammalian sperm nuclei. Chromosoma 100:32-36.

Pardoll DM, Vogelstein B, Coffey DS (1980): A fixed site of DNA replication in eukaryotic cells. Cell 19:527-536.

Parvinen M, Soder O, Mali P, Froysa B, Ritzem EM (1991): *In vitro* stimulation of stage-specific deoxyribonucleic acid synthesis in rat seminiferous tubule segments by Interleukin-1α. Endocrinology 129:1614-1620.

Peachey NM, Eckhardt CJ (1994): Structural studies of ordered monolayers using atomic force microscopy. Micron 25:271-292.

Peschon JJ, Behringer RR, Brinster RL, Palmiter RD (1987): Spermatid-specific expression of protamine 1 in transgenic mice. Proc Natl Acad Sci USA 84:5316-5319.

Picheral B (1971): Ultrastructure du noyau en rapport avec l'evolution des proteines basiques nucleaires au cours de la spermiogenese du Triton *Pleurodeles waltlii* Michah. J Microscopie 12:107-132.

Pirhonen A, Valtonene P, Linnala-Kankunnen A, Heiskanen ML, Mäenpää PH (1990): Primary structures of two protamines 2 variants (St2a and St2b) from stallion spermatozoa. Biochim Biophys Acta 1039:177-180.

Poccia DL (1991): Sp histones and chromatin structure in male germ line nuclei and male pronuclei of the sea urchin. In: Comparative spermatology 20 years after. Baccetti B (ed), Serono Symposia Publications, Raven Press Vol 75 pp 61-65.

Poccia DL, Green GR (1992): Packaging and unpackaging the sea urchin sperm genome. Trends Biochem Sci 17:223-227.

Poljak L, Käs E (1995): Resolving the role of topoisomerase II in chromatin structure and function. Trends Cell Biol 5:348-354.

Powell D, Cran DG, Jennings C, Jones R (1992): Spatial organisation of the genome in the mammalian sperm nucleus. In: Comparative spermatology 20 years after. Baccetti B (ed), Serono Symposia Publications, Raven Press Vol 75 pp67-71.

Prescott L, Deininger MA, Batzer , Hutchison CA, Marshall HE (1992): Master genes in mammalian repetitive DNA amplification. Trends Genet 8:307-311.

Rattner JB and Hamkalo BA (1978): Higher order structure in metaphase chromosomes. Chromosoma 69:373-379.

Razin A, Cedar H, Riggs AD (1984): Introduction and general overview. In: DNA methylation. Razin A, Cedar H, Riggs AD (eds), Springer-verlag, New York, Berlin, Heidelberg, Tokyo pp1-10.

Retief, JD, Rees JS, Westerman M, Dixon GH (1995a): Convergent evolution of cysteine residues in sperm protamines of one genus of marsupial, the Planigales. Mol Biol Evol 12:708-712.

Retief, JD, Krajewski C, Westerman M, Dixon GH (1995b): The evolution of protamine P1 genes in dasyurid marsupials. J Mol Evol 41:549-555.

Rhim JA, Connor W, Dixon GH, Harendza CJ, Evenson DP, Palmiter RD, Brinster RL (1995): Expression of an avian protamine in transgenic mice disrupts chromatin structure in spermatozoa. Biol Reprod 52:20-32.

Richardson WD, Davies HG (1980): Quantitative observations on the kinetics and mechanism of binding of electron stains to thin sections through hen erythrocytes. J Cell Sci 46:253-257.

Richmond TJ, Finch JT, Rushton B, Rhodes D, Kulg A (1984): Structure of the nucleosome core particle at 7 Å resolution. Nature 311:532-537.

Risley MS, Einheber S, Buncrot DA (1986): Changes in DNA topology during spermatogenesis. Chromosoma (Berl) 94:217-227.

Rodman TC, Pruslin FH, Allfrey VG (1984): Protamine-DNA association in mammalian spermatozoa. Exp Cell Res 150:269-281.

Roux C, Mathieson J, Dadoune JP (1987): Localisation immunocytologique des protamines du groupe HP1 dans le testicule humain et le spermatozöide éjaculé. Bull Ass Anat 71:65-69.

Russell LD, Lee IP, Ettlin R, Peterson RN (1983): Development of the acrosome and alignment, elongation and entrenchment of spermatids in procarbazine-treated rats. Tiss Cell 15:615-626.

Russell LD (1990): Spermatid-Sertoli tubulobulbar complexes as devices for elimination of cytoplasm from the head region of late spermatids of the rat. Anat Rec 194:233-246.

Russell LD, Russell JA, MacGregor GR, Meistrich ML (1991): Linkage of manchette microtubules to the nuclear envelope and observations on the role of the manchette in nuclear shaping during spermiogenesis in rodents. Am J Anat 192:97-120.

Sambrook J, Fritsch EF, Maniatis T (1989): Molecular Cloning: a laboratory manual. Cold Spring Harbor Laboratory Press, New York, USA.

Santi S, Rubbini S, Cinti C, Squarzoni S, Matteucci A, Caramelli E, Guidotti L, Maraldi NM (1994): Nuclear matrix involvement in sperm head structural organisation. Biol Cell 81:47-57.

Saperas N, Lloris D, Chiva M (1993): Sporadic appearance of histones, histone-l like proteins, and protamines in sperm chromatin of bony fish. J Exp Zool 265:575-586.

Saperas N, Ausio J, Domenec L, Chiva M (1994): On the evolution of protamines in bony fish: alternatives to the "retroviral horizontal transmission" hypothesis. J Mol Evol 39:282-295.

Sapienza C, Tran TH, Paquette J, McGowan R, Peterson MB (1989): A methylation mosaic model for mammalian genome imprinting. In: Progress in nucleic acid research and molecular biology. Cohn WE, Moldave K (eds), Academic Press Inc, San Diego pp145-156.

Sapsford CS, Rae CA, Cleland KW (1969): Ultrastructural studies on maturing spermatids and on Sertoli cells in the bandicoot, *Perameles nasuta* Geoffrey (Marsupialia). Aust J Zool 17:195-292.

Schechtman MG (1990): Characterisation of telomere DNA from *Neurospora crassa*. Gene 88:159-166.

Schmid CW (1991): Human Alu subfamilies and their methylation revealed by blot hybridisation. Nucl Acids Res 19:5613-5617.

Schmid C, Maraia R (1992): Transcriptional regulation and transpositional selection of active SINE sequences. Curr Opin Genet Dev 2:874-882.

Sealy L, Hartley J, Donelson J, Chalkley R, Hutchison N, Hamkalo BA (1981): Characterisation of a highly repetitive sequence DNA family in rat. J Mol Biol 145:291-318.

Selker EU (1990): DNA methylation and chromatin stucture: a view from below. Trends Biochem Sci 15:103-107.

Sen D, Crothers DM (1986): Condensation of chromatin: Role of multivalent cations. Biochemistry 25:1459-1464.

Sharpe RM (1993): Experimental evidence for Sertoli-germ cell and Sertoli-Leydig cell interactions. In: The Sertoli cell. Russell LD, Griswald MD (eds), Cache River Press, Clearwater, Florida pp331-347.

Sharpe RM (1994): Regulation of spermatogenesis. In: The physiology of reproduction. Knobil E, Neill JD (eds), Raven Press, New York pp1363-1434.

Sipski ML, Wagner TE (1977): The total structure and organisation of chromosomal fibres in eutherian sperm nuclei. Biol Reprod 16:428-440.

Slayter EM, Slayter HS (1992): Imaging: microscopy and diffraction. In: Light and electron microscopy. Cambridge University Press, Cambridge pp93-94.

Soon LLL, Breed WG (1996): Ultrastructure of nuclear condensation and localisation of DNA and proteins in the spermatozoa of a dasyurid marsupial, *Sminthopsis crassicaudata*. Mol Reprod Dev 43:217-227.

Sprando RL, Russell LD (1987): Comparative study of cytoplasmic elimination in spermatids of selected mammalian species. Am J Anat 178:72-80.

Stanker LH, Wyrobek A, Balhorn R (1987): Monoclonal antibodies to human protamines. Hybridoma 6:293-303.

Sterner R, Boffa LC, Chen TA, Allfrey VG (1987): Cell cycle-dependent changes in conformation and composition of nucleosomes containing human histone gene sequences. Nucleic Acids Res 15:4375-4391.

Suau P, Subirana JA (1977): X-ray diffraction studies of nucleoprotamine structure. J Mol Biol 117:909-926.

Subirana JA, Cozcolluela C, Palau J, Unzeta M (1973): Protamines and other basic proteins from spermatozoa of molluscs. Biochim Biophys Acta 31:364-379.

Subirana JA (1990): Proteins as counterions of DNA: a new model of nucleoprotamine structure. In: Water and ions in biomolecular systems. Vasilescu D, Loz J, Pack L, Pullmann B (eds), Advances in Life Sciences. Basel, Birkhauser Verlag pp63-70.

Sullivan KF, Hechenberger M, Masri K (1994): Human CENP-A contains a histone H3 related histone fold domain that is required for targeting to the centromere. J Cell Biol 127:581-592.

Suzuki M (1989): SPKK a new nucleic acid binding unit of protein found in histone. EMBO J 8:797-804.

Tamphaichitr N, Sobhon P, Taluppeth N, Chalermisarachai P (1978): Basic nuclear proteins in testicular cells and ejaculated spermatozoa in man. Exp Cell Res 117:347-356.

Tamphaichitr N, Sobhon P, Chalermisarachai P, Chutatape C (1982): Biochemical and ultrastructural characterisations of nucleoprotamine in human sperm heads treated with micrococcal nuclease and salt. Gam Res 6:235-255.

Tanhauser SM, Hecht NB(1989): Nucleotide sequence of rat protamine 2 gene. Nucl Acids Res 17:4395.

Temple-Smith PD (1984): Reproductive structures and strategies in male possums and gliders. In: Possums and gliders. Smith AP, Hume ID (eds), Aust Mammal Soc, Sydney pp89-106.

Therman E (1986): Human chromosomes: structure, behaviour, effects. Springer-Verlag, New York.

Thibault C, Gerard M (1973): Cytoplasmic and nuclear maturation of rabbit oocytes *in vitro*. Ann Biol Anim Biochim Biophys 13:145-156.

Thoma F, Koller T, Klug A: (1979): Involvement of histone H1 in the organisation of the nucleosome and of the salt-dependent superstructures of chromatin. J Cell Biol 83:403-427.

Toniolo C, Bonora GM, Marchiori F, Borin G, Fillippi B (1979): Protamines. II. Circular dichroism study of the three main components of clupeine. Biochim Biophys Acta 576:429-439.

Toniolo C (1980): Secondary structure prediction of fish protamines. Biochim Biophys Acta 624:420-427.

Tres LL, Kierszenbaum AL (1977): Premeiotic and meiotic prophase RNA synthesis in human testes. In: The testis in normal and infertile men. Troen P, Nanken HR, (eds), Raven Press, New York pp9-23.

Tullius TD, Dombroski BA, Churchill MEA, Kam L (1987): Hydroxyl radical footprinting: a high-resolution method for mapping protein-DNA contacts. Met Enzymol 155:537-558.

Turner BM (1991): Histone acetylation and control of gene expression. J Cell Sci 99:13-20.

Uschewa A, Auramova Z Tsanev R (1982): Tightly bound somatic histones in mature ram sperm nuclei. FEBS Lett 138:50-54.

van Holde KE (1988): Chromatin. Rich A (ed), Berlin-New York, Springer Verlag pp1-497.

van Holde KE (1993): The omnipotent nucleosome. Nature 362:111-112.

van Holde KE, Zlatanova J (1995): Chromatin higher order structure: chasing a mirage? Minireview. J Biol Chem 270:8373-8376.

Vaughn JP, Dijkwel PA, Mullender LHF and Hamlin JL (1990): Replication forks are associated with the nuclear matrix. Nucl Acids Res 18: 1965-1969.

Verdaguer N, Perello M, Palau J, Subirana JA (1993): Helical structure of basic proteins from spermatozoa. Comparison with model peptides. Eur J Biochem 214:879-887.

Vigers GPA, Lohka MJ (1991): A distinct vesicle population targets membranes and pore complexes to the nuclear envelope in *Xenopus* eggs. J Cell Biol 112:545-556.

Vogelstein B, Pardoll DM, Coffey DS (1980): Supercoiled loops and eukaryotic DNA replication. Cell 22:79-85.

von Holt C, De Groot P, Schwager S, Brandt WF (1984): The structure of sea urchin histones and considerations on their function. In: Histone genes: structure, organisation and regulation. Stein GS, Stein JL, Marzluff WF (eds), John Wiley, New York pp 65-105.

Walker H, Macgregor HC (1968): Spermatogenesis and the structure of the mature sperm in *Nucella lapillus*. J Cell Sci 3:95-104.

Ward WS, Coffey DS (1989): Identification of a sperm nuclear annulus: a sperm DNA anchor. Biol Reprod 41:361-370.

Ward WS, Partin AW, Coffey DS (1989): DNA loop domains in mammalian spermatozoa. Chromosoma 98:153-159.

Ward WS, Coffey DS (1990): Specific organisation of genes in relation to the sperm nuclear matrix. Biochem Biophys Res Commun 173:20-25.

Ward WS, Coffey DS (1991): DNA packaging and organisation in mammalian spermatozoa: comparison with somatic cells. Biol Reprod 44:569-574.

Ward WS (1993): Deoxyribonucleic acid loop domain tertiary structure in mammalian spermatozoa. Biol Reprod 48:1193-1201.

Warrent RW, Kim SH (1978): α-helix-double helix interaction shown in the structure of a protamine-transfer RNA complex and a nucleoprotamine model. Nature 271:130-135.

Widom J (1992): A relationship between the helical twist of DNA and the ordered positioning of nucleosomes in all eukaryotic cells. Proc Natl Acad Sci USA 89:1095-1099.

Wilcox AJ, Weinberg CR, O'Connor JF, Baird DD, Schlatterer JP, Caufield RE, Armstrong EG, Nisula BC (1988): Incidence of early loss of pregnancy. N Engl J Med 319:189-194.

Willard HF, Wayne JS (1987): Hierarchical order in chromosome specific human alpha satellite DNA. Trends Genet 3:192-197.

Williams SP, Athey BD, Muglia LJ, Schappe RS, Gough AH, Langmore JP (1986): Chromatin fibres are left-handed helices with diameter and mass per unit length that depend on linker length. Biophys J 49:233-248.

Wolffe AP (1994): Nucleosome positioning and modification: chromatin structures that potentiate transcription. Trends Biol Sci 19:240-244.

Woodcock CLF, Frado L-LY, Rattner JB (1984): The higher order structure of chromatin: evidence for a helical ribbon arrangement. J Cell Biol 99:42-52.

Woodcock CLF, Grigoryev SA, Horowitz RA, Whitaker N (1993): A chromatin folding model that incorporates linker variability generates fibres resembling the native structures. Proc Natl Acad Sci USA 90:9021-9025.

Woodcock CLF (1994): Chromatin fibres observed *in situ* in frozen hydrated sections. Native fibre diameter is not correlated with nucleosome repeat length. J Cell Biol 125:11-19.

Woodcock CLF, Horowitz RA (1995): Chromatin organisation re-viewed. Trends Cell Biol 5:272-277.

Worcester DL, Miller RG, Bryant PJ (1988): Atomic force microscopy of purple membranes. J Microsc 152:817-821.

Yanagimachi R, Noda YD (1970): Electron microscope studies of sperm incorporation into the hamster egg. Am J Anat 128:429-462.

Yanagimachi R (1994): Mammalian fertilisation. In: The physiology of reproduction. Knobil E, Neill JD (eds), Raven Press, New York pp189-318.

Yasuzumi G, Tanaka H (1985): Spermatogenesis in animals revealed by electron microscopy. VI. Research on the spermatozoon-dimorphism in a pond snail, *Cipangopaludina malleata*. J Biophys Biochem Cytol 4:621-632.

Yelick PC, Balhorn R, Johnson PA, Corzett M, Mazrimas JA, Kleene KC, Hecht NB (1987): Mouse protamine 2 is synthesised as a precursor whereas mouse protamine 1 is not. Mol Cell Biol 7:2173-2179.

Zabal MMZ, Czarnota GJ, Bazett-Jones DP, Ottensmeyer FP (1993): Conformation characterisation of nucleosomes by principal component analysis of their electron micrographs. J Micros 172:205-214.

Zalensky AO, Allen MJ, Kobayashi A, Zalenskaya IA, Balhorn R, Bradbury EM (1995): Well-defined genome architecture in the human sperm nucleus. Chromosoma 103:577-590.

Zini N, Mazzotti G, Santi P, Rizzoli R, Galanzi A, Rana R, Maraldi NM (1989): Cytochemical localisation of DNA loop attachment sites to the nuclear lamina and to the inner nuclear matrix. J Histochem 91:199-204.

APPENDIX 1

A. PREPARATION OF BUFFERS AND BLOCKING SOLUTIONS

A1. Phosphate buffered saline (ph 7.5)

Dissolve 0.70 g of Na_2HPO_4 (anhydrous), 0.16 g KH_2PO_4, and 8.5 g NaCl in distilled water. Adjust the pH to 7.5 and make up the solution to 1L.

A2. Washing buffer

Dissolve 4 g of sucrose and 4 g of polyvinylpyrrolidone (PVP) in 100 ml of PBS, pH 7.5.

A3. Tris buffered saline (ph 7.4)

Dissolve 4.38 g of NaCl and 1.21 g of Tris (Sigma or analytical grade) in 400-450 ml of dH_20. Adjust the pH with 1 N HCl and make up the final volume to 500 ml with dH_20.

A4. Ovalbumin (1%).

Measure out 0.5 g of Albumin and place in flask using funnel, wash down excess with PBS. Turn gently and leave until dissolved. Make up to 50 ml.

A5. Prehybridisation mix for Southern hybridisation

10% SDS	**5 ml**
20 x SSC	**30 ml**
5%Na-pyruvate	**1 ml**
distilled water	**63 ml**
Blocking reagent (Boehringer, Mannheim, W Germany)	**1g**

Measure out the above in a flask. Microwave on high at 20 sec intervals until the reagents dissolve. Incubate at 42°C before use.

A6. 20xSSC

Dissolve 175.3 g of NaCl and 88.2 g of sodium citrate in 800 ml of distilled water. Adjust pH to 7.0 with 10 N NaOH. Adjust the volume to 1 L with dH_20 and sterilize by autoclaving (Sambrook et al., 1989).

APPENDIX 2

FIXATIVES

A1. Glutaraldehyde (1.25%) + 4% paraformaldehyde

1) Dissolve 4 g of paraformaldehyde in 60 ml 6mM PBS (pH 7.2) at 60^{o}*{Use a magnetic stirrer in fume cupboard}*

2) When the solution is fairly clear, add 1-2 drops of 1N NaOH.

3) Dissolve in 4 g of sucrose and 4 g of polyvinylpyrrolidone (PVP) (10 000 MW) using the magnetic stirer.

4) Add 5 ml of 25% glutaraldehyde.

5) Adjust the pH to 7.2 by adding NaOH.

6) Make up the total volume to 100 ml.

A2. Glutaraldehyde (0.25%) + 4 % paraformaldehyde

1) Dissolve 4 g of paraformaldehyde in 60 ml of PBS at 60 ^{o}C,

2) When the solution is fairly clear, add 2-3 drops NaOH,

3) Add 1 ml of 25 % Glutaraldehyde,

4) Dissolve 4 g sucrose and 4 g PVP (10 000 MW)

5) Adjust the pH to 7.2 and make up to 100 ml.

APPENDIX 3

A. CONVENTIONAL TISSUE PROCESSING FOR TEM

1) Fix tissue for 12 - 18 h in 1.25 % Glutaraldehyde + 4% Paraformaldehyde prepared in 0.006 M PBS (pH 7.2) + 4% Sucrose and 4 % Polyvinylpyrrolidone (PVP) (10 000 MW). (see Fixatives, Appendix 2)

2) Wash in 2 changes of *washing buffer* (Appendix 1) for 20 - 30 min.

3) Post fix in 1% OsO_4 for 1 h (Wash in buffer for 15 min).

4) Dehydrate in the following ethanol concentrations:

30 %, 50 %, 70 %, 75 %, 80 %, 85 %, 90 %, 95%, 100 %, 100 % ethanol in CuSO4; 2x 30 min.

5) Propylene Oxide; 2 x 30 min

6) Infiltrate; **(2/1) Propylene oxide/Resin - Overnight**

(1/2) - 9 - 4 pm.

Pure resin; - 4 pm - Overnight.

7) Embed; next morning.

8) Polymerise at 60^{o}C for 24 h.

B. TISSUE PROCESSING WITH *EN BLOC* STAINING FOR TEM

1) Fix in 3% formaldehyde/3% glutaraldehyde in phosphate buffer at pH 7.4, at room temperature for 2-4 h.

2) Rinse 2 x 15 min in 0.2 M phosphate buffer.

3) Postfix: 2 % OsO_4 in phosphate buffer for 60 min.

4) Rinse in 0.2 M phosphate buffer for 15 min.

5) *En block* stain: Wash in maleate buffer pH 5.2 for 2 x 15 min.

Enbloc stain in 1 % uranyle acetate in maleate buffer, pH 6, at 4 ^{o}C in the dark for 1.5 h.

Wash in maleate buffer at pH 5.2 for 15 min.

6) Dehydrate in ethanol:

30 %, 50 %, 70 %, 75 %, 80 %, 85 %, 90 %, 95%, 100 %, 2x 100 % alcohol in CuSO4 for 30 min.

5) Propylene Oxide; 3 x 30 min

6) Infiltrate; (2:1) Propylene oxide/ TAAB Resin - Overnight/12 h

(1:2) - 9 - 5 pm/8 h

Pure resin - 4 pm - Overnight

7) Polymerise; (Embed in resin next morning) at 60^{o}C for 48 h.

C. PROCESSING OF TISSUES FOR IMMUNOGOLD LABELLING

1) Fix tissues for 4 h in 0.25 % Glutaraldehyde + 0.4 % Paraformaldehyde prepared in 0.006 M Phosphate Buffer + 4 % sucrose and 4 % PVP

2) Wash in two changes of Washing Buffer for 20-30 min.

***Note: No post-fixation with OsO_4**

3)Dehydrate in ethanol:

30 %, 50 %, 70 %, 75 %, 80 %, 85 %, 90 %, 95%, 100 %, 2x 100 % alcohol in CuSO4 for 30 min.

4) Infiltrate in:

LR White resin (hard grade) / Abs in CuSO4; 1 : 1 ratio for 4 h / overnight.

Pure resin (LRW)

5) Embed the following day using capsules and incubate overnight at 50 ^{o}C.

APPENDIX 4

STAINING OF SECTIONS FOR TEM

A1. Uranyl acetate

1. Prepare a 2% solution of uranyl acetate in 70% alcohol in a disposable tube.

2. Leave on rotator for about 30 min to dissolve.

3. Centrifuge for 15 min.

4. Make small "boats" out of dental wax and place in a petri dish. Pipette on a small amount of 70% alcohol around the boats.

5. Millipore uranyl acetate into the boats, add grids and cover petri dish with a black box (uranyl stains in the dark).

6. Stain for 15 min.

7. Dip grids in 70% alcohol about 20 times then in distilled water for about the same time and finally drop the grids into the beakers and swirl the containers briefly.

8. Dry the grids using pieces of filter paper.

A2. Lead citrate

1. Mix 1.33 g of lead nitrate with 1.74 g of sodium citrate and 30 mls of distilled water in a 50 ml volumetric flask. Shake throughly for 1 min and intermittently for 30 min, to ensure complete conversion of lead nitrate to lead citrate.

2. Add 8.0 ml of NaOH and dilute the suspension to 50 ml with distilled water. Mix by inversion. The resulting staining solution (pH 12.0) is stable for 6 months in a stoppered bottle and should be centrifuges before use.

3. Centrifuge lead stain for 15 min.

4. To one edge of a petri dish add 10-20 pellets of NaOH.

5. Pipette a few drops of stain into the other chamber of the petri dish and float on the grids.

6. Add a pipette full of water to the NaOH and place the lid on the petri dish.

7. Stain for 12 min.

8. Wash the grids buy dipping them (about 20 times) in two changes of distilled water dropping them in the last beaker. Swirl the beaker gently before collecting the grids and drying them with filter paper.

APPENDIX 5

A. CANTILEVER/TIP SPECIFICATIONS (TOPOMETRIX TECHNICAL BRIEFS)

The AFM cantilever has a "V"-shaped design, with the probe tip integrated onto the underside of the cantilever at the far end.

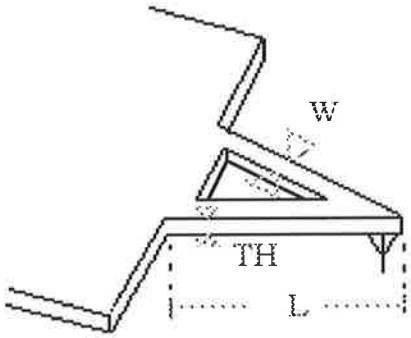

V-TYPE CANTILEVER

CANTILEVER SPECIFICATIONS

ITEM	CANTILEVER 1700
Geometry	V
Material	Si3N4
L-arm length (μm)	200
W-arm width (μm)	18
TH-Thickness (μm)	0.6
Force constant (N/m)	0.032
Resonance Frequency (kHz)	17
Tip Type	SUPERTIP™

TIP SPECIFICATIONS

ITEM	SUPERTIP™
Material	**Diamond-like Carbon**
Geometry	**Pyramidal + Needle 0.15μm (Needle) base diameter** 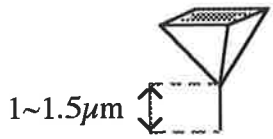
Aspect Ratio	**~10:1**
Tip Radius	**<20 nm**

APPENDIX 6

A. PROTOCOL FOR ELECTROPORATION

A1. Materials

Bacteria species used:	*E. coli* (DH5α)
Molecules electroporated:	pBluescript and PCRscript vectors

Before the Pulse

Cell growth medium:	L-Broth (LB)[4]
Growth phase at harvest OD_{600}:	0.5
Pre-pulse incubation:	10 to 20 sec on ice
Wash solution:	Distilled deionized water. Cells frozen in 10% glycerol

The Pulse

Electroporation temperature:	Ice, 0°C
Electroporation medium:	10% glycerol
Cell density:	10^{10} cells/ml
Vol of cells:	40 μl
DNA concentration:	1-100 ng
Vol of DNA:	0.5-1 μl
Instruments used:	Gene Pulser® Apparatus Pulse Controller
Cuvette gap:	0.2 cm
Voltage:	2.5 kV
Field strength:	12.5 kV/cm
Capacitor:	25 μF
Resistor:	200 Ω (Pulse Controller)
Time constant:	4.5 to 4.7 msec

After the Pulse

Outgrowth medium:	SOC[5]
Outgrowth temperature:	37°C
Length of incubation:	30-40 min
Selection method or assay used:	Ampicillin resistance
Electroporation efficiency:	10^7 to 10^{10} transformants/μg DNA

---

[4]L-Broth: 1% Bactotryptone, 0.5% Bacto yeast extract, 0.5% NaCl.
[5]SOC: 2% Bacto tryptone, 0.5% Bacto yeast extract, 10 mM NaCl, 2.5 mM KCl, 10 mM $MgCl_2$, 10 mM $MgSO_4$, 20 mM glucose.

A2. Procedure for high efficiency electro-transformation of E *coli*

Preparation of cells

1. Inoculate 1 litre of LB with 1/100 volume of fresh overnight culture.

2. Grow cells at 37°C with vigorous shaking to an ABS_{600} of 0.5 to 0.7 (the best results are obtained with cells that are harvested at early-to mid-log phase; the appropriate cell density therefore depends on the strain and growth conditions).

3. To harvest, chill the flask on ice for 15 to 30 min, and centrifuge in a cold rotor at 4000 xg_{max} for 15 min. Note: Keep the cells as close to 0°C as possible (in an ice-water bath) throughout their preparation.

4. Remove as much of the supernatant (medium) as possible. It is better to sacrifice the juice by pouring off a few cells than to leave any supernatant behind. Resuspend pellets in a volume of 1 litre of ice-cold sterile 10% glycerol taking care not to lyse them. Centrifuge as in step 3.

5. Resuspend in 0.5 litre of ice-cold sterile 10% glycerol. Centrifuge as in step 3.

6. Resuspend in ~20 ml of ice-cold 10% glycerol. Centrifuge as in step 3.

7. Resuspend to a final volume of 2 to 3 ml in ice-gold 10% glycerol. The cell concentration should be about $1\text{-}3x10^{10}$ cells/ml.

8. This suspension may be frozen in aliquots on dry ice, and stored at -70°C. The cells are good for at least 6 months under these conditions.

A3. Electro-transformation and plating

1. Gently thaw the cells at room temperature and then immediately place them on ice. Remove sterile cuvettes from their pouches and place them on ice. Place the white chamber slide on ice.

2. In a cold, 1.5 ml polypropylene tube, mix 40 μl of the cell suspension with 1 to 2 μl of DNA (DNA should be in a low ionic strength buffer such as TE[6]). Mix well and allow to sit on ice until transferring contents to a chilled cuvette.

3. Set the Gene Pulser apparatus at 25 μF, Set the Pulse Controller to 200 Ω. Set the Gene Pulser apparatus to 2.5 kV when using the 0.2 cm cuvettes. Set it to 1.8 kV when using the 0.1 cm cuvettes.

4. Transfer the mixture of cells and DNA to a cold electroporation cuvette, and shake the suspension to the bottom. Place the cuvette in a chilled safety chamber slide. Push the slide into the chamber until the cuvette is seated between the contacts in the base of the chamber.

5. Pulse once at the above settings.

6. Remove the cuvette from the chamber and immediately add 1 ml of SOC medium to the cuvette and quickly but gently re suspend the cells with a Pasteur pipette. (This rapid addition of SOC after the pulse is very important in maximizing the recovery of transformants.)

7. Transfer the cell suspension to a 17x100 mm polypropylene tube and incubate at 37°C for 1 h. (Shaking the tubes at 225 rpm during this incubation may improve the recovery of transformants.)

8. Check and record the pulse parameters. The time constant should be between 4 and 5 ms. The field strength can be calculated as actual volts (kV)/cuvette gap (cm).

9. Plate on selective medium.

---

[6]DNA containing too much salt will make the sample too conductive and cause arcing at high voltages.

APPENDIX 7

A. HARVESTING OF THE CELLS AND PREPARATION OF SLIDES

1. Soak slides in Decon 90 detergent for at least 2 h, then rinse in running tap water. Rinse the slides in distilled water and three changes of ethanol and drain dry.

2. Following incubation with 5-BrdU for 6-7 h, add colchicine solution (100 μg/ml) at 4 drops per 10 ml of culture for 20 min.
Note: Colchicine is a very poisonous plant extract which stops the formation of a mitotic spindle allowing the chromosomes to spread, but it also contracts the chromosomes.

3. Centrifuge the tube for 10 min at 1300 rpm, (352 x g, r=18.7 cm).

4. Remove the supernatant by spray suction pump.

5. Add a large excess of hypotonic 0.075 M KCl solution, leaving space for about 20% fixative, resuspend by repeated inversion and leave in 37°C water for 20 min.
Note: The KCl is 1/2 isotonic and it swells the lymphocytes and destroys the erythrocytes by bursting them.

6. Make up 120 ml of fixative: 3 parts methanol: 1 part acetic acid in a fume hood.

7. Add 20% by volume of fixative. Mix by inversion. Centrifuge for 10 min at 1300 rpm and remove the supernatant.

9. Add about 2 ml of fixative, mix with the Pasteur pipette and transfer to a 10 ml tube. Rinse the original tube by repeating, to a volume of 8 ml (1st full fix). Centrifuge for 10 min at 1300 rpm, remove the supernatant.

11. Add 8 ml of fixative. Resuspend the cells with the pipette (2nd full fix). Centrifuge for 10 min at 1300 rpm, remove the supernatant.

12. Add 8 ml of fixative. Resuspend the cells with the pipette (3rd full fix). Centrifuge for 10 min at 1300 rpm, remove the supernatant.

13. Add 2 ml of fixative and resuspend the cells. From a height of about 5 cm, place 2 drops on a slide and allow to dry.

14. Add fixative to a volume of 8 ml in the tube of cells and store at -20°C.

Breed, W.G., Leigh, C.M., Washington, J.M., and Soon, L.L.L., (1994) Unusual nuclear structure of the spermatozoon in a marsupial,*Sminthopsis crassicaudata*. *Molecular Reproduction and Development, v. 37 (1), pp. 78-86.*

Soon, L.L.L. and Breed, W.G. (1996) Ultrastructure of nuclear condensation and localization of DNA and proteins in spermatozoa of a dasyurid marsupial, Sminthopsis crassicaudata.
Molecular Reproduction and Development, v. 43 (2), pp. 217–227, February 1996